

RELATIONS BETWEEN PORE WATER PRESSURE, STABILITY AND
MOVEMENTS IN REACTIVATED LANDSLIDES

A THESIS SUBMITTED TO
THE GRADUATE SCHOOL OF NATURAL AND APPLIED SCIENCES
OF
MIDDLE EAST TECHNICAL UNIVERSITY

BY

BORA GÜNDOĞDU

IN PARTIAL FULFILLMENT OF THE REQUIREMENTS
FOR
THE DEGREE OF MASTER OF SCIENCE
IN
CIVIL ENGINEERING

FEBRUARY 2011

Approval of the thesis:

**RELATIONS BETWEEN PORE WATER PRESSURE, STABILITY AND
MOVEMENTS IN REACTIVATED LANDSLIDES**

submitted by **BORA GÜNDOĞDU** in partial fulfillment of the requirements for
the degree of **Master of Science in Civil Engineering Department, Middle East
Technical University** by,

Prof. Dr. Canan Özgen _____
Dean, Graduate School of **Natural and Applied Sciences**

Prof. Dr. Güney Özcebe _____
Head of Department, **Civil Engineering**

Assist. Prof. Dr. Nejan Huvaj-Sarıhan _____
Supervisor, **Civil Engineering Dept., METU**

Examining Committee Members:

Prof. Dr. Ufuk Ergun _____
Civil Engineering Dept., METU

Assist. Prof. Dr. Nejan Huvaj-Sarıhan _____
Civil Engineering Dept., METU

Prof. Dr. Erdal Çokça _____
Civil Engineering Dept., METU

Prof. Dr. Candan Gökçeoğlu _____
Geological Engineering Dept., Hacettepe University

Dr. Aslı Özkeskin-Çevik _____
Civil Engineering Dept., METU

Date: 11.02.2011

I hereby declare that all information in this document has been obtained and presented in accordance with academic rules and ethical conduct. I also declare that, as required by these rules and conduct, I have fully cited and referenced all material and results that are not original to this work.

Name, Last name : BORA, GÜNDOĞDU

Signature :

ABSTRACT

RELATIONS BETWEEN PORE WATER PRESSURE, STABILITY AND MOVEMENTS IN REACTIVATED LANDSLIDES

Gündoğdu, Bora

M.Sc., Department of Civil Engineering

Supervisor: Asst. Prof. Dr. Nejan Huvaj-Sarihan

February 2011, 100 pages

Slope movements cause considerable damage to life and property in Turkey as well as in the world. Although they do not typically cause loss of life, slow landslide movements can severely damage structures, interrupt the serviceability of lifelines; and, related stabilization efforts can be too costly. Most of these slow-moving landslides are reactivated landslides in stiff clays and shales, and they are mainly triggered by rainfall induced high pore water pressures. In this study, a number of reactivated, slow-moving landslide case histories with extensive pore pressure and movement data are selected for further analysis. For these landslides, the relation between pore water pressures, factor of safety and rate of movements of the slide are investigated by using limit equilibrium and finite element methods. It is found that there is a nonlinear relationship between these three variables. Sensitivity of slow moving landslides to changes in pore water pressure is developed by defining the percent change in factor of safety and percent change in pore pressure coefficient, for 10-fold change in velocity. Such relations could especially be useful in planning required level of remediation, for example, to decide on how many meters the ground water level should be lowered at a certain piezometric location, so that the stability increases to a desired level of F.S., and movement rates are reduced to an acceptable slow rate.

Keywords: Reactivated Landslides, Pore Water Pressure, Slope Stability, Velocity

ÖZ

REAKTİVE HEYELANLARDA BOŞLUK SUYU BASINCI, DURAYLILIK VE HEYELAN HAREKETLERİ ARASINDAKİ İLİŞKİLER

Gündoğdu, Bora

Yüksek Lisans, İnşaat Mühendisliği Bölümü

Tez Yöneticisi : Y. Doç. Dr. Nejan Huvaj-Sarihan

Şubat 2011, 100 sayfa

Heyelan hareketleri dünyada olduğu gibi Türkiye’de de ciddi boyutlarda can ve mal kaybına yol açmaktadır. Yavaş heyelan hareketleri, genellikle can kaybıyla sonuçlanmasa da, yapılarda ciddi anlamda hasara yol açabilir; kritik altyapı hizmetlerinde kesintiye neden olabilir ve oldukça masraflı stabilizasyon yöntemleri gerektirebilir. Bu tür heyelanların çoğunluğu sert kil ve şeyl türü malzemelerde yeniden kayan heyelanlardır ve yağmurun yol açtığı yüksek boşluk suyu basıncı duraysızlığın temel nedenidir. Bu çalışmada, yavaş hareket gözlenen reaktive heyelan vakalarından birkaçı seçilerek detaylı analizler yapılmıştır. Bu heyelanlar için, boşluk suyu basıncı, duraylılık ve heyelan hareketleri arasındaki ilişkiler, limit denge ve sonlu elemanlar metodları kullanılarak araştırılmıştır. Bu üç değişken arasında doğrusal olmayan ilişkiler tespit edilmiştir. Yavaş hareket eden heyelanların boşluk suyu basıncındaki değişimlere olan hassasiyeti, heyelan hareket hızındaki her 10-kat değişim için duraylılık ve boşluk suyu basıncı katsayısındaki yüzde değişimler tanımlanarak ifade edilmiştir. Bu tür ilişkiler özellikle gereken iyileştirme seviyesinin ve riskin azaltılmasının planlanmasında, örneğin stabilitenin istenilen güvenlik katsayısına yükseltilmesi ve hareket hızlarının kabul edilebilir yavaş hızlara düşürülmesi için belirli bir piyezometre ölçüm noktasında yeraltı su seviyesinin kaç metre düşürüleceğine karar verilmesinde yararlı olabilir.

Anahtar Kelimeler: Reaktive Heyelanlar, Boşluk Suyu Basıncı, Şev Stabilitesi, Hareket Hızı

To My Family

ACKNOWLEDGMENTS

This research has been carried out under the supervision of Asst. Prof. Dr. Nejan Huvaj-Sarihan in the Geotechnical Engineering Division of Civil Engineering Department in the Middle East Technical University.

The author wishes to express his sincere appreciation to Asst. Prof. Dr. Nejan Huvaj-Sarihan for her guidance and helpful advices throughout the research.

The technical assistance of author's colleagues and the effort of geotechnics division are gratefully acknowledged.

The author offers sincere thanks to his family for their unshakable faith in him, their patience and confidence in him. They receive many indebted thanks.

This research was supported by a Marie Curie International Reintegration Grant (grant agreement no: PIRG05-GA-2009-249186, FOLADIS) within the 7th European Community Framework Programme.

TABLE OF CONTENTS

ABSTRACT	iv
ÖZ	v
ACKNOWLEDGMENTS.....	vii
TABLE OF CONTENTS.....	viii
LIST OF TABLES.....	xi
LIST OF FIGURES	xiii
CHAPTER	
1. INTRODUCTION	1
1.1 Background and Motivation.....	1
1.2 Objective of the Study.....	2
1.3 Scope	3
2. LITERATURE REVIEW.....	4
2.1 Reactivated Landslides.....	4
2.2 Shear Strength Parameters.....	5
2.2.1 Drained Shear Strength	5
2.2.2 Drained Residual Shear Strength.....	7
2.3 Slow Landslides.....	10
2.3.1 General Information.....	10
2.3.2 Landslide Classifications.....	13
2.3.2.1 Morphology Classification	13
2.3.2.2 Intensity Classification	13
2.4 Rainfall-controlled Movement.....	14
2.4.1 Pore Pressures	14

2.4.2 Storm Response	17
2.4.3 Seasonal Response	19
2.5 General Considerations on Slope Stability Methods	20
2.6 Slope Monitoring	22
3. METHODOLOGY	27
3.1 Modeling Framework.....	27
3.2 Stability Analyses	29
3.3 Deformation Modeling	29
3.3.1 Finite Element Analysis	29
3.3.1.1 Material Models	30
3.3.1.2 Boundary Conditions.....	31
3.3.1.3 Initial Conditions.....	31
3.3.1.4 Calculation Type	31
3.3.2 Kinematic Analysis	32
4. ANALYSES OF LANDSLIDE CASE HISTORIES	33
4.1 Vallcebre Landslide	33
4.1.1 Overview	33
4.1.2 Monitoring Data.....	34
4.1.3 Stability Analyses	35
4.2 San Martino Landslide	43
4.2.1 Overview	43
4.2.2 Monitoring Data.....	43
4.2.3 Stability Analyses	44
4.3 Steinernase Landslide.....	48
4.3.1 Overview	48
4.3.2 Stability Analyses	49

4.4 Triesenberg Landslide	53
4.4.1 Overview	53
4.4.2 Stability Analyses	53
4.5 Babadag Landslide.....	57
4.5.1 Overview	57
4.5.2 Stability Analyses	58
4.6 Finite Element Analyses.....	64
4.7 Kinematic Analyses	70
5. DISCUSSION OF RESULTS	74
5.1 Results of Stability Analyses.....	74
5.2 Results of Deformation Analyses	83
5.3 Results of Kinematic Analyses.....	83
6. CONCLUSIONS	84
6.1 Conclusions	84
6.2 Future Work Recommendations	86
REFERENCES	88
APPENDICES	95
APPENDIX A.....	95
APPENDIX B.....	97

LIST OF TABLES

TABLES

Table 2.1 - Varnes classification system (after modifications) in terms of mode of slope failure (1978).....	13
Table 2.2 – Velocity Classification (IUGS 1995, Cruden and Varnes 1996)	14
Table 2.3 – Descriptions of methods of analysis (Pockoski and Duncan, 2000)	22
Table 4.1 - Shear strength parameters derived from different tests: Minimum strength measured in direct shear, ring shear and triaxial tests for fissured shale; minimum strength measured in direct shear for clayey siltstone and residual strength measured on a pre-existing shear surface in fissured shale (Corominas et al., 2005).....	38
Table 4.2 – Parameters used in kinematic analyses with correlation coefficients	71
Table 5.1 – Percent change in factor of safety for 10-fold change in velocity	76
Table 5.2 – Change in r_u for 10-fold change in velocity.....	81
Table 5.3 - Change of FS for 1 m rise in groundwater level.....	82
Table A.1 - General information about landslide cases	95
Table A.2 - Material properties of landslide cases	96
Table B.1 – Slope stability analyses input and results with corresponding velocities (Vallcebre).....	9797
Table B.2 – Slope stability analyses input and results with corresponding measured velocities (San Martino).....	9898
Table B.3 - Slope stability analyses input and results with corresponding measured velocities (Steinernase)	99
Table B.4 - Slope stability analyses input and results with corresponding measured velocities (Triesenberg).....	100

LIST OF FIGURES

FIGURES

Figure 2.1 – Different stages of slope movements (Leroueil, 2001)	4
Figure 2.2 - a) general description of intact, fully softened and residual shear strengths b) intact, fully softened and residual shear strengths of London clay (Mesri and Shahien, 2003)	6
Figure 2.3 - Secant residual friction angle relationships with liquid limit, clay-size fraction, and effective normal stress (Stark et al., 2005)	8
Figure 2.4 - Empirical information on fully softened strength and residual strength (Mesri and Shahien 2003).	9
Figure 2.5 - (a) slickensided shear surface within the fissured shale in Vallcebre slide in Spain (Corominas et al. 2005), (b) distinct shear surface observed in Lexington apartments slide, in Nashville, Tennessee, reactivated in 2003 (courtesy of Mr. John Wolosick of Hayward Baker Inc.).....	11
Figure 2.6 – Relative factor of safety versus velocity for (a) earthflow cases, (b) debris slide cases (Bonnard and Glastonbury, 2005).....	12
Figure 2.7 – Relation between storm response and rainfall for Uxbridge, near the Mam Tor landslide in England (Skempton et al., 1989).....	18
Figure 2.8 – Typical slice and forces for method of slices (USACE, 2003).....	21
Figure 2.9 – Standard inclinometer arrangement (Mikkelsen, 1996).....	24
Figure 2.10 – Percentages of different methods of displacement measurement (Mansour et al., 2010).....	25
Figure 2.11 – Displacements measured by inclinometers (a) at the San Martino landslide (Bertini et al., 1984), (b) at Triesenberg landslide (Francois et al. 2007)	26
Figure 3.1 - Schematization to model the kinematic reponse of landslides to rainfall (Leroueil, 2001 and Calvello et al, 2008)	27
Figure 3.2 – A part of the procedure followed before and after stability analyses	28

Figure 4.1- Cross-section of the Vallcebre landslide - without vertical exaggeration (Reproduced from the cross-section A-A' by Corominas et al., 2005)	34
Figure 4.2 – Piezometric data and landslide velocity at S2 (Corominas et al., 2005)	35
Figure 4.3 – Shear stress envelopes for the Vallcebre landslide	37
Figure 4.4 – Output of limit equilibrium slope stability analysis for Vallcebre landslide with the piezometric condition P14 (see Appendix).....	39
Figure 4.5 – Relationships between relative factor of safety, groundwater level and pore pressure coefficient for the boreholes S2, S5 and S9 at the lower slide of the Vallcebre landslide.....	41
Figure 4.6 – Relation between relative factor of safety and the rate of movement (as observed at station S2) of the Vallcebre landslide	42
Figure 4.7 – Relation between pore pressure coefficient and slide velocity of Vallcebre landslide at S2.....	42
Figure 4.8 – Cross-section of San Martino landslide (Bertini et al., 1984)	43
Figure 4.9 – Piezometric level and displacement rate at station B (Bertini et al., 1984)	44
Figure 4.10 – Shear stress envelopes for the weathered zone of the marly clay bedrock. Solid lines represent the envelope obtained from Mesri and Shahien (2003) data (Huvaj-Sarihan, 2009).....	45
Figure 4.11 – Output of slope stability analysis for San Martino landslide with the piezometric condition P14 (see Appendix)	45
Figure 4.12 – Relationships between relative factor of safety, groundwater level and pore pressure coefficient for the boreholes B3 and C6 of the San Martino landslide	46
Figure 4.13 – Relation between the relative factor of safety and rate of movement (as observed at station B3) of the San Martino landslide.....	47
Figure 4.14 - Relation between pore pressure coefficient and slide velocity of San Martino landslide at B3.....	47
Figure 4.15 – Cross-section of Steinernase landslide (Reproduced from Laloui et al., 2008)	48
Figure 4.16 - Output of slope stability analysis for Steinernase landslide with the piezometric condition P3 (see Appendix).....	50

Figure 4.17 - Relation between the depth of groundwater level from the ground surface (as measured at two piezometric locations), relative factor of safety and pore pressure coefficient of the Steinernase landslide.....	51
Figure 4.18 - Relation between the relative factor of safety and rate of movement (as observed at station B3C) of the Steinernase landslide.....	52
Figure 4.19 – Relation between pore pressure coefficient and slide velocity of Steinernase landslide at B3C.....	52
Figure 4.20 – Cross-section of Triesenberg landslide (no vertical exaggeration) (modified from François et al., 2007).....	53
Figure 4.21 - Output of slope stability analysis for Triesenberg landslide with the piezometric condition P10 (see Appendix).....	54
Figure 4.22 - Relation between the depth of groundwater level from the ground surface (as measured at B8) and the relative factor of safety of the Triesenberg landslide	55
Figure 4.23 - Relation between the factor of safety and rate of movement (as observed at station B) of the Triesenberg landslide.....	56
Figure 4.24 – Relation between pore pressure coefficient and slide velocity of Triesenberg landslide at B.....	56
Figure 4.25 – Cross-section of Babadag landslide (Cevik and Ulusay, 2005).....	57
Figure 4.26 – Approximate boundaries of the main sliding body of Babadag (February 2011).....	58
Figure 4.27 - Direct shear test results for 0.035 mm/min shearing rate (modified from Cevik, 2003).....	60
Figure 4.28 – Shear stress envelope for the Babadag landslide	60
Figure 4.29 - A view from the landslide showing main sliding body and its components.....	62
Figure 4.30 – Relation between relative factor of safety and pore pressure coefficient of Babadag landslide.....	63
Figure 4.31 – Relation between slide velocity and pore pressure coefficient of Babadag landslide.....	64
Figure 4.32 – Total displacements (as shading) of simplified San Martino landslide model at time P3	66

Figure 4.33 – Total displacements (as arrows) of simplified San Martino landslide model at time P3	67
Figure 4.34 – Deformation analyses results of San Martino landslide	68
Figure 4.35 – Deformation analyses results of Vallcebre landslide	68
Figure 4.36 – Deformation analyses results of Steinernase landslide	69
Figure 4.37 - Nonlinear empirical relationship between relative factor of safety and rate of displacement for (a) Triesenberg, (b) Vallcebre, (c) San Martino, (d) Steinernase landslides	71
Figure 4.38 – Results of kinematic analysis for Triesenberg landslide	72
Figure 4.39 - Results of kinematic analysis for Vallcebre landslide	72
Figure 4.40 - Results of kinematic analysis for San Martino landslide	73
Figure 4.41 - Results of kinematic analysis for Steinernase landslide	73
Figure 5.1 - Relative factor of safety against slide velocity of the four selected landslides in this study (shown by black symbols) in comparison with results of other slides reported by Bonnard and Glastonbury (2005)	75
Figure 5.2 – Relation between landslide velocity and pore pressure coefficient r_u of selected cases	79
Figure 5.3 – Relation between landslide velocity and pore pressure coefficient r_u of selected cases with mudslide cases of Bonnard and Glastonbury (2005)	80

CHAPTER 1

INTRODUCTION

1.1 Background and Motivation

Landslides are one of the main disasters to cause damage in the world. According to the World Disaster Report (2009) due to wet mass movements, 7410 people are reported as killed between the years of 1999 and 2008. In this time interval the total amount of their estimated direct damage exceeded 2 billion US dollars. In Turkey, 45% of disasters are results of slope movements, having the second place after earthquakes in terms of affected people (Gökçe et al., 2008).

All types of slope movement may cause considerable damage to property and life in all around the world. However, unlike rapid movements, slow movements are not expected to typically cause life loss if proper precautions like evacuation and/or stabilization of the slope are taken. Slow landslides can severely damage structures, interrupt the serviceability of lifelines such as highways, railways and pipelines. According to the U.S. Transportation Research Board, in the United States, annual costs for the repair of minor slope failures by state departments of transportation is more than \$100 million. Similarly, the Canadian railway industry deals with reactivated slow-moving earth slides since 1800's, especially in the Thompson River Valley at which slides typically move with rates of 2 - 10 cm per year, and railways require continuous maintenance work associated with these movements (Eshraghian, 2007). Mansour et al. (2010) describe that "the vulnerability of these facilities to slow moving slides has sometimes been underestimated, although the velocity of some classes of slow slides is uncontrollable". For example, in Turkey, at Babadag district of Denizli, villagers suffered about 60 years from a slow moving, deep-seated

landslide with rates of 4 to 15 cm/year. It did not cause loss of life; but it caused buildings to tilt, structures to settle and crack significantly, in addition to damage in the roads, pipelines and other infrastructure that required continuous repair and replacement over the years. In fact, the major part of allocation of resources of the local municipality for decades was the repair cost of village roads at the crown of the slow-moving Babadag slide.

Slow moving landslides are typically deep landslides (>5 m thickness) occurring in cohesive soils, especially in stiff clays and clay shales, and moving along a distinct basal shear surface. These landslides show seasonal variations in their rate of movement depending on the rainfall/snowmelt-caused increase in the pore water pressure acting on the failure surface. They are referred to as “active” or “reactivated” landslides, displaying displacement rates in “extremely slow” and “very slow” category (<1.6 m/year) according to Cruden and Varnes (1996) rate of movement classification. When pore water pressure increases, the shear resistance along the basal shear surface decreases, and movement rate of the sliding mass increases. In this study, simplified relations between the pore water pressure in the ground and movement rates will be investigated. Such relations could be useful in dealing with slow moving landslides. Because, slow moving large masses are typically environmentally and economically not feasible to stabilize and for many legislative, economic and cultural reasons permanent evacuation may not be a choice. In this context, establishment of early warning systems and alarm levels for increasing rate of movements could be a reasonable solution for living with slow moving landslides.

1.2 Objective of the Study

In recent years, some researchers have suggested linear or nonlinear relations between the factor of safety, movement rate and pore pressures for slow moving landslides (Glastonbury and Fell 2002, Bonnard and Glastonbury 2005, Corominas et al. 2005, Eshraghian et al. 2008, Laloui et al. 2008).

The objective of this study is to explore the relations between pore water pressure, factor of safety and rate of movement in slow-moving reactivated landslides in cohesive soils. Such relations can be useful (1) to understand the significance of a possible error in the pore water pressures, on the calculated factor of safety of the slope (as it was noted by Bishop in 1955), (2) in classifying slow moving reactivated landslides in terms of their sensitivity, which may help in prioritization of allocation of money and resources in monitoring and early warning works for more critical slopes, (3) in early warning systems to predict the time of hazardous movements, (4) in planning required level of remediation and risk mitigation, for example, to decide on how many meters the ground water level should be lowered at a certain piezometric measurement location, so that the stability increases to a desired level of F.S., and movement rates are reduced to an acceptable slow rate.

1.3 Scope

The scope of this thesis is to cover the intermediate steps to lead further development of an ideal early warning system. The selected landslide cases in this study are all translational or roto-translational active slow moving landslides. Reactivations of the landslides are due to changes in hydraulic boundary conditions. The common features of the landslides is thought to serve to a better local understanding of the intermediate relationships that are mentioned above. The steps include 2-D limit equilibrium slope stability analyses under different groundwater conditions, deformation analyses and kinematic analyses to compute velocities from pore pressures. Through these steps relationships between factor of safety and groundwater levels, relative factor of safety and rate of movements, pore pressures and rate of movements are formed.

The thesis is divided into 6 Chapters. Chapter 2 gives an overview of the literature on this topic. Chapter 3 introduces the methodology of analyses. Chapter 4 encloses analyses of landslide case histories and Chapter 5 discusses the results and Chapter 6 gives conclusions.

CHAPTER 2

LITERATURE REVIEW

2.1 Reactivated Landslides

Different stages of slope movements are considered by Vaunat et al. (1994) and Leroueil et al. (1996). The reactivation stage include occasional reactivation and active landslide phases (Figure 2.1) which occur interchangeably during a time interval.

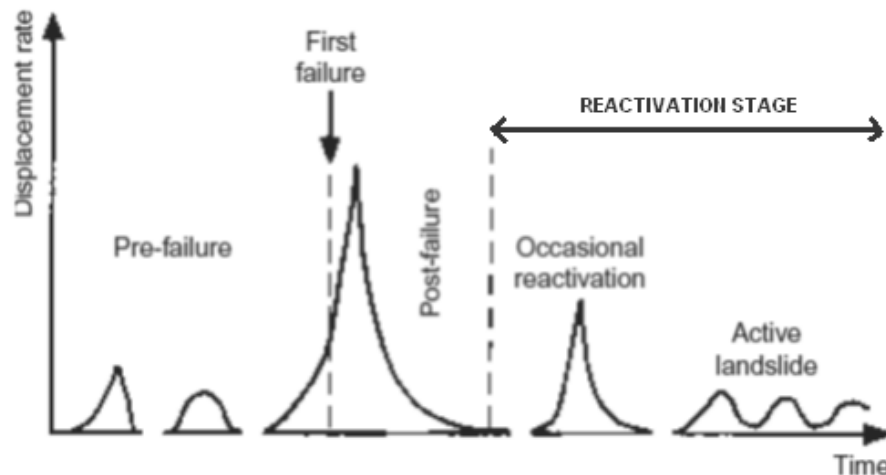


Figure 2.1 – Different stages of slope movements (Leroueil, 2001)

According to Brooker and Peck (1993) a reactivated slide is a landslide in which the shearing resistance on the failure surface is everywhere reduced to the residual strength. In reactivated landslides the entire landslide mass has already experienced some level of movement and has been separated from the stable ground by a slip surface that has reached the residual condition. Therefore, a shear strength equal to

the residual shear strength is available on the preexisting shear surface of old landslides as it was proposed by Skempton in 1964.

Reactivation of a landslide may be due to many triggering forces acting on a pre-sheared surface. In this study, since translational or roto-translational landslides are selected as case studies, driving forces do not change drastically with time. The stability is mainly controlled by the shear resistance of the soil in the shear plane, which is controlled by the changing pore water pressures. It can be well observed that the selected slow moving landslides are reactivated by a critical accumulation of subsurface water.

2.2 Shear Strength Parameters

2.2.1 Drained Shear Strength

In any slope stability analyses, the choice of appropriate shear strength parameters possess a great role among others like the geometry of the slope, initial loading conditions, boundary conditions and other material parameters. There are two types of shear strength; the undrained shear strength to be used in total stress analysis and the drained shear strength to be used in effective stress analysis.

As mentioned in the preceding section, in reactivated landslides the shear strength mobilized in the field is the residual shear strength of the material in the shear zone. In order to review the drained shear strength characteristics of overconsolidated clays, a typical shear stress-displacement curve of an intact sample is illustrated in Figure 2.2 (a). As also stated by Skempton (1985), after peak strength, a “fully softened” condition is attained at relatively small displacements due to an increase in water content. This decrease in strength is caused by the opening of joints and fissures in the stiff clay, and related dilation, increase in water content and softening. A “fully softened strength” is defined when the volumetric strain levels off. If we

continue to shear the material, shearing strains become concentrated in a thin shear zone, and the shearing resistance continues to decrease until finally a residual strength is reached. The loss in strength between the fully softened and residual strengths is caused primarily by the orientation of the platy clay particles parallel to the direction of shearing. The drop of shear strength from intact to fully softened and residual conditions are shown in Figure 2.2 (b) at which Mesri and Shahien (2003) used data from triaxial compression, direct shear, and ring shear tests in London clay. A noticeable curvature of shear strength envelope is seen at the intact strength envelope since swelling and softening is more pronounced as effective normal stress decreases toward zero. It can be seen in Figure 2.2 (b) that the relationship between shear strength and effective normal stress is curved (for the intact, fully softened and residual conditions) and there is no shear strength at zero effective normal stress.

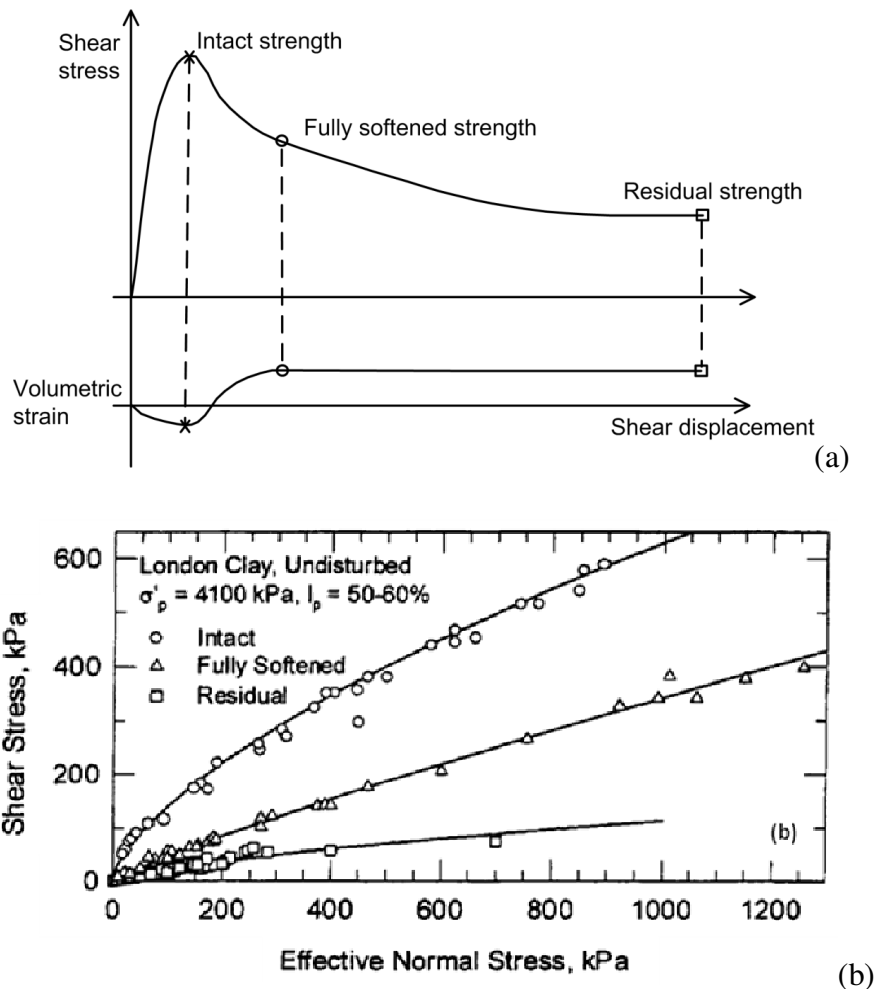


Figure 2.2 - a) general description of intact, fully softened and residual shear strengths b) intact, fully softened and residual shear strengths of London clay (Mesri and Shahien, 2003)

2.2.2 Drained Residual Shear Strength

A drained failure condition due to drained shear strength is usually valid during reactivation of pre-sheared slip surface that has reached a residual shear strength condition (Stark et al., 2005). As early as in 1964, by Skempton, it was noted that drained residual strength of stiff clays is mainly related to the type of clay mineral, quantity of clay-size particles and the alignment of particles along a shear plane. Therefore, correlations between some index properties of stiff clays and the residual shear strength could be expected (Lupini et al. 1981; Skempton 1985; Stark and Eid 1996, Mesri and Shahien 2003). The liquid limit indicates clay mineralogy, whereas the clay-size fraction indicates quantity of particles smaller than 0.002 mm. Hence, when the liquid limit and clay-size fraction are increased, the drained residual strength decreases.

On the other hand Mesri and Shahien (2003) suggest that “residual conditions may also be present on part of the slip surface of first-time natural or excavated slopes failures in stiff clays and clay shales”. In fact, they claim that intact, fully softened and residual conditions may be mobilized along different elements on the slip surface of a first-time slope failure. Picarelli et al. (2006) contribute with a conclusion that “the operative strength in first-time slides in overconsolidated clay is often less than the peak bulk strength measured in the laboratory”. The reason to this phenomena is not well described by any, but it is mostly believed that swelling due to stress decrease rules a reduction of the peak shear strength (Picarelli et al., 2006).

As Skempton (1985) indicated, field residual strength can be obtained by multiple reversal shear box tests on intact or on cut-plane samples. Besides Stark and Eid (1993) have suggested the modified Bromhead ring shear apparatus to measure the residual and fully softened strengths, which was than used by researchers as Stark et al. (2005). The change of secant residual friction angle with respect to liquid limit, clay-size fraction and effective normal stress is given in Figure 2.3, where the data was obtained from ring shear tests carried out by Bromhead ring shear device.

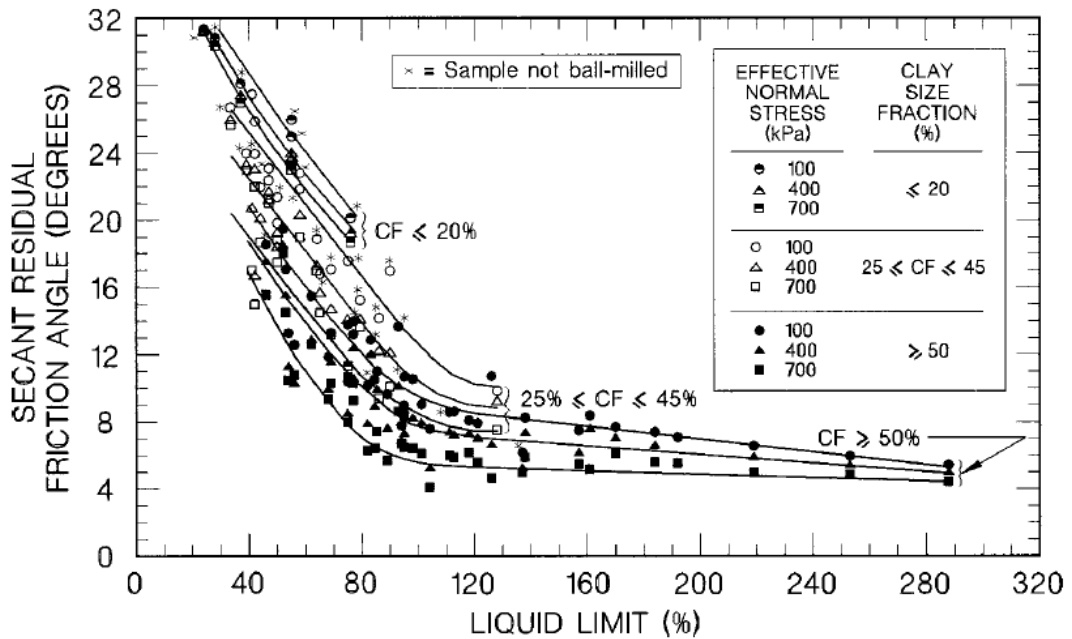


Figure 2.3 - Secant residual friction angle relationships with liquid limit, clay-size fraction, and effective normal stress (Stark et al., 2005)

Mesri and Shahien (2003) proposed that a correlation between residual shear strength and liquid limit or plasticity index is expected because residual shear strength is controlled by the fundamental factors of particle size and plateyness. They represented the curved shear strength envelope in terms of secant friction angle, which decreases as the effective normal stress increases. Based on extensive data from direct shear and ring shear tests on various natural stiff clays and shales, they proposed the relations shown in Figure 2.4. In the absence of site-specific laboratory residual shear strength tests, these relations can be used to estimate shear strength for stability analysis. However, Mesri and Shahien (2003) noted that such empirical correlations are not applicable to clays or shales that are composed of clay minerals that are not plate-shaped, or are exceptionally aggregated. It has been noted in the recent literature that, sample preparation procedure may have a significant effect on Atterberg limits and complete disaggregation of Atterberg limit samples is especially required for the correlations between residual friction angle and liquid limit or plasticity index, as clay minerals also disaggregate in the shear zones in the field (Stark and Eid 2005).

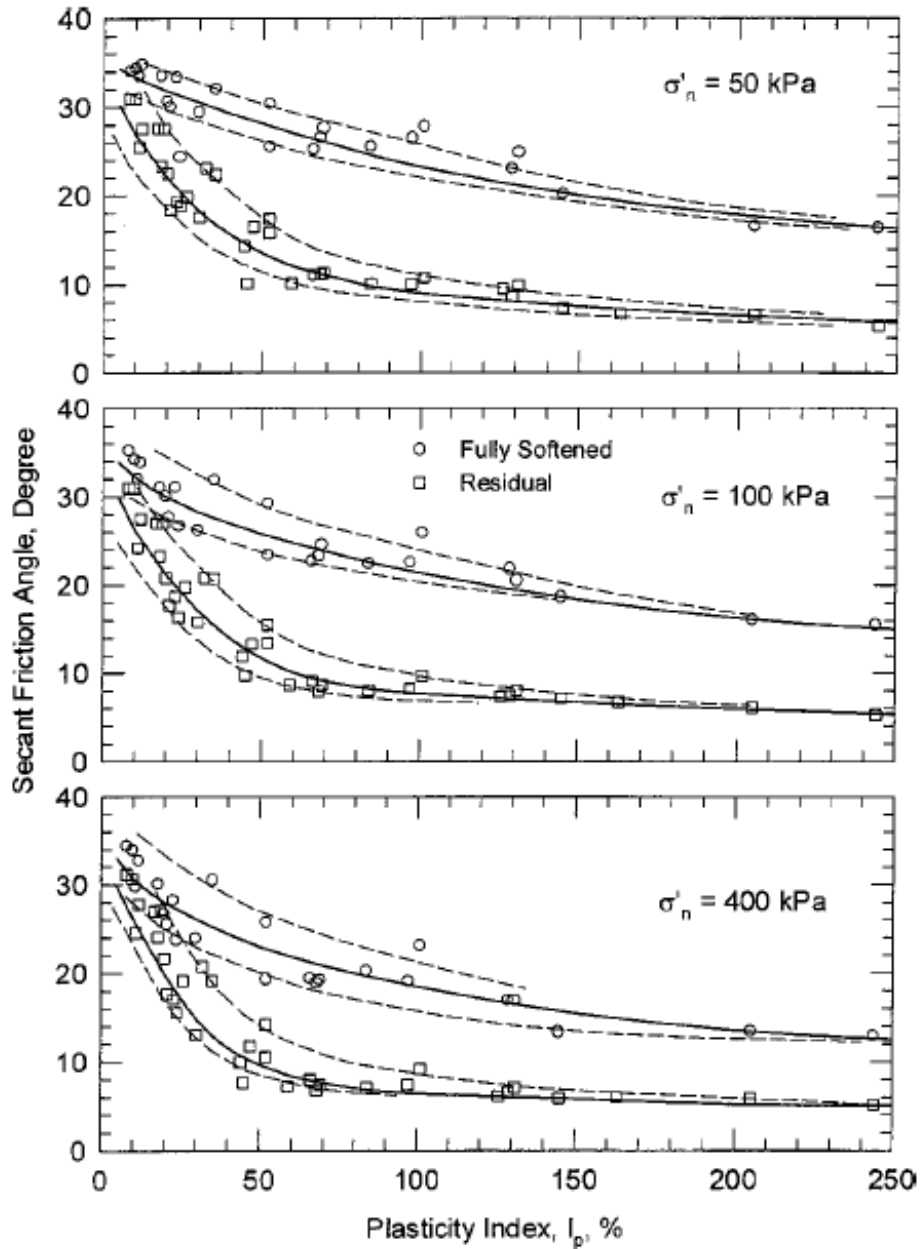


Figure 2.4 - Empirical information on fully softened strength and residual strength (Mesri and Shahien 2003).

In this thesis, residual shear strength values are either back-calculated from reactivated landslides using the pore pressures at the time of failure or derived from laboratory direct shear test measurements, if exist and checked with the Mesri and Shahien (2003) range of values.

2.3 Slow Landslides

2.3.1 General Information

Common features of slow landslides are listed by Bonnard and Glastonbury (2005). In general, slow landslides

- (i) have pre-sheared basal surfaces of rupture, typically having completely developed shear zones showing a line of discontinuity in the profile view (Figure 2.5);
- (ii) have translational movement with little or no internal deformation, generally along a basal shear surface as a rigid body. For example, for the mudslides studied by Glastonbury and Fell (2008), about 80% of the movement observed at the ground surface was taking place along a basal rupture surface;
- (iii) can be shallow or deep-seated, “slide” type reactivated landslides;
- (iv) are common in fine grained soils, especially in stiff clays and shales; and
- (v) slide movement is mostly controlled by fluctuations in pore water pressures. However, the degree of sensitivity to pore water pressure fluctuations is varying between different slides. Glastonbury and Fell (2008) observed that the sensitivity to groundwater level changes may be linked to the “difference between rupture surface inclination and basal friction angle”. The slide is more sensitive when the difference is greater than zero.



(a)



(b)

Figure 2.5 - (a) slickensided shear surface within the fissured shale in Vallcebre slide in Spain (Corominas et al. 2005), (b) distinct shear surface observed in Lexington apartments slide, in Nashville, Tennessee, reactivated in 2003 (courtesy of Mr. John Wolosick of Hayward Baker Inc.)

The visualization of sensitivity to the changes in pore water pressure is reached by plotting relative factor of safety from slope stability analyses against slide velocity in logarithmic scale. Glastonbury and Fell (2002) have conducted infinite slope stability analyses on several selected cases to calculate the safety factors and normalized the factors by introducing “the relative factor of safety” concept. In the concept of relative factor of safety, the least stable condition of slow moving active landslides is considered to represent a relative factor of safety of unity. The rest of the conditions are normalized against this condition. This concept is adopted in this study but instead of the infinite slope analysis, method of slices is used in calculating the safety factors.

Glastonbury (2002) noted that three mudslide cases, La Chenaula, Alvera and Earthflow 2, showed relatively high sensitivity to groundwater fluctuations with 1 to 3% decrease in relative factor of safety causing 10-fold increase in rate of movements (Figure 2.6). Two other mudslides, Alani Paty and La Mure show relatively less sensitivity to groundwater fluctuations: a change in F.S. of 5% and 16.3% were required for a 10-fold change in the velocity. Glastonbury (2002) also noted that faster moving slides appear to be less sensitive to fluctuations in groundwater levels.

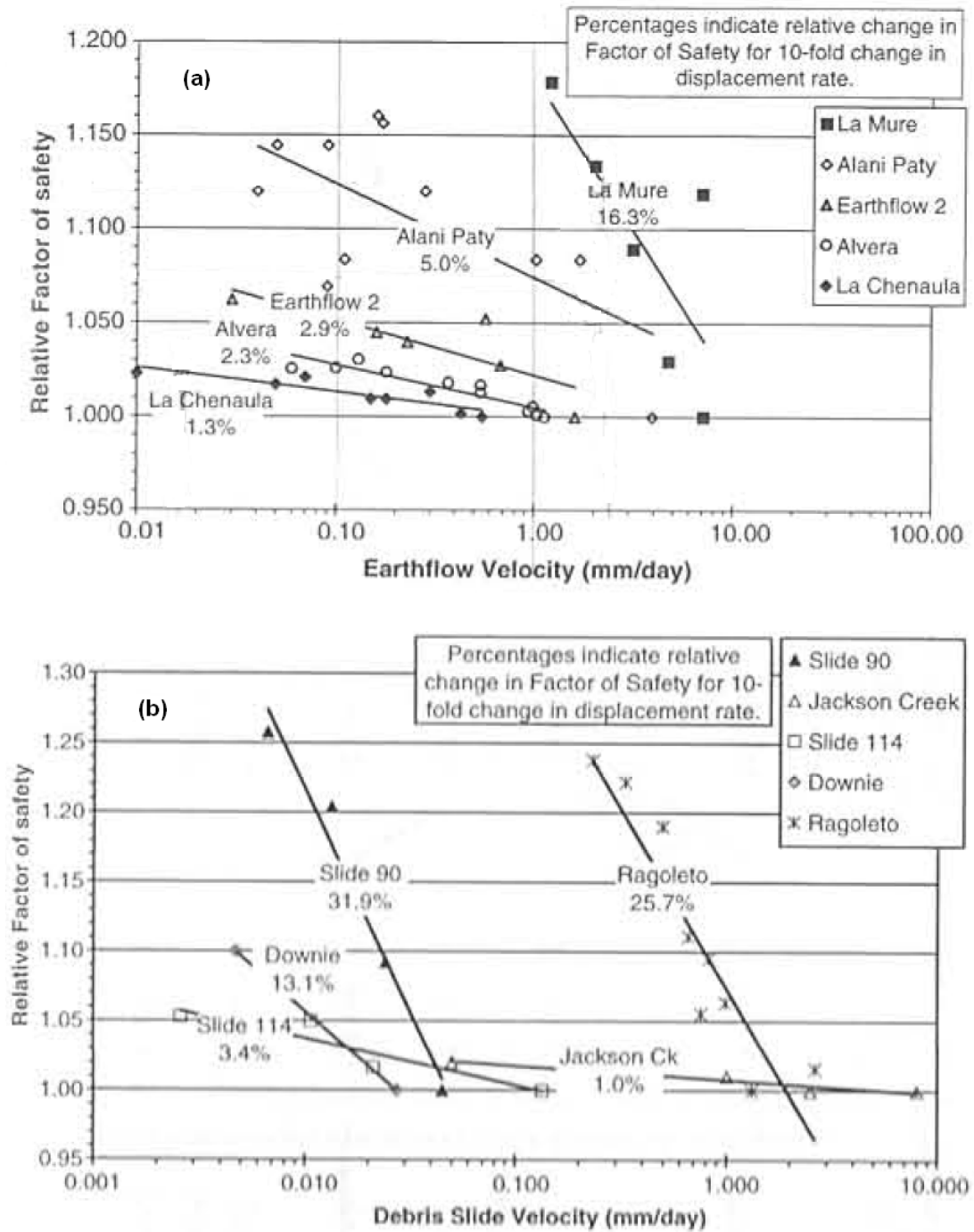


Figure 2.6 – Relative factor of safety versus velocity for (a) earthflow cases, (b) debris slide cases (Bonnard and Glastonbury, 2005)

The relation between rate of movement, F.S. and piezometric level essentially depends on the shear stress level (Vulliet and Hutter 1988; Leroueil et al. 1996). For about 0.10 increase in the F.S. (a 10% increase), the rate of movements were suggested to decrease by about 10-times (Energren and Imrie 1996; McFarlane and

Jenks 1996; Leroueil 2001). Leroueil (2001) noted that typically, when the factor of safety is increased by about 5%, the rate of displacement decreases by two orders of magnitude.

2.3.2 Landslide Classifications

2.3.2.1 Morphology Classification

A common classification of slope instabilities considers the morphology of the moving mass. Varnes (1978) classification with modifications of Cruden and Varnes (1996) involves basically the type of movement and the type of material; and divides slope instabilities into 21 different classes (Table 2.1). The landslide cases in this study fall into the classes marked as bold at Table 2.1.

Table 2.1 - Varnes classification system (after modifications) in terms of mode of slope failure (1978)

TYPE OF MOVEMENT			TYPE OF MATERIAL		
			ENGINEERING SOILS		BEDROCK
			Predominantly fine	Predominantly coarse	
Falls			Earth fall	Debris fall	Rock fall
Topples			Earth topple	Debris topple	Rock topple
Slides	Rotational	Few units	Earth slump	Debris slump	Rock slump
			Earth block slide	Debris block slide	Rock block slide
	Translational	Many units	Earth slide	Debris slide	Rock slide
			Lateral Spreads	Earth spread	Debris spread
Flows			Earth flow (soil creep)	Debris flow	Rock flow (deep creep)
Complex			Combination of two or more principal types of movements		

2.3.2.2 Intensity Classification

There are various suggestions to classify a landslide considering its intensity. The bulk volume of the sliding body, movement rate or possible/observed damage of the

landslide can be considered relatedly. According to Calvello et al. (2009) “the maximum movement velocity” is the most accepted parameter of intensity among others. The well-known classification is suggested by IUGS (1995) and Cruden and Varnes (1996) which is based on the maximum movement velocity just after failure (Table 2.2). Due to its convenience this classification is referred throughout this thesis every time when the velocity of a landslide is described. The landslides considered in this thesis are in the “very slow” and “extremely slow” moving landslide category. They will be referred to as “slow moving landslides” in the rest of this thesis.

Table 2.2 – Velocity Classification (IUGS 1995, Cruden and Varnes 1996)

Velocity Class	Velocity Description	Typical Velocity Limits	in mm/day
7	Extremely rapid	> 5 m/s	> 4.3×10^8
6	Very rapid	3 m/min – 5 m/s	4.3×10^6 – 4.3×10^8
5	Rapid	1.8 m/hr – 3 m/min	4.3×10^4 – 4.3×10^6
4	Moderate	13 m/mo – 1.8 m/hr	433 – 4.3×10^4
3	Slow	1.6 m/yr – 13 m/mo	4 – 433
2	Very slow	16 mm/yr – 1.6 m/yr	4.4×10^{-2} – 4
1	Extremely slow	< 16 mm/yr	< 4.4×10^{-2}

2.4 Rainfall-controlled Movement

According to a recently published technical note of Mansour et al. (2010) 64% of studied landslides are triggered by rainfall which is followed by stream incision with 23%. Anthropogenic activities, reservoir filling and fluctuations, mining activities, snow melt and earthquakes are other main triggering factors with decreasing order having percentages of less than 20.

2.4.1 Pore Pressures

Positive pore water pressure (to be called as “pore pressure” at the rest of this thesis) below the groundwater table reduces the available shear strength along the sliding

surface by reducing effective stress. Hence slope stability decreases if pore pressure increases.

The response of pore pressure to rainfall events may be rapid or gradual. The degree of pore pressure increase at a slope depend on intensity of rainfall, runoff, infiltration and evapotranspiration related to the properties of slope surface and materials composing the slope, for example, the unsaturated and saturated permeability of the soil. More specifically, rapid response of pore pressure to rainfall is due to preferential pathways of infiltrating water to the depths like fissures or cracks made by previous landslides (Van Asch and Buma, 1996; Matsuura et al., 2008). In a case described by Corsini et al. (2005), “while the movement on the deeper sliding surface has been practically continuous before and after the water table rise, the movement on the shallower sliding surfaces has been more influenced by smaller water table fluctuations related to precipitation pattern.”

Rapid increase of pore pressure and consequently groundwater level, however, usually occur after heavy rainfall exceeding a certain threshold in a certain time interval which are found for many cases. This type of response is the case of storm response which is explained in Section 2.4.2.

In the analysis of slow moving landslides, pore pressure fluctuations, either rapid or gradual, are important. Since the displacements of slow, very slow and extremely slow moving landslides are intermittent, fluctuations in groundwater levels determine the stability condition of them. Moreover if a slide is already moving, increase in pore pressure cause to accelerate and decrease in pore pressure cause to decelerate until the movement stops. In some cases, movements do not stop even factor of safety is greater than the unity. For example, Fell et al. (2000) presented data from Salledes slide in France, and indicated that even when the factor of safety was 1.1, movements were occurring with rates up to 1 mm/day. Eshraghian (2007) noted, based on movement records of the slides in the Ashcroft area in Canada, that

extremely slow reactivation of movement started when the F.S. approached 1.1 or less.

In recent years, some researchers have suggested linear or nonlinear relations between the movement rate and pore pressures on the pre-existing shear surfaces (Glastonbury and Fell 2002, Bonnard and Glastonbury 2005, Huvaj-Sarihan 2009). Calvello et al. (2008) summarized the models in two categories, namely, phenomenological models and physically based models. Phenomenological models include empirical relationships between soil movements and triggering factors whereas physically based models concern the mechanical behaviour of the soil.

Corominas et al. (2005) suggested a model to predict both landslide displacements and velocities at Vallcebre landslide with a viscous term added in the momentum equation. It is shown that, using similar rheological parameters for the entire landslide, displacements are accurately calculated. The Authors reported a non-linear relationship between pore pressure and velocity.

Laloui et al. (2008) used coupled finite element hydrogeological and geomechanical models to analyse the behaviour of Steinernase landslide. The model was applied to reproduce the mechanism and behavior under different event possibilities.

In this thesis, pore pressures are incorporated and represented by the pore pressure ratio, r_u , which is defined as

$$r_u = \frac{u}{\gamma * h} \quad \text{Eq.2.1}$$

where u = pore pressure, γ = unit weight and h = thickness of the slide.

The pore pressure ratio correlates the pore pressure with the total pressure at any point on the slide.

Eshraghian et al. (2008) showed a nonlinear correlation between the movement rate and the average pore pressure ratio, r_u , on the rupture surface of a slide in Canada. A nonlinear relationship between the rate of movement and the F.S. was suggested by Vulliet and Hutter (1988).

Bishop (1955) noted that “It is useful from the design point of view to know the influence of possible variations in construction pore pressure on the factor of safety, and for this purpose the factor of safety may be plotted directly against average pore pressure ratio”. Understanding the sensitivity of a slope to changes in pore water pressure is also useful in order to quantify the significance of the error in the pore water pressures used in the slope stability analyses. This was pointed out by Bishop (1955), as well as by Yucemen & Tang (1975) in their study of evaluation of uncertainties in the long term stability of soil slopes.

2.4.2 Storm Response

Skempton et al. (1989) described a slow; ancient but still active; landslide at Mam Tor in the North Derbyshire of United Kingdom. This was one of the first landslide cases investigated through detailed observations. Although this landslide was known to be moving for about a century, published data related to rainfall, piezometric levels and displacements go back to 1965 and followed in the last decade by many researchers as Waltham and Dixon (2000), Rutter et al. (2003), Walstra et al. (2004), Dixon and Brook (2006) and Walstra et al. (2007).

Skempton et al. (1989) differentiate storm response with so-called seasonal response by defining the movement owing to storm response as “the movement caused by a transient rise in piezometric level Δh above the level corresponding to a state of

limiting equilibrium (F.S = 1.0) with the static residual strength". Thus storm response is accepted as the ratio between groundwater level change and rainfall magnitude, $\Delta h/R$, i.e. increase in groundwater level, Δh , is approximately directly proportional to the rainfall amount, R . The range of the storm response is given as between 1 and 18, generally restricted between 4 and 6 (Figure 2.7).

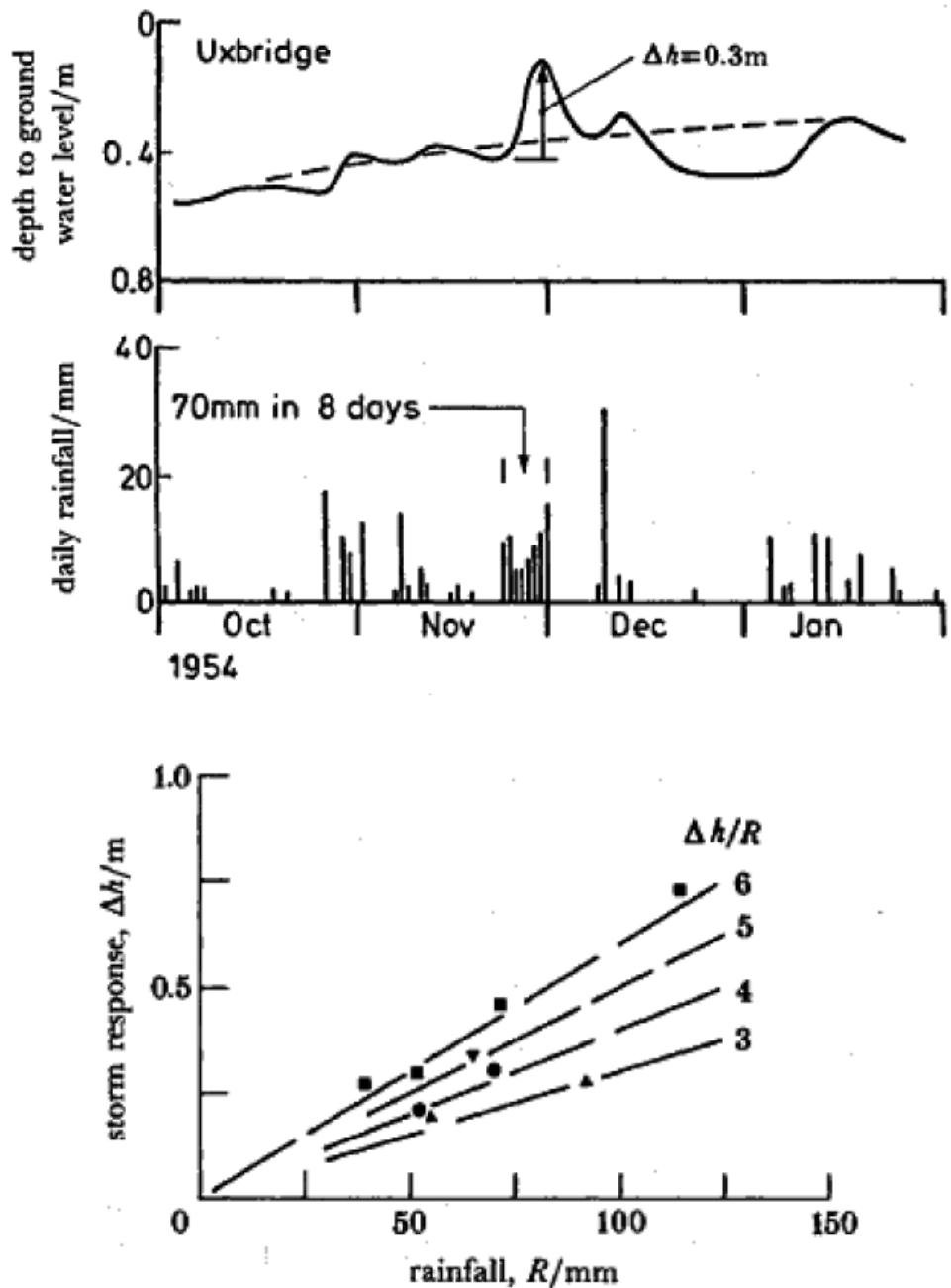


Figure 2.7 – Relation between storm response and rainfall for Uxbridge, near the Mam Tor landslide in England (Skempton et al., 1989)

Glastonbury and Fell (2002) claimed that slide cases with high silt, sand and gravel fractions like La Mure and Alani Paty slides display greater storm response values than those cases with lower coarse fractions. Furthermore slides with high storm response values show faster induction process. If the storm response $\Delta h/R$ of certain materials can be known, at least in a range, this could be a useful information for future early warning systems in slow moving landslides.

2.4.3 Seasonal Response

According to Mansour (2009) “the likely trigger of movement in slow moving earth slides of moderate thickness is the seasonal changes in the boundary conditions that are almost affected by the hydrological variations over the year.”

Basically, if the landslide responds to long periods of high cumulative rainfall or effective infiltration, for example, to multiple storms during periods of several days or weeks, rather than single meteorological events (Corsini et al., 2005), seasonal response dominates. Matsuura et al. (2008) defined the concept of critical pore water pressure as “a certain pore water pressure threshold at which landslide displacement begins by loss of dynamic balance”.

Displacements continue through the rainy season and then cease when precipitation or infiltration inputs become sparse. Picarelli et al. (2004) investigated both first time and reactivated landslides that are triggered by rainfall and came to the opinion that slow and long-duration landslides in stiff clays and shales show intermittent movements due to seasonal fluctuations of piezometric levels, i.e. changes in pore water pressures. Such changes in boundary conditions lead to changes in the effective stresses and decrease the mobilized shear strength along shear surfaces.

Tacher et al. (2005) modeled the displacement behavior of the La Frasse landslide in Switzerland by making use of geomechanical simulations of changes in hydraulic conditions. It is suggested to consider the contribution of groundwater feeding by the geological bodies in the slide rather than infiltration, if the long-term movement component dominates.

The mobility of slow moving landslides are discussed by Van Asch et al. (2007) by compiling three case studies. An important observation is that at one of the cases the movement response to changes in groundwater level was not the same during a rise as compared to a fall in the piezometric level. This difference is explained by undrained conditions revealing during rapid changes in the stress field.

A rainfall triggering model is proposed by Montrasio et al. (2009) which defines a safety factor relevant to the seasonal rainfall for landslides, the stability of which are directly controlled by rainfall. This model takes into account the geometric characteristics of the slope, the geotechnical properties, and strength parameters of the soil. Montrasio et al. (2009) propose that knowing the seepage behavior of slopes, a seasonal factor of safety can be directly calculated without the need of calculation of pore pressures at the slip surface.

2.5 General Considerations on Slope Stability Methods

In limit equilibrium methods, the factor of safety is calculated using one or more of the equations of static equilibrium at the sliding mass. The sliding mass is bounded by a potential slip surface and the surface of the slope. In many limit equilibrium methods, the soil mass above the slip surface is divided into a finite number of vertical slices in order to handle static equilibrium. This approach is called method of slices. A slice in the sliding mass and forces acting on this slice are illustrated in Figure 2.8. The forces are:

W : slice weight

E : horizontal (normal) forces on the sides of the slice

X : vertical (shear) forces between slices

N : normal force on the bottom of the slice

S : shear force on the bottom of the slice

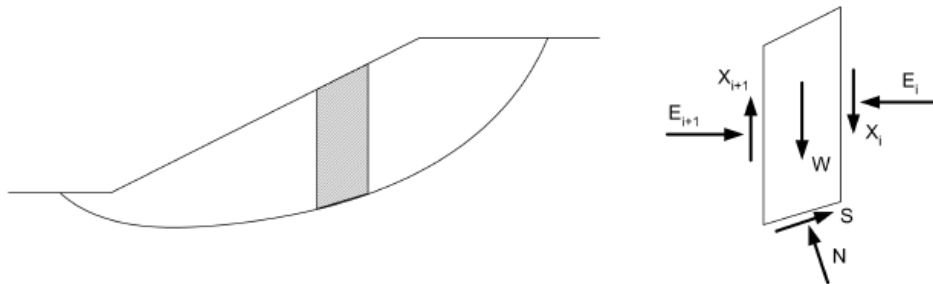


Figure 2.8 – Typical slice and forces for method of slices (USACE, 2003)

There are various methods proposed in the literature for limit equilibrium slope stability analyses. In different methods different assumptions, called as side force assumptions, are considered in order to overcome unknowns in equilibrium equations. Pockoski and Duncan (2000) reported comparisons between different methods, force-moment equilibrium and assumptions used in each method (Table 2.3).

Table 2.3 – Descriptions of methods of analysis (Pockoski and Duncan, 2000)

Method					Assumptions	Comments
	Overall Moment Equilibrium	Individual Slice Moment Equilibrium	Horizontal Force Equilibrium	Vertical Force Equilibrium		
Swedish Circle	Yes	No	No	No	Circular Slip Surface	Only for $\phi=0$
Ordinary Method of Slices (Fellenius 1927)	Yes	No	No	No	Circular Slip Surface Side Forces Parallel to Base	Conservative Very inaccurate for high pore water pressures
Bishop's Modified Method (Bishop 1955)	Yes	No	No	Yes	Circular Slip Surfaces Side Forces Horizontal	Very inaccurate for high pore water pressures
Morgenstern and Price's Method (Morganstern and Price 1965)	Yes	Yes	Yes	Yes	Slip surface of any shape Pattern of Side Force Orientations	Much engineering time required to vary side force assumptions.
Spencer's Method (Spencer 1967)	Yes	Yes	Yes	Yes	Slip surface of any shape Side Forces Parallel	Simplest Method
Corps of Engineers Modified Swedish (1970)	No	No	Yes	Yes	Slip surface of any shape Side Forces Parallel to Slope	High factor of safety
Lowe & Karafiath (1960)	No	No	Yes	Yes	Slip surface of any shape Side Force Orientations Average of Slope and Slip Surface	Best side force assumption
Janbu Simplified (Janbu 1954)	No	No	Yes	Yes	Slip surface of any shape Side Forces Horizontal	Low Factor of Safety
GLE - General Limit Equilibrium	Yes	Yes	Yes	Yes	Slip surface of any shape Pattern of Side Force Orientations	Much engineering time required to vary side force assumptions.
GoldNail Method* (Golder)	Yes	*	Yes	Yes	Slip surface of any shape Normal Stress Distribution	Toe circles only
SNAIL Method (CALTRANS)	No	No	Yes	Yes	Slip surface of any shape Two or three wedges, with side force angle = ϕ	Limited shapes of slip surfaces

Spencer's method takes into account all equilibrium types and solves any shape of slip surface by adopting a frictional center of rotation. Thus, in this study Spencer's method is selected to analyze translational or roto-translational landslides. In this method the interslice forces are assumed to have constant inclination throughout the slope.

2.6 Slope Monitoring

The most widely used monitoring devices in relation to landslide studies are inclinometers and piezometers. Inclinometers are typically installed at several different locations along the length of the slope, and they define the depth of the slip surface, the thickness of the shear zone, and the rate of movement. In addition, they indicate whether there is any internal deformation within the landslide body, allowing us to compare the movements at the ground and at the slip surface. Piezometers are widely used to measure the pore water pressure at a point, typically by a sensor located at the tip of the piezometer. There are various types of

inclinometers and piezometers, the details of which are beyond the scope of this thesis.

Models of landslides for the computation of landslide displacements from pore pressure data require accurate monitoring of landslides. Cascini et al. (2010) describe that the main limitation of this type of models is the lack of reliable measurements of pore pressures along slip surfaces. Although it is possible to monitor the global changes in the groundwater level, it is mostly difficult to set up piezometers on the slip surface. However all of the pore pressure data used in this study are at or very close to the sliding surfaces.

Aside from the location of the monitoring device, the measurement period is also important. The piezometer accurately measures the pore water pressure at the sensor (tip of the piezometer) over an extended time period; long-term slow landslides may be covered by regular measurements ranging from days or weeks to years and decades.

Instruments are needed to measure pore pressures as well as surface or subsurface displacements along the slope. The input data of this study is acquired by the measurements of devices including inclinometers (Figure 2.9), wire extensometers (Corominas et al., 2000), piezometers, EDMs and GPS networks.

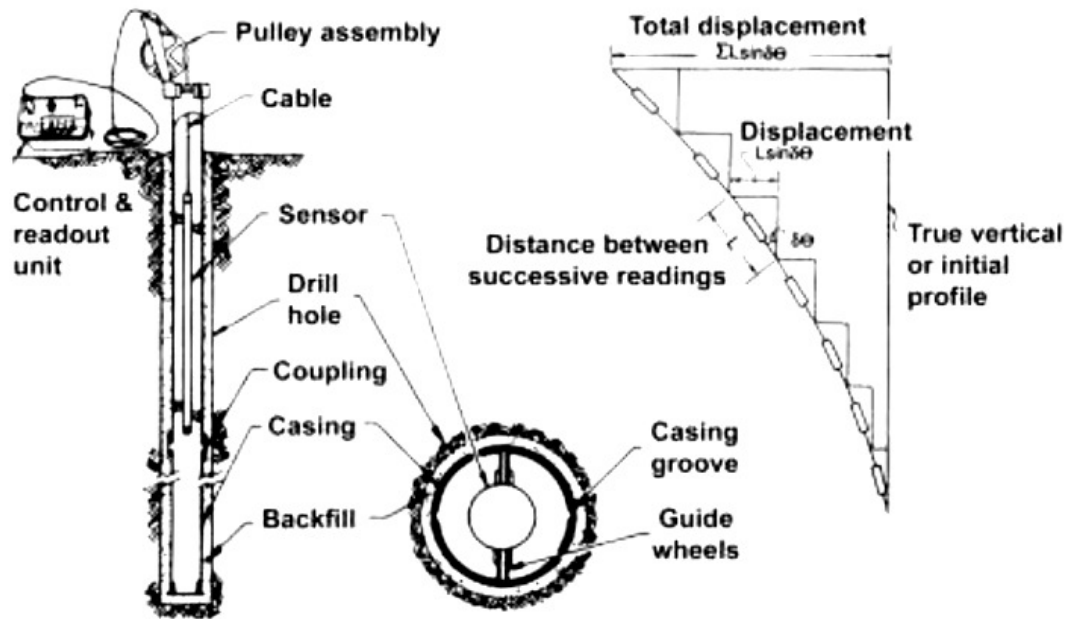


Figure 2.9 – Standard inclinometer arrangement (Mikkelsen, 1996)

On Figure 2.10 percentages of different displacement measurement methods are given at which about 50 slow moving landslides all around the world are compiled by Mansour et al. (2010). From the pie chart one can notice that inclinometers are still most widely used having over half of the percentages, which are followed by on-field surface surveying methods with about 30 %. On the other hand lately developed remote measurement techniques share the remaining percentages with extensometers and geomorphologic evidence. It should be noted that for some landslide cases more than one measurement method is used.

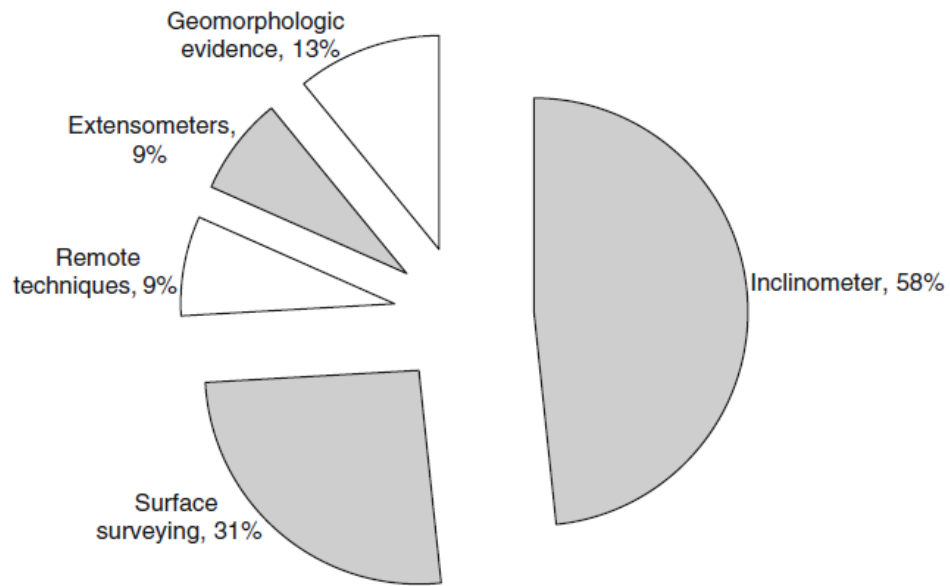
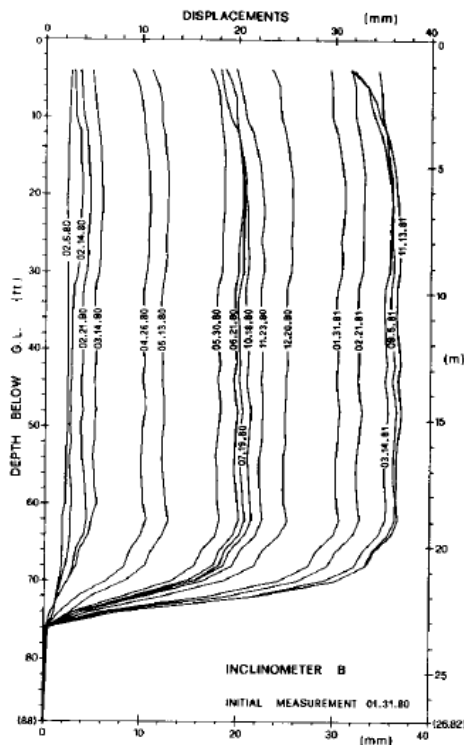
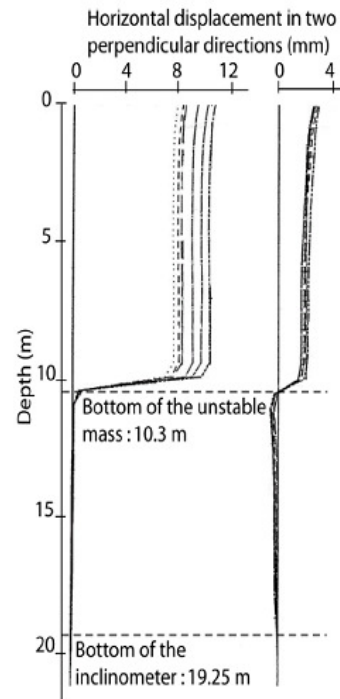


Figure 2.10 – Percentages of different methods of displacement measurement (Mansour et al., 2010)

Translational landslides are assumed to exhibit rigid block type movements which are well observed at the cases in this study. Figure 2.11 shows an example of movement data from the San Martino slide at two inclinometers at different locations on the slope. Here surface movements are almost equivalent to movements at the slip surface, such that they are representative of each other. As can be seen from this specific case, the thickness of the shear zone can also be determined by inclinometer results where displacements vary over a certain range for any certain inclinometer location at the bottom of the moving body. For example, for San Martino landslide the thickness of the shear zone seems to be about 1.5 m (5 ft) as can be seen from the inclinometer data in Figure 2.11.



(a)



(b)

Figure 2.11 – Displacements measured by inclinometers (a) at the San Martino landslide (Bertini et al., 1984), (b) at Triesenberg landslide (Francois et al. 2007)

The assumption of rigid block movement is practically useful since monitoring data on surface movements in landslides are more commonly available as compared to movements measured at the sliding surface, especially after the development of airborne SAR and LIDAR interferometry. Moreover, it allows more slow moving landslide case histories to be investigated, and possible early warning systems to be based on remote or on field surface movement measurements. Early warning studies based on the movements measured at the ground surface would typically be on the safe side. This is because, in general, the deformations observed at the ground surface in landslides are larger, instead of being smaller, than the movements in the shear zone.

CHAPTER 3

METHODOLOGY

3.1 Modeling Framework

The main framework to be followed in modeling is schematized by Leroueil (2001) and modified by Calvello et al. (2008) to relate different variables in the natural process of the landslide mechanism (Figure 3.1).

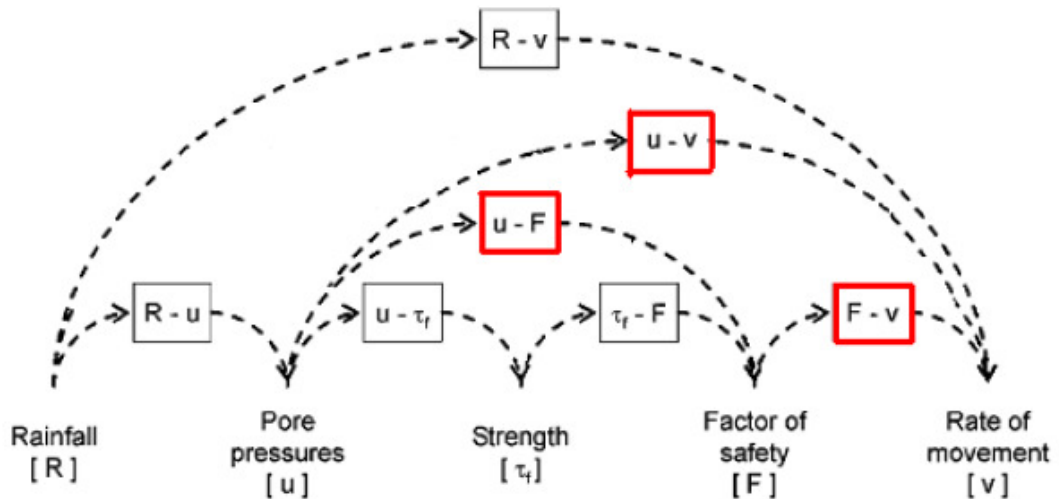


Figure 3.1 - Schematization to model the kinematic response of landslides to rainfall (Leroueil, 2001 and Calvello et al, 2008)

In an ideal (and currently not existing) early warning system, we could predict the rate of movement from the given input of rainfall data (R-v relationship in Figure 3.1), without the need of intermediate steps. But to accomplish this, it is first needed to build the intermediate relationships at local scales by as many consistent cases as possible. This kind of early warning system is currently not available although studies on this topic continue to make progress (Cascini et al. 2010, Ferrari et al. 2010). Within the confines of this thesis, the relations between the pore pressures,

factor of safety and rate of movements (u-F, F-v and u-v relationships shown in Figure 3.1.) are investigated. It should be noted here that, the use of a “factor of safety” concept (as in “F.S.>1.0 stable, F.S.<1.0 unstable”) may not seem very meaningful for a landslide that already has F.S. at or very close to 1.0, and already moving. However, in this study, the factor of safety is still considered as an indication of the safety level, since it is widely used by geotechnical engineers in relation to landslide studies. Accepting such a limitation, for example, Glastonbury and Fell (2002), and Bonnard and Glastonbury (2005) developed relations between “relative F.S.” and rate of movement. Therefore, it is also used in this study by normalizing the F.S. with respect to the lowest F.S. obtained for the given case for the worst piezometric condition, and using “relative factor of safety” term.

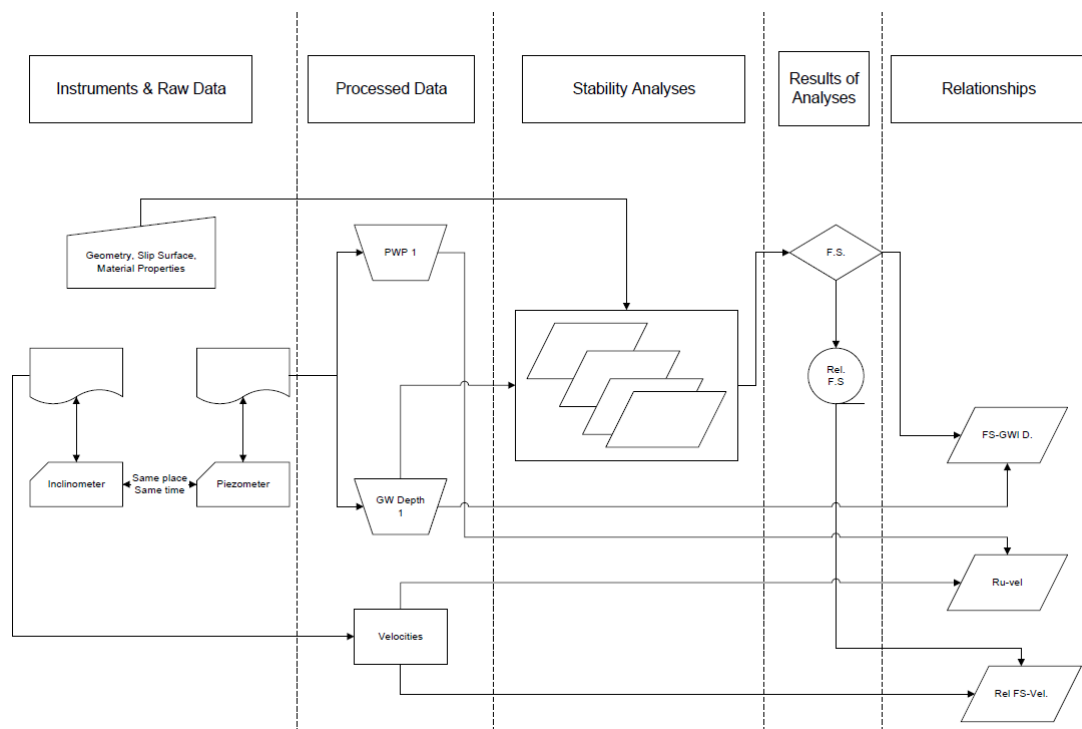


Figure 3.2 – A part of the procedure followed before and after stability analyses

Figure 3.2 shows a part of the procedure of obtaining necessary relationships for an individual landslide case in this study. The procedure begins by selecting the landslide cases with extensive piezometric and displacement data and followed by processing the data into desired parameters. Such parameters are then used in the analyses along with information on geometry, the slip surface and material

properties. Combination of output of analyses and corresponding input allow to form necessary relationships. Details on the procedure is given under analyses chapter. Two dimensional slope stability analyses, finite element models and a kinematic model are incorporated for geomechanical and hydrological analysis of the selected landslide cases. The next section introduces the fundamentals of the modeling phase followed by explanation of each analysis type used.

3.2 Stability Analyses

The limit equilibrium analyses are executed by utilizing SLIDE v5.0 2D Limit Equilibrium Slope Stability Analysis Program. The method to calculate the factor of safety values is selected as Spencer's method. The sliding bodies are divided into 25 slices and calculations are done with 0.5% tolerance in maximum number of iterations of 50.

Failure surfaces are determined and entered by the output of inclinometer measurements as well as published field observations such as tension cracks or heave at the toe. Shear strength used in slope stability analyses are residual values which are either back-calculated or laboratory measured. Detailed information on the determination of failure surfaces and shear strength values are given in the following sections, when needed.

3.3 Deformation Modeling

3.3.1 Finite Element Analysis

PLAXIS 2D Version 8 is utilized to model deformation behavior of landslides under different observed groundwater conditions. The model used in analyses is 15-noded plane strain model with very fine meshed element distribution.

Slip surfaces are modeled with interface elements having virtual thickness factor of 0.100. Since 15-node soil elements are used, the corresponding interface elements are defined by five pairs of nodes. The virtual thickness of slip surfaces correspond to the multiplication of virtual thickness factor and the average element size. A general meshing parameter representing the average element size, l_e , is calculated from outer geometry dimensions such that:

$$l_e = \sqrt{\frac{(x_{max} - x_{min})(y_{max} - y_{min})}{n_c}} \quad (\text{Eq. 3.1})$$

where x_{max} , x_{min} , y_{max} , y_{min} are the maximum and minimum geometry dimensions given by user and n_c is the factor representing the global coarseness. Very fine coarseness have an estimate value of $n_c = 400$ which refers to around 1000 elements.

3.3.1.1 Material Models

The lack of laboratory-derived material properties required for advanced material constitutive models forced us to the usage of simple material model as the elastic-plastic Mohr-Coulomb model for all layers including slip surfaces. Although the representation of material behavior by this model is generally correct at soil layers, it can not serve better than a first-order approximation of the real slip surface behavior. If necessary data could be obtained; advanced constitutive material models would give better results. In this study it is preferred to work with known data and simple models rather than estimated data and corresponding complex models.

3.3.1.2 Boundary Conditions

For all cases boundary conditions are set to standard fixities of PLAXIS 2D which refer to the boundary conditions at which (i) the lowest and highest x-coordinates of vertical geometry lines acquire a horizontal fixity, i.e. $u_x = 0$; (ii) the lowest y-coordinate of horizontal geometry lines acquire a full fixity, i.e. $u_x = u_y = 0$.

3.3.1.3 Initial Conditions

Since by nature the landslide slopes as well as some parts of groundwater tables are not horizontal, the initial loading by the K_0 -condition would give misleading results. Instead, gravity loading is exerted at the beginning of each analysis set. This way initial stresses are built by applying the self-weight of the model.

3.3.1.4 Calculation Type

Updated mesh analysis with updated water pressures option is selected with the plastic calculation type to compensate the effects of large displacement simulations. From time to time even slow moving landslides face large local or global displacements that are to be differentiated by smaller long-term rate of displacements. Moreover water pressures are continuously recalculated referring to the new positions of stress points.

Note that, arc-length control option in iterative procedure control parameters is deactivated since it causes spontaneous unloading for displacement-controlled calculations although the soil body is far from collapse.

3.3.2 Kinematic Analysis

In order to compute the rate of displacements from the output of a groundwater analysis or simply from measured groundwater levels, kinematic analysis is needed. Velocities are predicted by making use of an assumed non-linear empirical relationship taking into account observed minimum and maximum velocities as well as the maximum factor of safety values in a certain time interval. Finally, the calculations are optimized by regression analyses. The procedure is adopted from Calvello et al. (2008).

The non-linear relationship used is given below, which is valid for $F \leq F_{\max}$:

$$v(t) = v_{\min} 10^{\left(\frac{1 - \log F}{\log F_{\max}}\right) \log \frac{v_{\max}}{v_{\min}}} \quad (\text{Eq.3.2})$$

In this relationship; t is the time, F_{\max} is an upper limit of factor of safety above which velocity of the slide is assumed to be zero and at which the velocity equals to v_{\min} . v_{\max} corresponds to a maximum value of rate of displacement at the factor of safety of unity. As can be seen from this equation, to be able to use this approach, one has to know, or estimate, the minimum and maximum velocities.

CHAPTER 4

ANALYSES OF LANDSLIDE CASE HISTORIES

4.1 Vallcebre Landslide

4.1.1 Overview

The translational Vallcebre landslide is located in Upper Llobregat basin of Eastern Pyrenees of Spain. The materials composing the landslide body are fissured shales and clayey siltstone underlied by limestone bedrock. All of the material is of Upper Cretaceous to Lower Palaeocene age. Observations since 1996 show that the landslide is triggered by rainfall; and the response is immediate (Corominas et al., 2005). However the rate of displacement is almost constant having velocities between 0.2 and 0.5 mm/day. The sliding body has a volume of approximately $20 \cdot 10^6 \text{ m}^3$ and an average slope angle of 10 degrees. The shear surface is determined by inclinometers at the lower slide by Corominas et al. (1999) and it is nearly parallel to the slope surface. The slide has three main units; upper, intermediate and lower. In this study only the lower unit is considered since it is the most unstable unit. A typical cross-section of the slide is given in Figure 4.1.

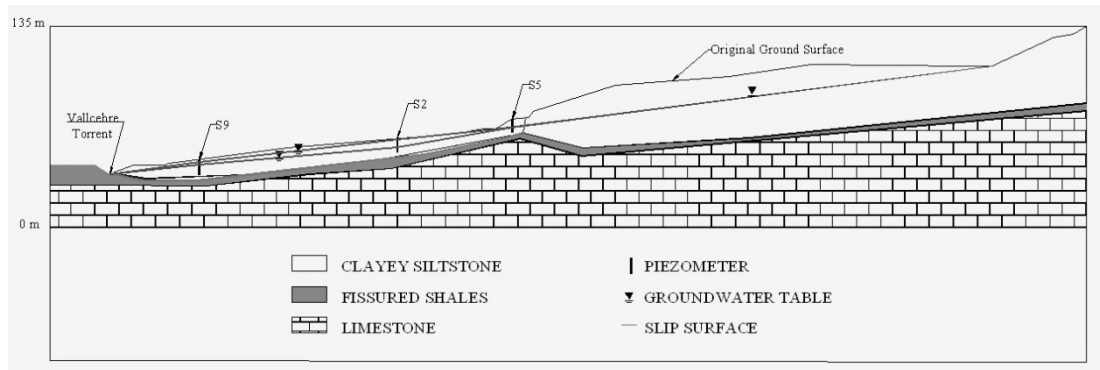


Figure 4.1 - Cross-section of the Vallcebre landslide - without vertical exaggeration (Reproduced from the cross-section A-A' by Corominas et al., 2005)

4.1.2 Monitoring Data

The monitored data of change in groundwater table depth and displacements at the lower slide are extracted from Corominas et al. (2005). The data from three boreholes (S2, S9, and S5) measured between November 1996 and October 1998 is used in this study. Different from other cases, the displacements given are the results of wire extensometer measurements along boreholes. Borehole wire extensometers allow the measurement of the relative displacement between two points, one in the sliding mass that is moving and the other in the stable soil. Therefore it is needed to convert wire displacements to superficial displacements by making use of the suggested conversion functions at the Vallcebre landslide (Corominas et al., 2000). The simplified relationship between wire displacement and superficial displacement for approximately 30 cm of shear zone thickness at station S2 is used.

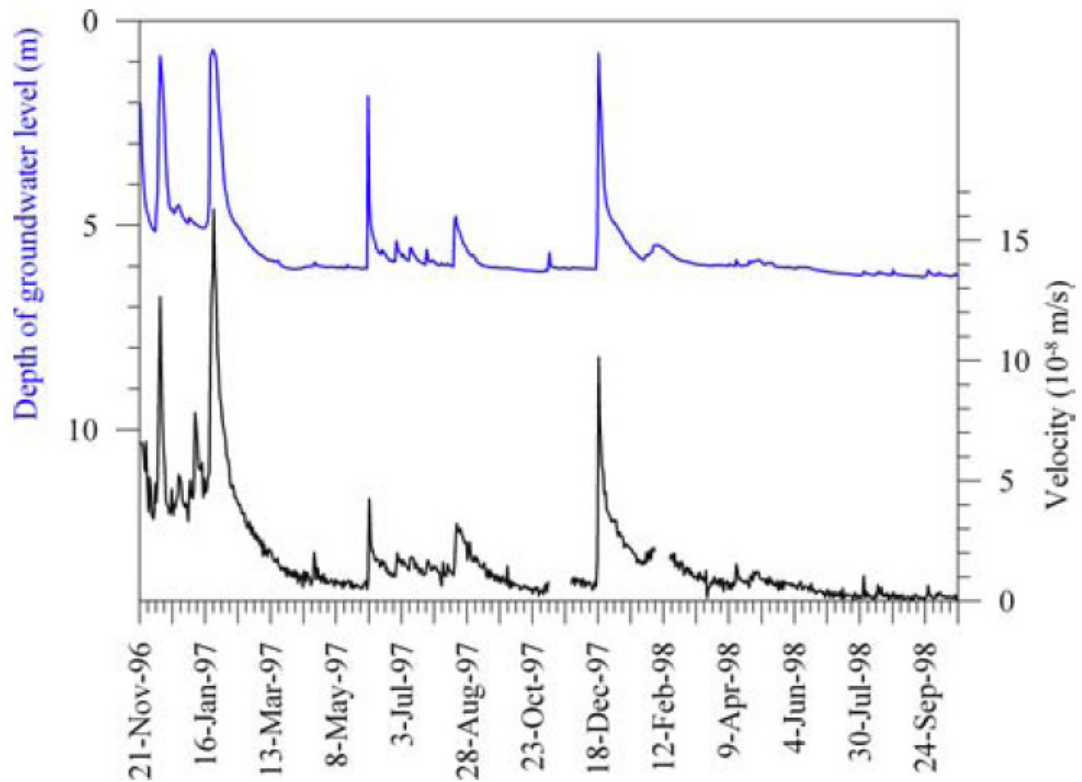


Figure 4.2 – Piezometric data and landslide velocity at S2 (Corominas et al., 2005)

A close relationship between the changes in depth of groundwater level and landslide velocity is reported (Figure 4.2) referring to measurements taken from the borehole wire extensometer at borehole S2 (Figure 4.1). Corominas et al. (2005) described that there exists “a strong level of synchronism” between the two measurements.

4.1.3 Stability Analyses

The groundwater levels corresponding to the displacement data are determined to analyze the static stability of the slope. For each selected time of measurement groundwater depths are calculated and inserted in the analysis. A total of 17 analyses are executed to span the selected time interval.

From the empirical data on residual friction angle proposed by Mesri and Shahien (2003), for 50 kPa, 100 kPa and 400 kPa, secant friction angles are obtained for various I_p values (Figure 2.4). Thus for each I_p value three secant friction angle are found for the given stress range. In order to calculate corresponding shear stresses, nonlinear envelope curves are found with the Equation 4.1 proposed by Mesri and Abdel-Ghaffar (1993) and modified by Mesri and Shahien (2003).

$$s(r) = \sigma'_n \tan(\phi'_r)_s^{100} \left(\frac{100}{\sigma'_n} \right)^{1-m_r} \quad (\text{Eq. 4.1})$$

where $(1 - m_r) = \text{slope of } \log \left[\frac{\tan(\phi'_r)_s}{\tan(\phi'_r)_s^{100}} \right] \text{ versus } \log \left(\frac{100}{\sigma'_n} \right)$.

$s(r)$ = residual shear strength

σ'_n = effective normal stress

ϕ'_r = residual friction angle

and $(\phi'_r)_s^{100}$ = secant residual friction angle at $\sigma'_n = 100$ kPa.

A non-linear failure envelope is determined for fissured shales using the equation (Equation 4.1) and the residual average curves proposed by Mesri and Shahien (2003). The non-linear envelope for $I_p=60\%$ shows most compatible curve (Figure 4.3) with the laboratory measured residual values of Corominas et al. (2005). As reported by Corominas et al. (2005) laboratory direct shear tests on pre-sheared surfaces collected from the field gave a cohesion of zero, a residual friction angle of 7.8 degrees (for effective normal stress range up to 800 kPa), and the plasticity index of the material was about 20%. It should be noted that, when one look at the database on residual friction angle of stiff clays and plasticity index in Figure 2.4 from Mesri and Shahien (2003), one can see that for a material with $I_p=20\%$ residual friction angle of 7.8 degrees is not possible. This discrepancy could be explained in several ways: either the material tested in direct shear tests and plasticity tests are not the same material, or the material is not fully disaggregated in the sample preparation of plasticity index test (which caused the clay particles to have a lower water holding

capacity around the clay particles), or the material contains nonplatey clay minerals. Plasticity index value of about 60 % matches with the reported 7.8 degrees secant residual friction angle. In fact, Mesri and Shahien (2003) reported that for stiff clays, clay shales, claystones, and mudstones, pulverization and complete disaggregation of the sample is needed in order to truly represent the state of these materials in the shear zone of landslides. Sample preparation and disaggregation can significantly influence the plasticity index value obtained in the laboratory (Stark et al., 2005).

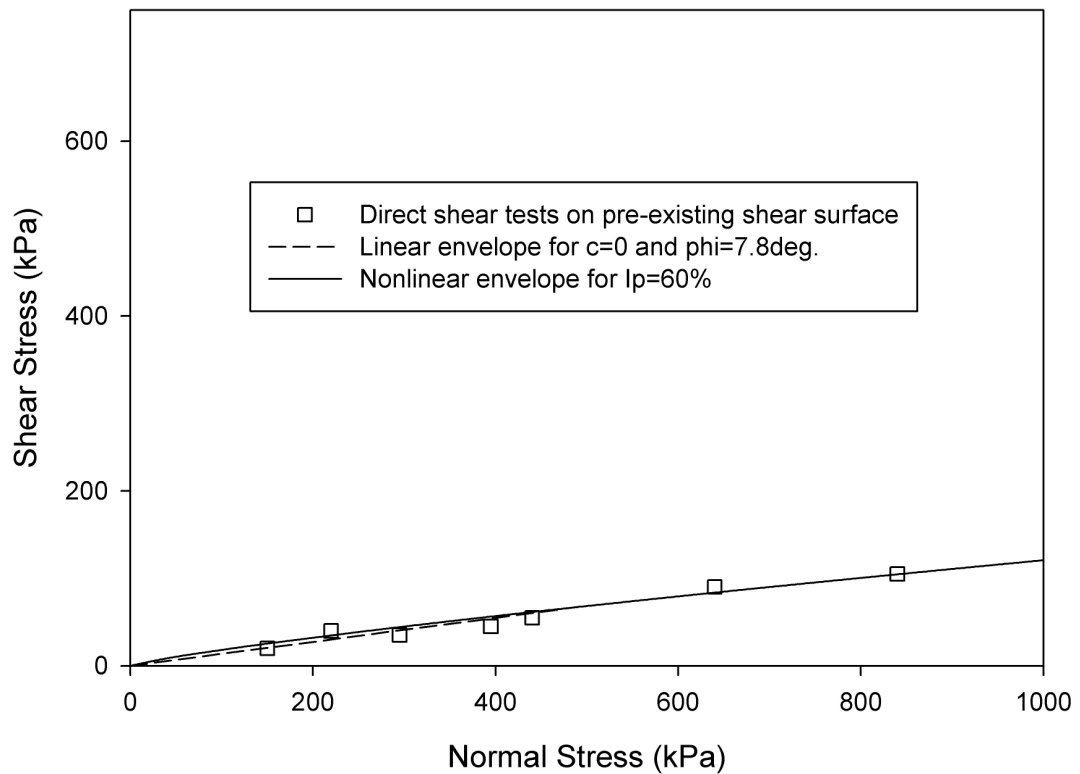


Figure 4.3 – Shear stress envelopes for the Vallcebre landslide

The planar sliding surface is introduced to the program in correspondence with the failure surface determined by inclinometers at the lower slide (Corominas et al., 1999).

Table 4.1 - Shear strength parameters derived from different tests: Minimum strength measured in direct shear, ring shear and triaxial tests for fissured shale; minimum strength measured in direct shear for clayey siltstone and residual strength measured on a pre-existing shear surface in fissured shale (Corominas et al., 2005)

Material	Range of Normal Stress	c' (kPa)	Ø' (°)
Fissured Shale	$0 < \sigma'_n < 200$ kPa	0	23.4
	$200 < \sigma'_n < 700$ kPa	44	11.8
Clayey Siltstone	$0 < \sigma'_n < 400$ kPa	0	33
Shear Surface	$0 < \sigma'_n < 800$ kPa	0	7.8

Analyses are conducted with material properties given in Table 4.1 where shear strength parameters were derived by Corominas et al. (2005) from minimum strength measured in direct shear, ring shear and triaxial tests for fissured shale; minimum strength measured in direct shear for clayey siltstone and residual strength measured on a pre-existing shear surface in fissured shale. The results are given for each piezometric level (Appendix). The analyses take into account all three water levels at boreholes simultaneously.

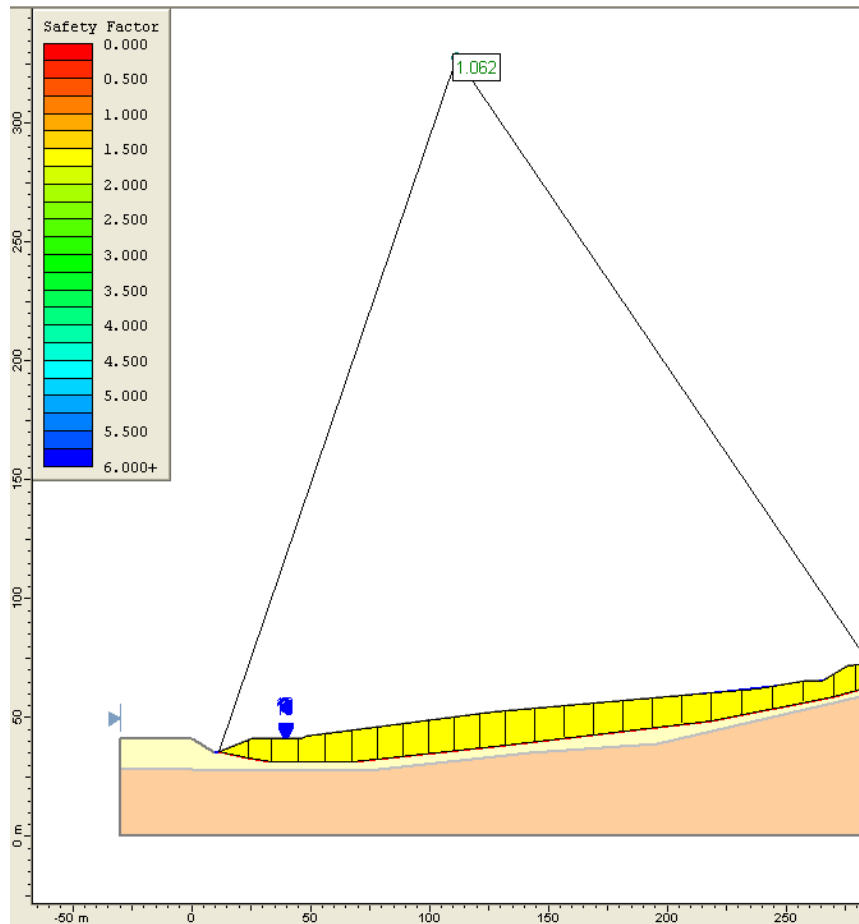


Figure 4.4 – Output of limit equilibrium slope stability analysis for Vallcebre landslide with the piezometric condition P14 (see Appendix)

The factor of safety values determined from static stability analyses are close to the unity from above and also below, implying that the landslide is moving “continuously”. Thus, the values do not refer to the stability condition due to creep effects but to the degree of global instability against the changes in boundary conditions like groundwater levels, i.e. pore pressure fluctuations. Dynamic stability analyses including elasto-plastic and/or viscous effects would give meaningful results if the information related to the creep behavior of the material is known.

As explained in preceding sections of this thesis, relations between pore pressures, factor of safety and rate of movement (u - F , F - v , u - v in Figure 3.1) are of interest. The change of stability with respect to groundwater increase at each inspected borehole is shown by plotting relationships between relative factor of safety, depth of groundwater level and pore pressure coefficient (Figure 4.5). Pore pressure

coefficient ru is calculated for each borehole separately by using the measured water levels and total normal stress values for each borehole, instead of averaging ru values over the whole slope. This approach seems reasonable and practical, since for a real life landslide, an average ru of the whole slope may not be known, however ru at a specific location can be measured and known, therefore can be used in relations of pore pressure and movement rate. The concept of relative factor of safety is proposed by Glastonbury and Fell (2002). In the concept of relative factor of safety, the least stable condition; i.e. highest measured groundwater level; of slow moving active landslides is considered to represent a relative factor of safety of unity. The rest of the conditions are normalized against this condition.

Despite the gap in the given data of the boreholes S2 and S5 the relationship between the groundwater level (represented also by ru) and relative F.S. at the upper part of the lower slide is linear (Figure 4.5). At the toe section represented by the borehole S9 the relationship follows a nonlinear trend. However, if the data from all three boreholes is considered, an overall nonlinear relationship could be visualized. Factor of safety against depth of groundwater level (or pore pressure coefficient) plot is not expected to be linear since (i) the thickness of the sliding mass and groundwater tables are not purely translational as in an infinite slope, and (ii) shear strength envelope used is nonlinear, therefore shear strength of the soil decreases nonlinearly as the pore water pressure increases and effective vertical stress decreases.

Relations between relative factor of safety and rate of movement, and between pore water pressure and rate of movement are also studied for borehole location S2 where the maximum amount of ground surface movement is observed in Vallcebre landslide. In the proceeding sections of the thesis, the results of these relations for several analyzed landslide cases will be gathered and conclusions will be reached.

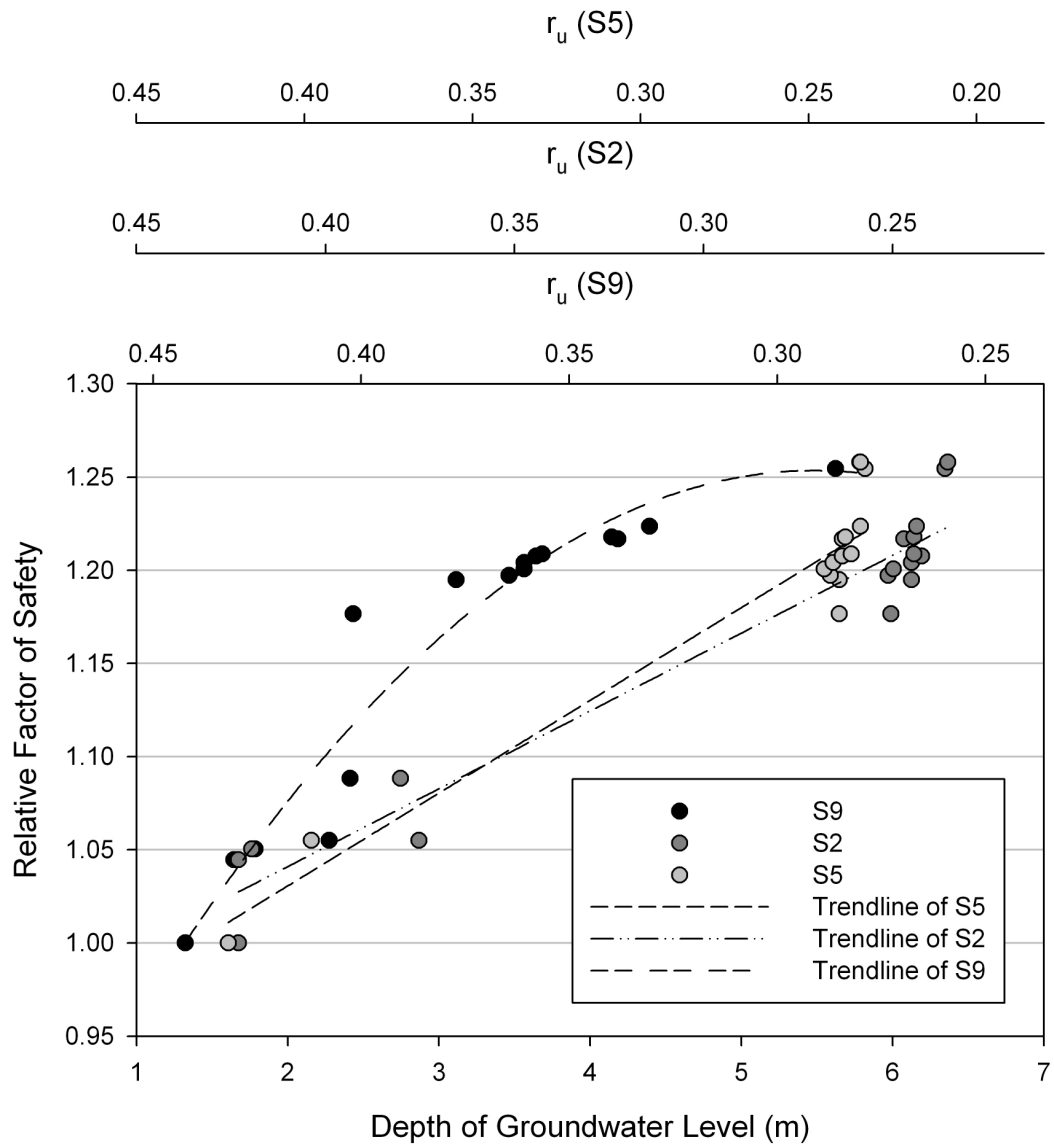


Figure 4.5 – Relationships between relative factor of safety, groundwater level and pore pressure coefficient for the boreholes S2, S5 and S9 at the lower slide of the Vallcebre landslide

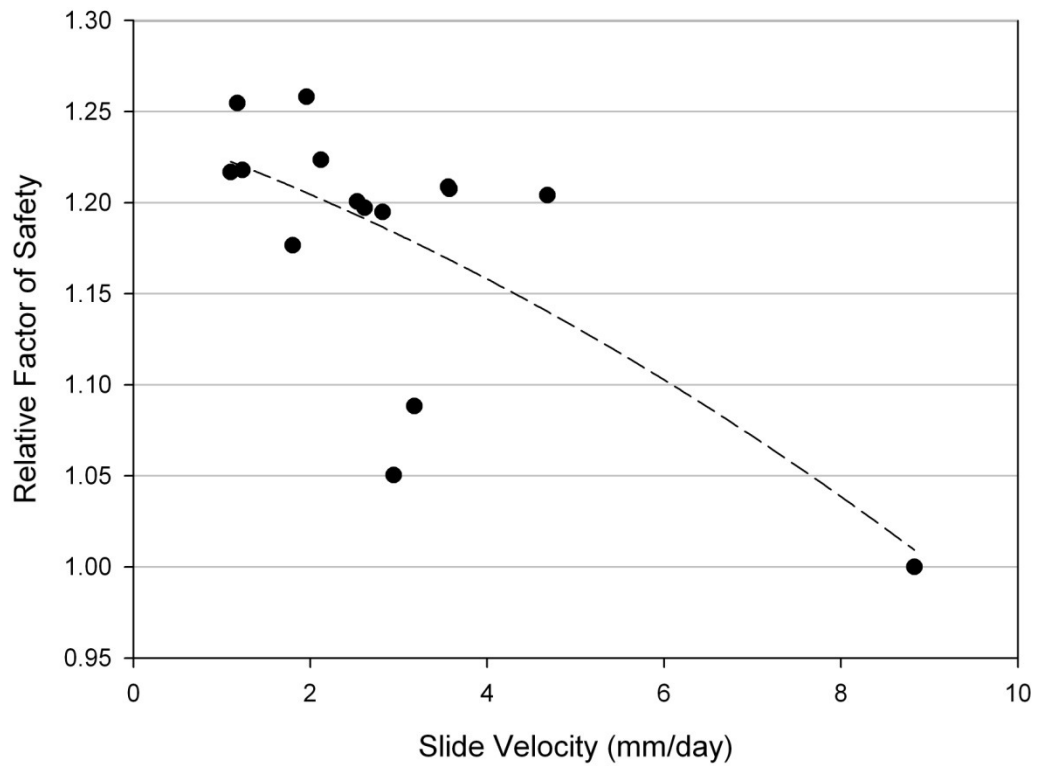


Figure 4.6 – Relation between relative factor of safety and the rate of movement (as observed at station S2) of the Vallcebre landslide

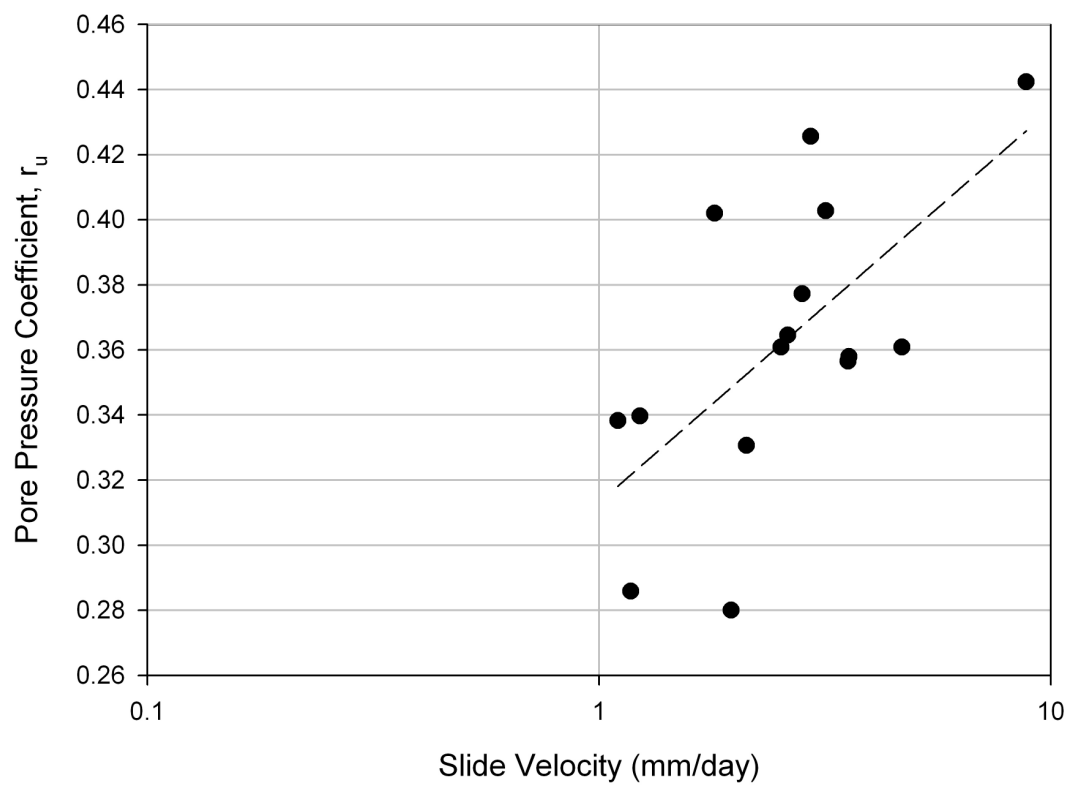


Figure 4.7 – Relation between pore pressure coefficient and slide velocity of Vallcebre landslide at S2

4.2 San Martino Landslide

4.2.1 Overview

The San Martino landslide is located in the Central Italy, near the shore of Adriatic Sea, at the side of Gran Sasso and Laga Mountains. The toe of the landslide is at the drainage basin of San Martino river (Figure 4.8). The materials composing the slope are silty clay colluvial cover and weathered marly clay. The underlying bedrock formation of marly clays are of middle-upper pliocene age. Bertini et al. (1984) have investigated the slide between 1980 and 1982 through detailed surface and subsurface observations.

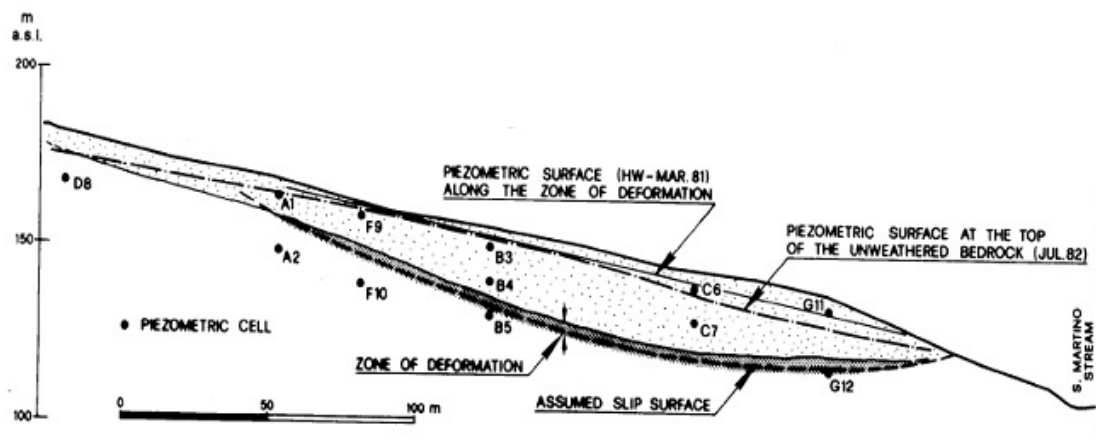


Figure 4.8 – Cross-section of San Martino landslide (Bertini et al., 1984)

4.2.2 Monitoring Data

Daily rainfall data from pluviometers and measured piezometric levels within the colluvium have referred to a close relationship between them; generally immediate response to rainfall events was encountered. Inclinometric measurements without having relative displacements within the colluvial cover suggested that the movement occurred as a rigid body. The average rate of displacement is given as 2 cm/year (Bertini et al., 1984) where the movement is sensitive to pore water pressure fluctuations in the colluvial cover.

Figure 4.9 shows the close relationship between fluctuations in piezometric level and rate of displacements at Station B during the observation period of two years.

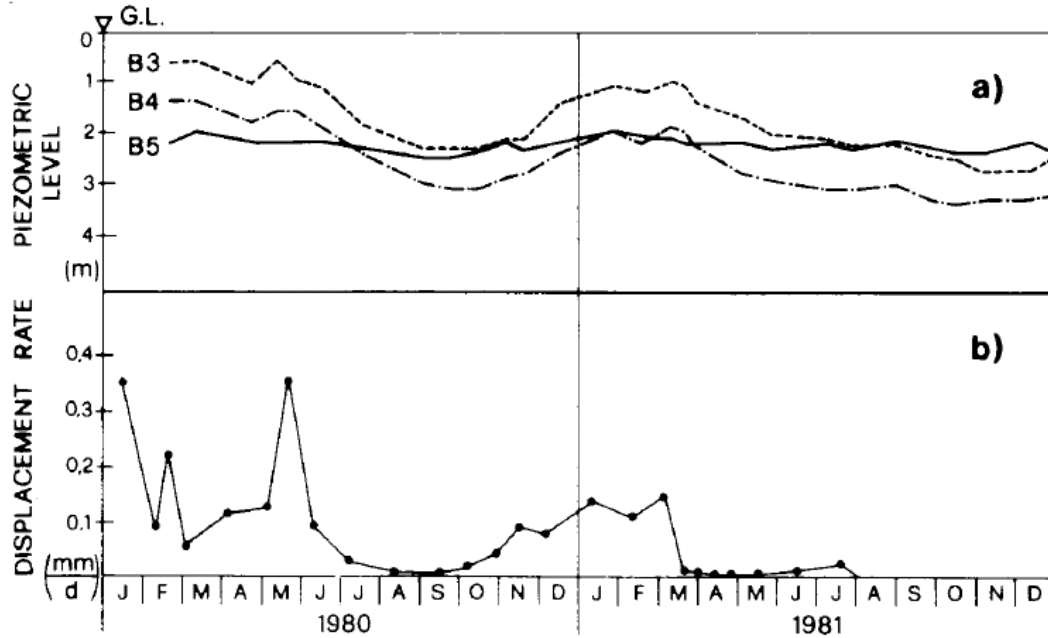


Figure 4.9 – Piezometric level and displacement rate at station B (Bertini et al., 1984)

4.2.3 Stability Analyses

It was observed that the response of the San Martino landslide is seasonal, such that continuous and even low intensity rainfalls change groundwater levels more than short intense rains.

Huvaj-Sarihan (2009) used the high groundwater level observed in March 1981 to back-calculate the nonlinear shear strength envelope which corresponded to the average residual shear strength for $I_p=27\%$ with the procedure of Mesri and Shahien (2003). The lowerbound of reversal direct shear test results on weathered marl (Bertini et al., 1984) coincided with the back-calculated mobilized strength (Figure 4.10).

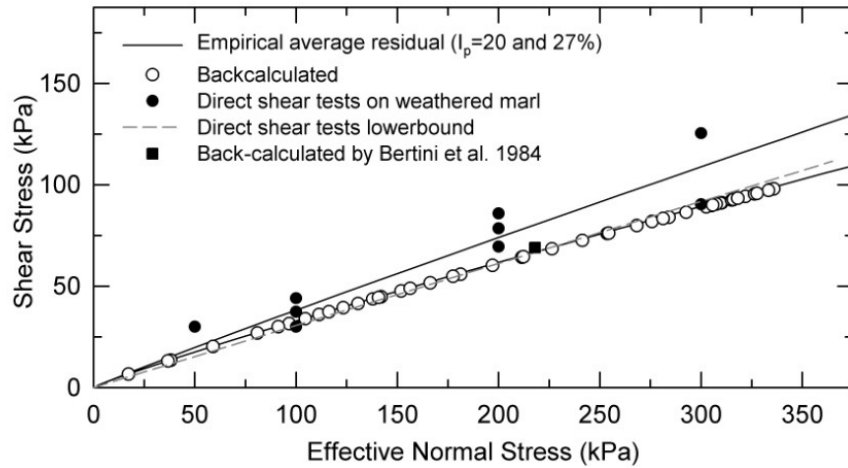


Figure 4.10 – Shear stress envelopes for the weathered zone of the marly clay bedrock. Solid lines represent the envelope obtained from Mesri and Shahien (2003) data (Huvaj-Sarihan, 2009)

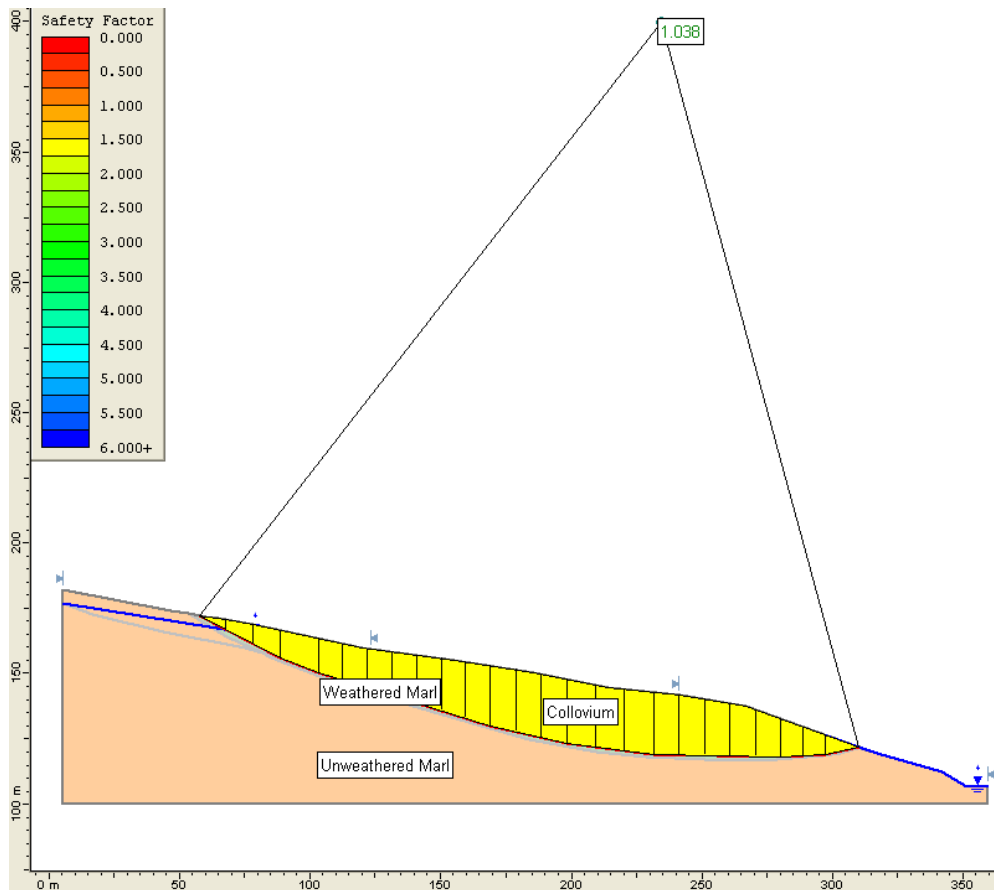


Figure 4.11 – Output of slope stability analysis for San Martino landslide with the piezometric condition P14 (see Appendix)

Figure 4.11 shows the output for the piezometric condition P14 with the input geometry, slices, material boundaries, slope limits, groundwater table, failure surface and analysis properties.

Relative factor of safety values corresponding to each depth of groundwater tables with pore pressure coefficients are correlated at two piezometric locations from the given piezometric data of Bertini et al. (1984) (Figure 4.12). Figure 4.13 shows the plot of rate of movements against relative calculated factor of safety where rate of movements are derived from the horizontal displacement data. Figure 4.14 shows relation between pore pressure coefficient and slide velocity at B3.

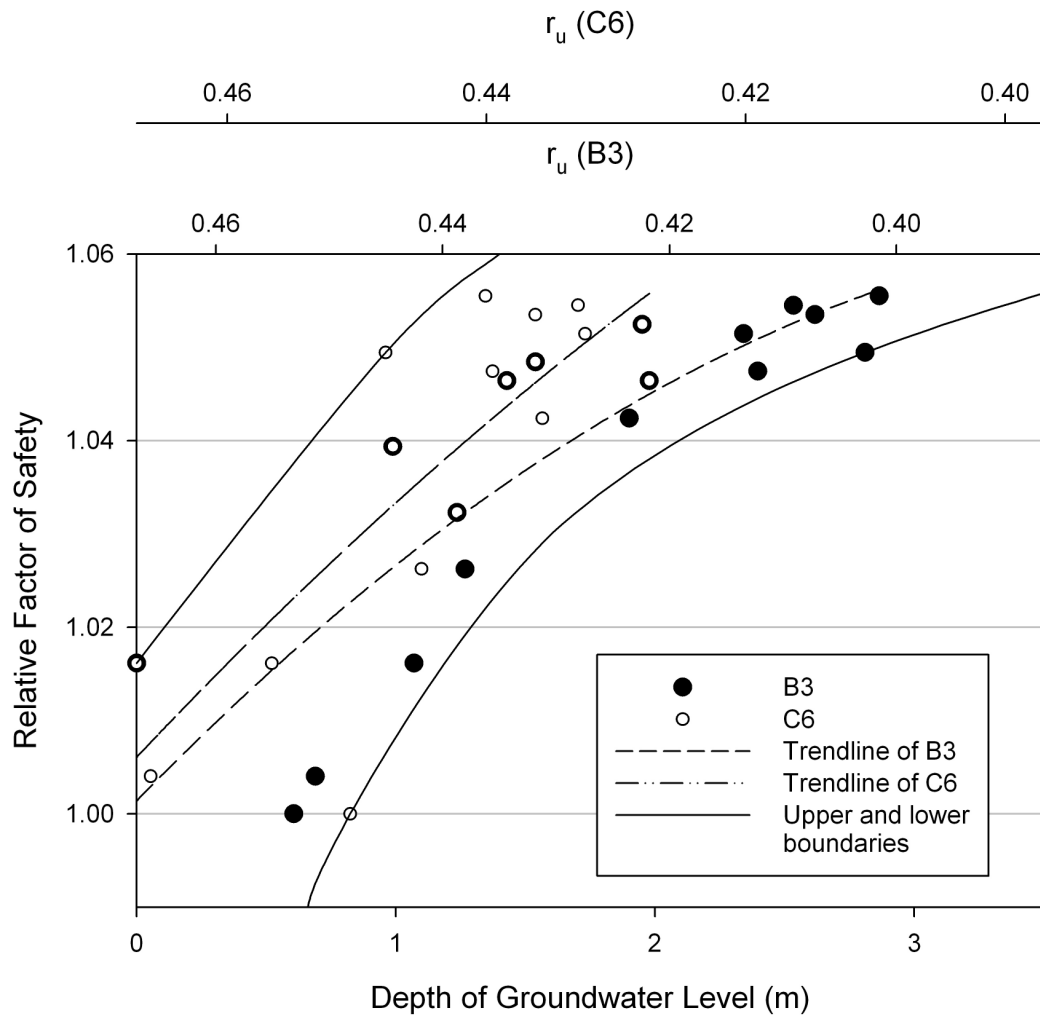


Figure 4.12 – Relationships between relative factor of safety, groundwater level and pore pressure coefficient for the boreholes B3 and C6 of the San Martino landslide

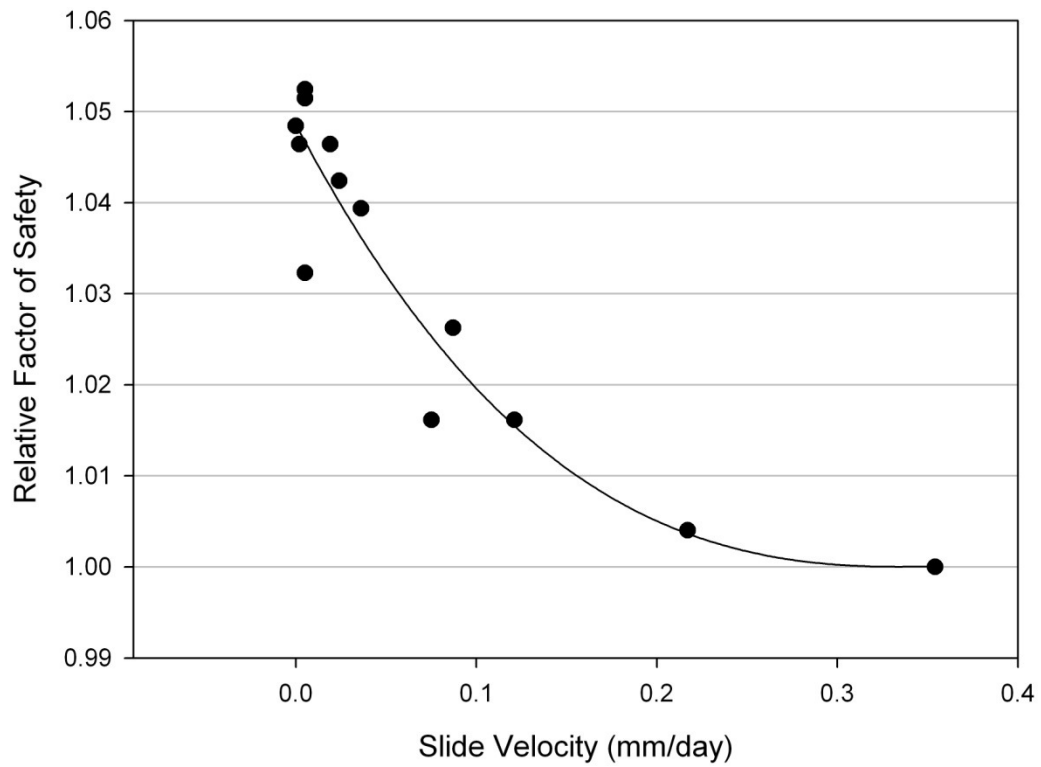


Figure 4.13 – Relation between the relative factor of safety and rate of movement (as observed at station B3) of the San Martino landslide

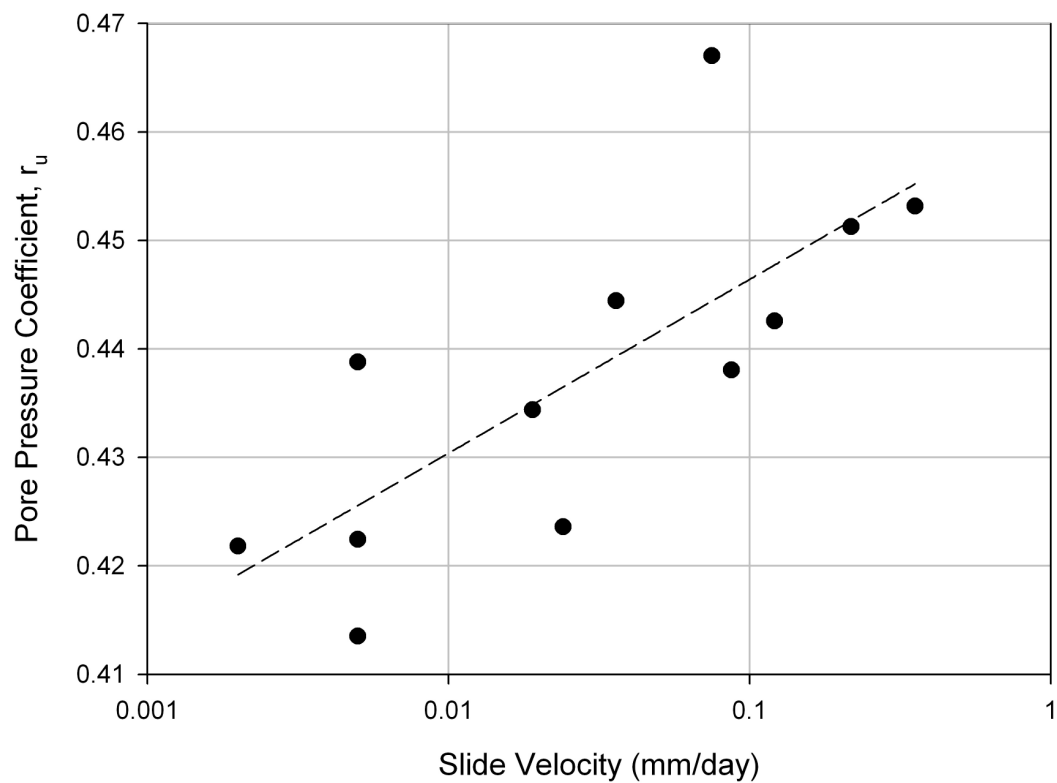


Figure 4.14- Relation between pore pressure coefficient and slide velocity of San Martino landslide at B3

4.3 Steinernase Landslide

4.3.1 Overview

The Steinernase landslide is located in the canton of Aargau in Switzerland. Monitoring data including displacements from inclinometers and piezometric elevations are available since 1986 (Laloui et al., 2008). The active zone of the slope have dimensions of about 300 m x 230 m. Laloui et al. (2008) studied the landslide by analyzing hydrogeological and geomechanical finite element models. They identified that fluctuations in pore water pressure along the slope determine the acceleration and deceleration phases of the movement. Surface monitoring and inclinometer data have suggested that the sliding surfaces are bounded between the main scarp and cantonal road at the toe (Figure 4.15). Although the failure mechanism involves multiple sliding surfaces, the deepest sliding surface is used in this study since it carries the greatest risk to endanger the infrastructure facilities (railway, highway and cantonal road) near the toe. Instabilities occur completely in the colluvial soil cover which is underlied by alluvium and bedrock, at the bottom and at the rest of the slope, respectively. Monitoring data of 2000 and 2001 is used in this study.

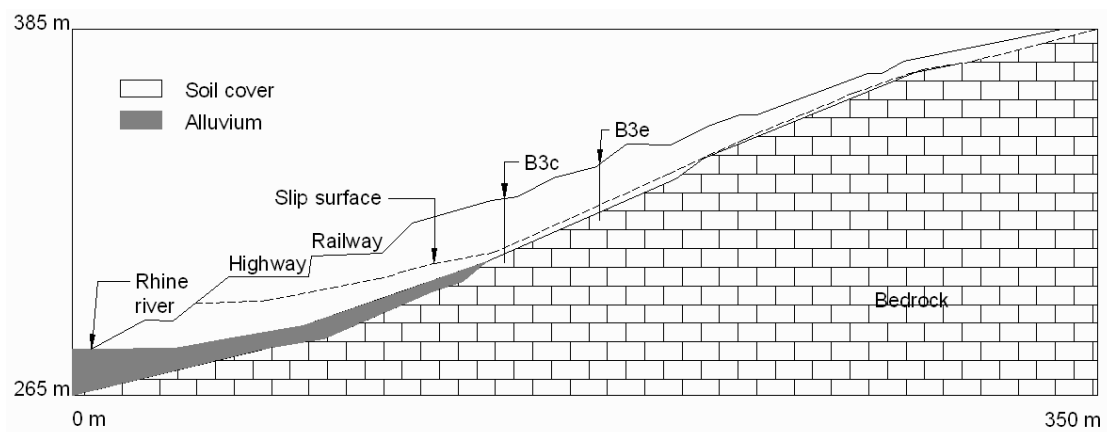


Figure 4.15 – Cross-section of Steinernase landslide (Reproduced from Laloui et al., 2008)

4.3.2 Stability Analyses

The output for the piezometric condition P3 of the Steinernase landslide is given at Figure 4.16. This figure also includes the input geometry, slices, material boundaries, slope limits, groundwater table and failure surface.

The landslide movements are occurring in the soil cover, which is mostly a silty material containing 15-30% clay-size fraction. Shearing resistance parameters reported by Laloui et al. (2008) from direct shear tests, performed on “specimens collected from the slip surfaces”, were in the range of $24^{\circ} - 27^{\circ}$. According to Mesri and Shahien (2003) secant residual friction angle versus plasticity index relationship, these friction angles could correspond to a material with I_p in the range of 10-20%, which seems reasonable for this silty material containing small amount of clay size fraction. However, it should be noted that the residual condition, which is defined by the alignment of plate-shaped clay particles parallel to the direction of shear, do not typically occur in mostly silty materials.

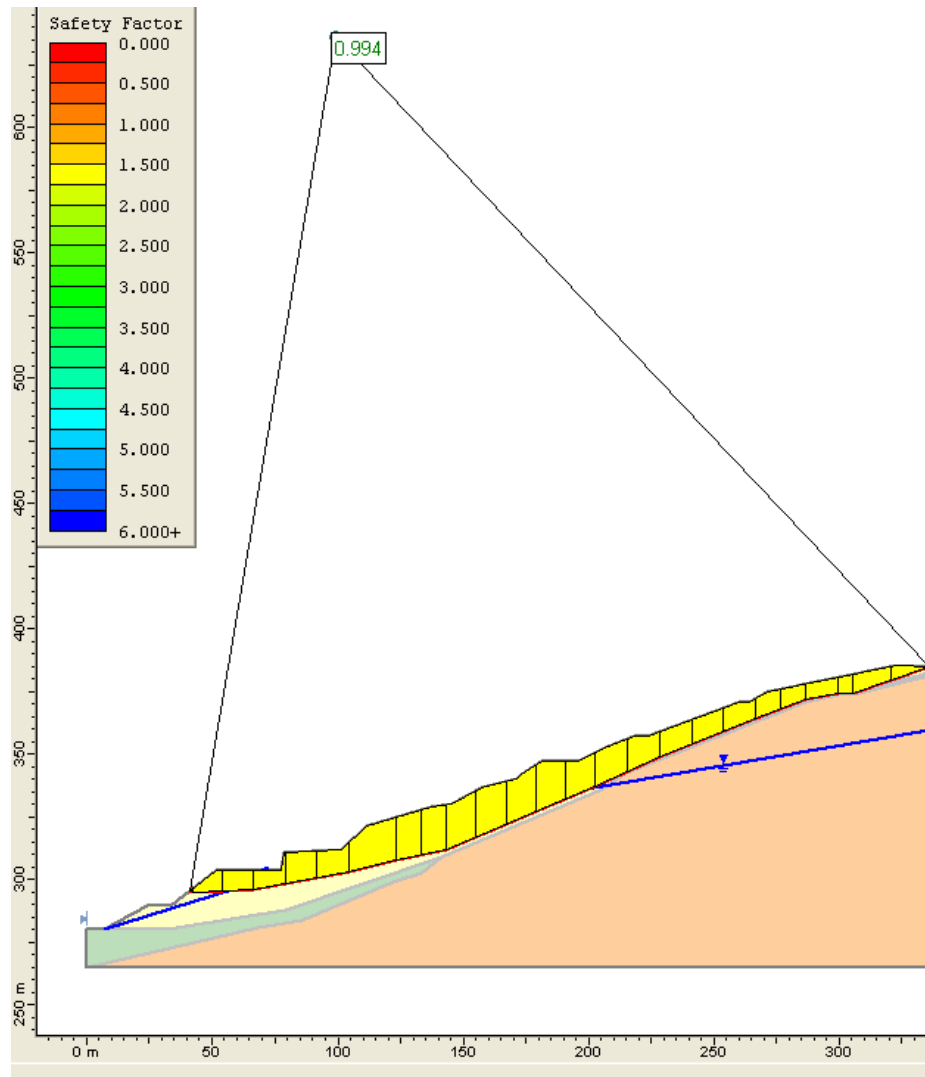


Figure 4.16 - Output of slope stability analysis for Steinernase landslide with the piezometric condition P3 (see Appendix)

Relative factor of safety versus depth of groundwater level plot including pore pressure coefficients (Figure 4.17) for Steinernase landslide imply a non-linear relationship for both of the two piezometric locations considered. The observed velocities fall into “extremely slow” category by having velocities less than 0.05 mm/day. Small to moderate increase in factor of safety reduce the slide velocities greatly where the range of difference of factor of safety is approximately 11%.

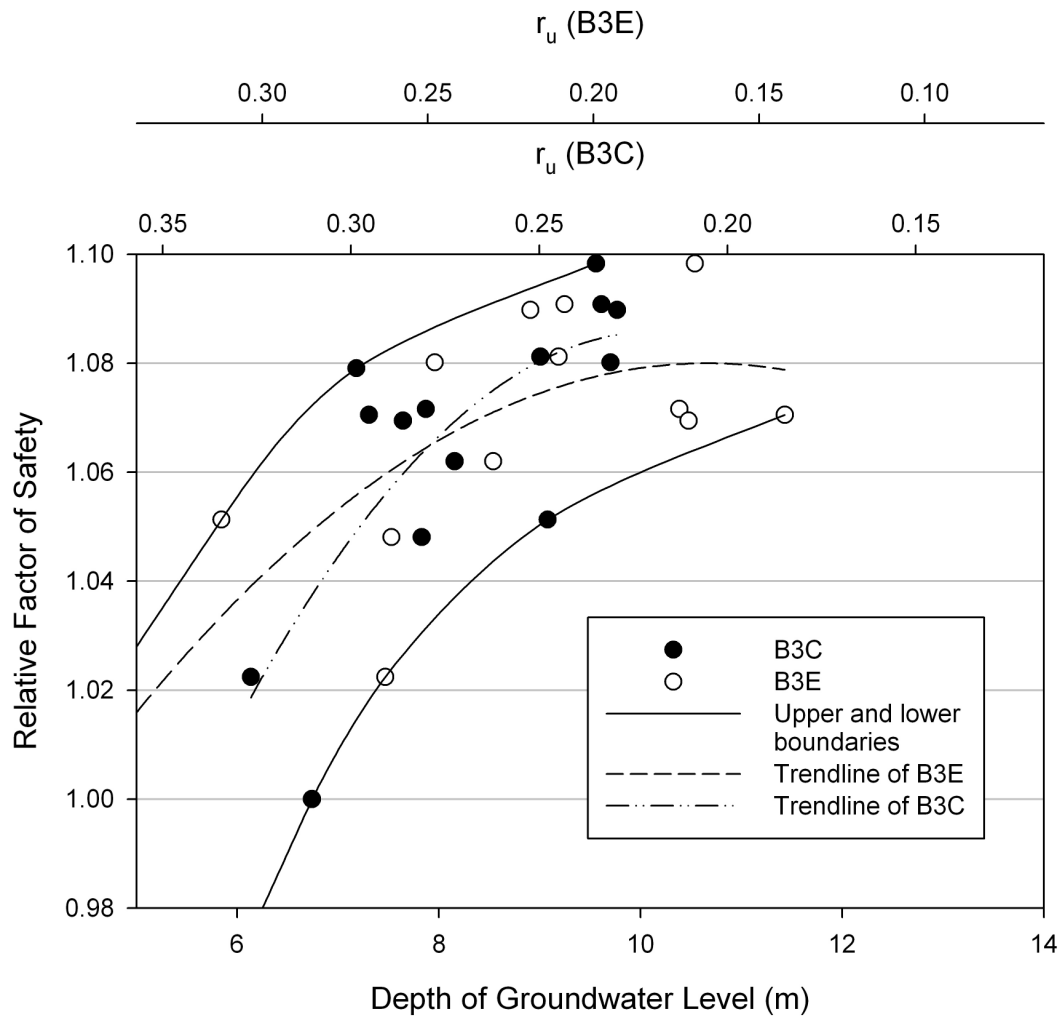


Figure 4.17 - Relation between the depth of groundwater level from the ground surface (as measured at two piezometric locations), relative factor of safety and pore pressure coefficient of the Steinernase landslide

Since the deepest sliding body is considered for the Steinernase landslide, the response of the pore pressures to rainfall events are lagged. On the other hand, more superficial smaller sliding surfaces may respond earlier and cause local slides along the slope. But as mentioned before the deepest slide carries the greatest risk to endanger the infrastructure facilities. Hence it is sufficient to consider only the deepest slide during a preparation of an early warning system.

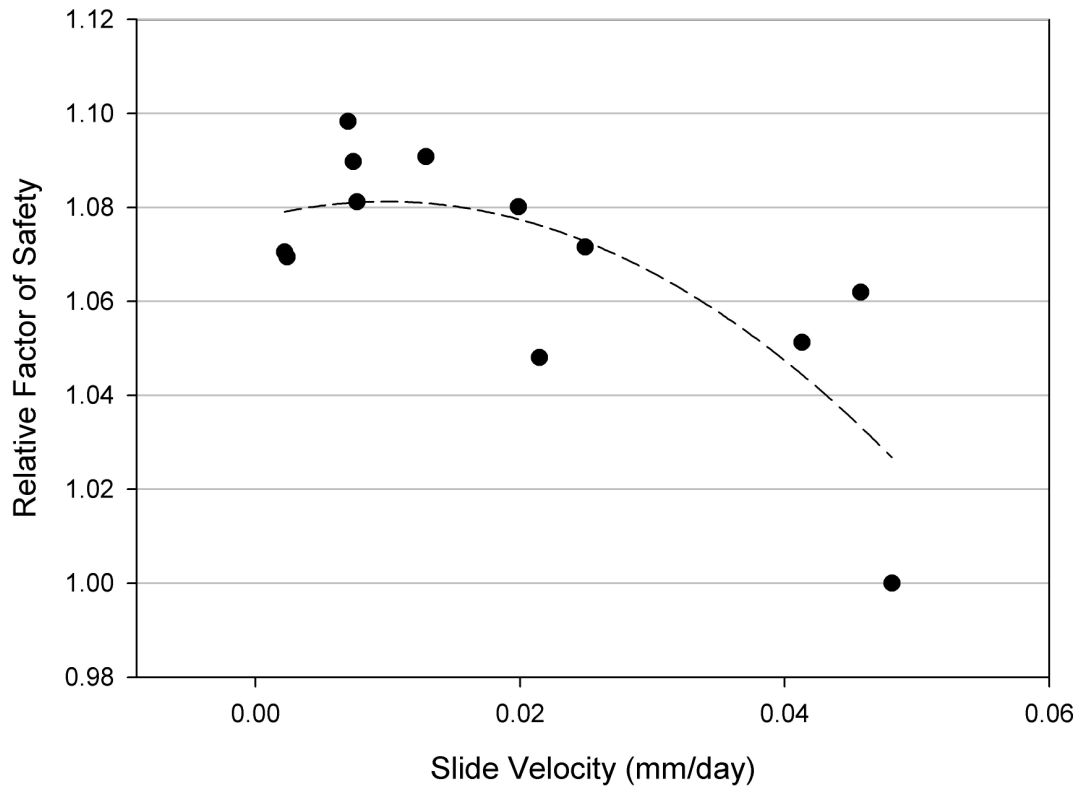


Figure 4.18 - Relation between the relative factor of safety and rate of movement (as observed at station B3C) of the Steinernase landslide

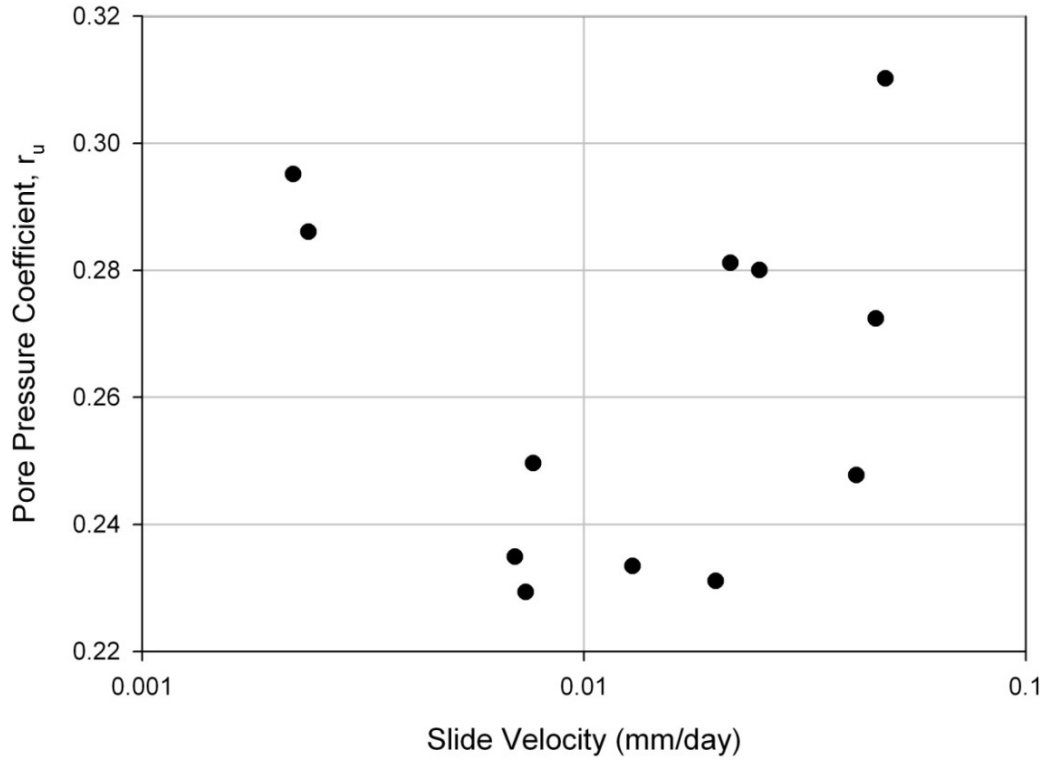


Figure 4.19 – Relation between pore pressure coefficient and slide velocity of Steinernase landslide at B3C

4.4 Triesenberg Landslide

4.4.1 Overview

The Triesenberg landslide in the Principality of Liechtenstein on a slope of the Rhine valley risks important Triesen and Triesenberg villages nearby. Investigations by François et al. (2007) include inclinometer, GPS, piezometer and flow data along with laboratory test to assess mechanical properties of slope forming materials. Approximately 1 m thick slip surface was observed at an average depth of 10-20 m on the 24 degrees inclined slope (Figure 4.20). The average velocity observed was up to 3 cm/year within the loose soil cover; composed of limestone, sandstone, dolomite, flysch and Quaternary deposits in clayey silt. Underlying bedrock and deep seated landslide contain schist, limestone, sandstone and flysch. The water table is generally 20-30 m below the soil surface at the top but it reaches the slope surface at the bottom. The main triggering force of movements was found to be the variations in pore water pressures in the slope (François et al., 2007). Displacements and pore pressures data of the year 2000 is used in this study.

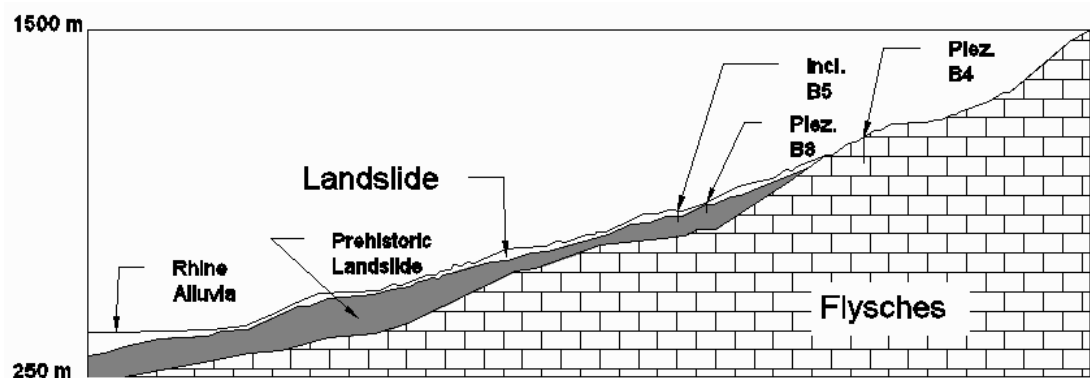


Figure 4.20 – Cross-section of Triesenberg landslide (no vertical exaggeration)
(modified from François et al., 2007)

4.4.2 Stability Analyses

To characterize the material, François et al. (2007) took several samples of soil at different locations near the slip surface, but not necessarily within the slip surface

zone, as the slip surface could not be precisely located in the boreholes. The material is classified as CL to SC with $I_p=11-13\%$. Triaxial tests carried out on this material gave a peak friction angle of 25 degrees with zero cohesion. Therefore, this material is most probably not at the residual condition (of alignment of plate-shaped clay particles parallel to the direction of shear).

The relation between the depth of groundwater level from the ground surface, pore pressure coefficient and the calculated relative factor of safety of the Triesenberg landslide is given at Figure 4.22. The relationship follows a perfectly linear trend consistent with the relation between rate of movement and relative factor of safety (Figure 4.23). This is most probably due to: (i) very long and thin slide mass which resembles a theoretical infinite slope cross section, in which total normal stress and pore water pressure is almost constant along the length of the slope, (ii) there is no significant difference between nonlinear and linear shear strength envelope for materials with very low plasticity. Therefore a linear relationship, as it would occur in infinite slope analysis, can be expected.

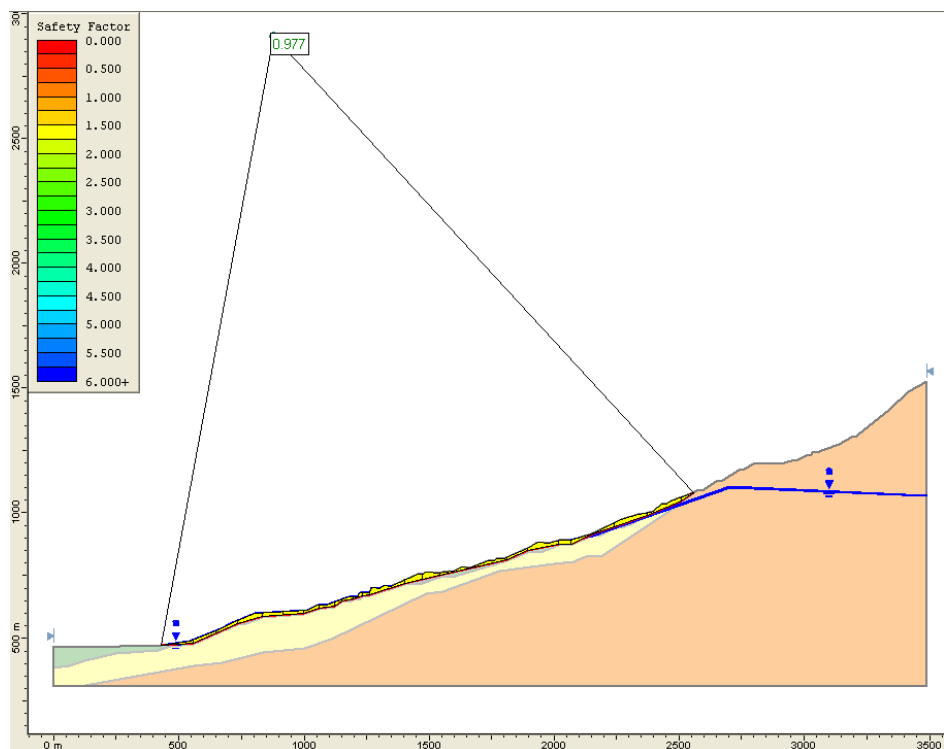


Figure 4.21 - Output of slope stability analysis for Triesenberg landslide with the piezometric condition P10 (see Appendix)

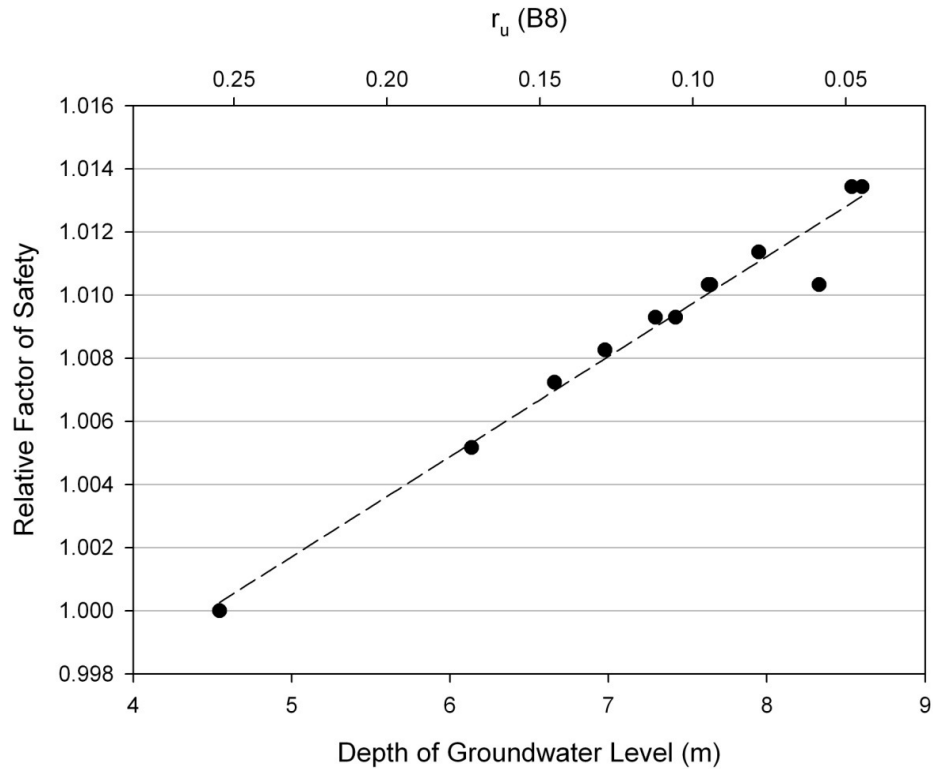


Figure 4.22 - Relation between the depth of groundwater level from the ground surface (as measured at B8) and the relative factor of safety of the Triesenberg landslide

As the factor of safety values range at about 1.6 % against the change of rate of movement between 0.1 to 0.6 mm/day, slight increase in the pore pressures, and consequently decrease in factor of safety values accelerates the movements greatly. Since the active slip surface is at an average depth of 10-20 m below the ground surface, the increase in pore pressure do not occur immediately after rainfall events. This implies that to build an efficient early warning system, either hydraulic conditions of the landslide should be well integrated in the analyses or the pore pressures along the slip surface should be monitored continuously.

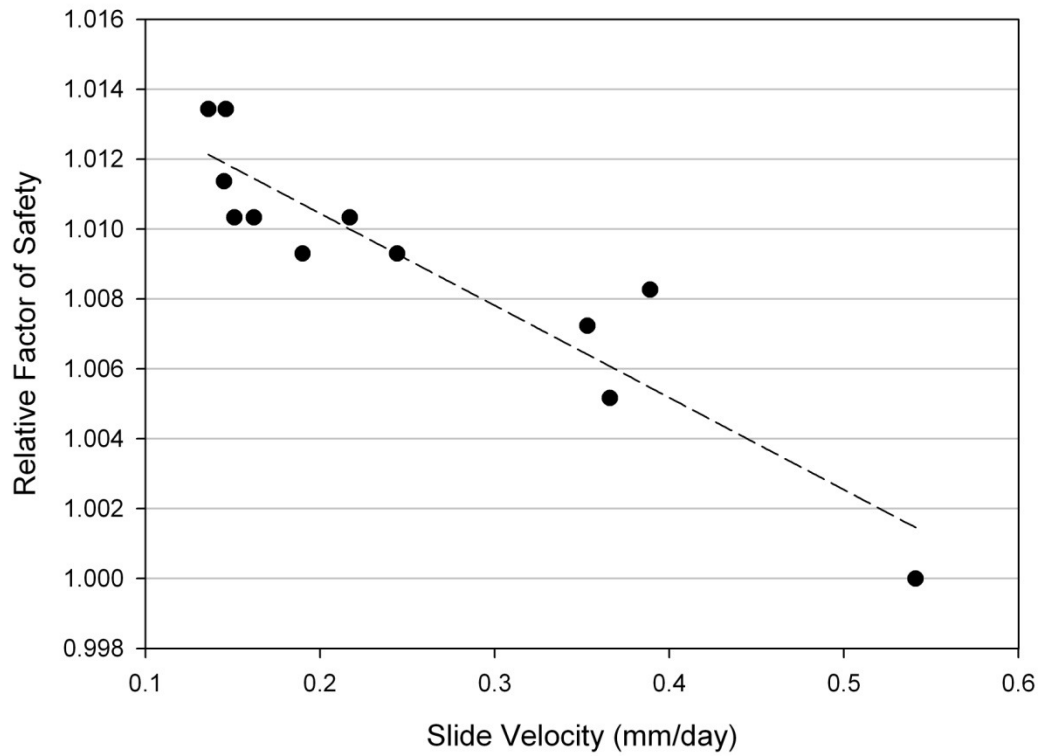


Figure 4.23 - Relation between the factor of safety and rate of movement (as observed at station B) of the Triesenberg landslide

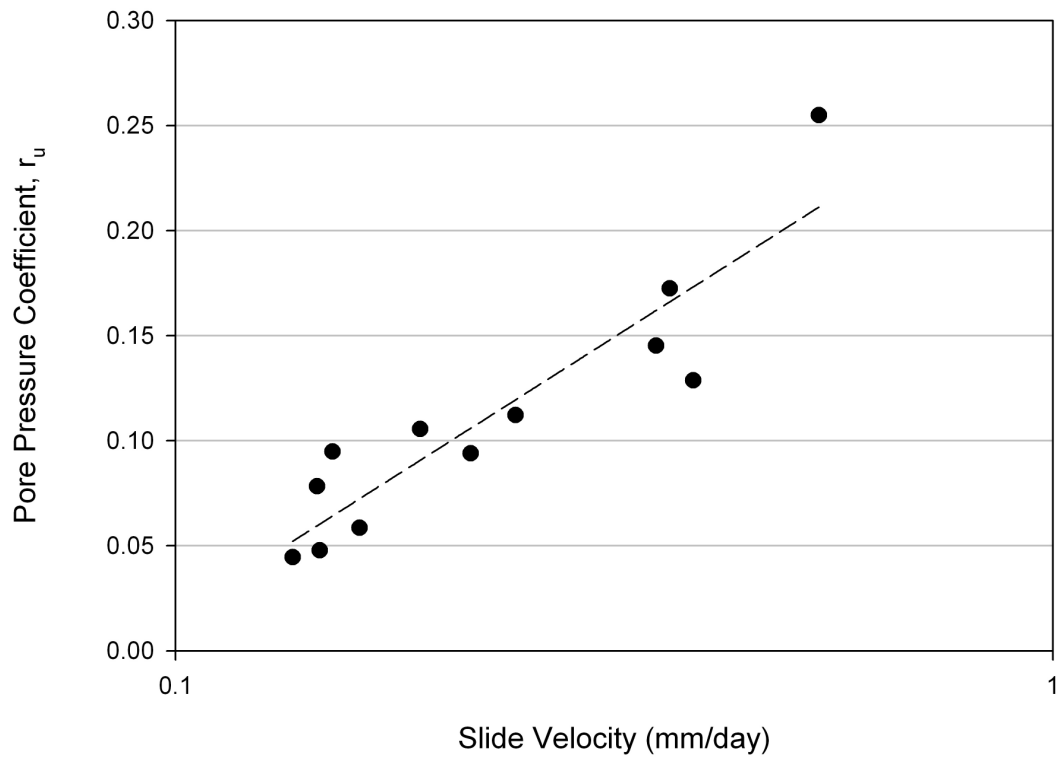


Figure 4.24 – Relation between pore pressure coefficient and slide velocity of Triesenberg landslide at B

4.5 Babadag Landslide

4.5.1 Overview

Babadag is near the west coast of Turkey and 30 km away from the centre of the town Denizli in Aegean region and is located at southern hills of Büyük Menderes graben. The district is in between deep and narrow valleys with occasionally high elevated slopes (Kayıhan and Demirci, 2007). It has a population of 5000 and is known as a historic center of textile industry and it is still producing.

The village of Babadag suffered from a long-term landslide which is sliding since 1940 at a continuous rate of up to 15 cm per year (Cevik and Ulusay, 2005). The main sliding body have a width of 430 m and a length of 650 m (Ozpınar et al., 1999) (Figure 4.26). The landslide is observed by various investigators at different times by making use of various techniques and instruments.

The previous investigations of the displacement of the sliding body were done through aerial photography (Cevik, 2003), relative measurement technique (Ulusay et al., 2006) and movement observation network (Cevik and Ulusay, 2004). Pore pressure and related groundwater level data are taken from Cevik (2003).

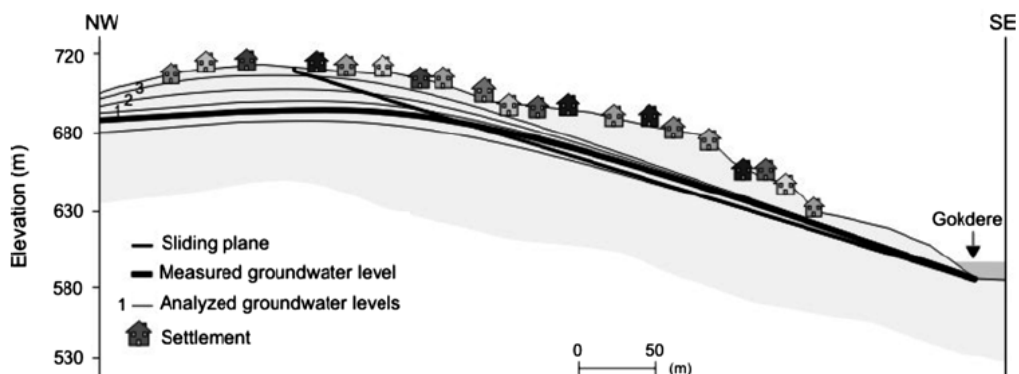


Figure 4.25 – Cross-section of Babadag landslide (Cevik and Ulusay, 2005)



Figure 4.26 – Approximate boundaries of the main sliding body of Babadag (February 2011)

4.5.2 Stability Analyses

The instability of Babadag is caused by planar failure surfaces along bedding planes. Due to the lack of inclinometer data along the slope, the main failure surface cannot be determined precisely. The planar failure surface used in the analyses connects the toe of the slope with the tension crack at highest elevation. It is known that the mass behind that tension crack moves at a very slow rate (Tano et al., 2006), close to zero, implying stationary condition.

Strain controlled laboratory direct shear tests carried out in a 6x6 cm square direct shear box by Cevik (2003) are considered in this study. 34 representative intact block samples taken from the field (samples including the interface between the marl and sandstone members) were assembled in the upper and lower halves of the shear box. Information was not provided on the plasticity of the materials tested. Cevik (2003) noted that since the samples were easily disaggregating when wetted, the laboratory direct shear tests were carried out providing water by a pipette in a controlled manner

and keeping the sample moist during the test. The normal stress range used in the tests was 40-720 kPa by considering maximum 45 m of overlaid material.

Three shearing rates were used in the tests by Cevik (2003); 0.25mm/min, 0.08mm/min and 0.035mm/min for first, second and third group of samples, respectively. Since (i) ASTM D3080 suggests using a slow shearing rate to determine the drained shear strength parameters, (ii) Babadag landslide is a “very slow” landslide (rates of movement on the order of 3×10^{-5} - 3×10^{-3} mm/min according to the classification by Cruden and Varnes, 1996), and (iii) shearing at fast rates give an increased resistance (literature summarized in Huvaj-Sarihan, 2009); Cevik (2003) tests carried out at the lowest rate of 0.035 mm/min were considered in this study. Shearing was carried out up to shearing displacements of 9 mm, and most of the samples reached residual condition after about 4 mm of displacements as can be seen from Figure 4.27. The difference between the peak and residual shear strength values were insignificant and it can be concluded that the samples were at or very close to residual condition. As noted by Morgenstern (1977) and Mesri and Shahien (2003), large shearing deformations may not be necessary in bedded deposits where shearing is restricted to bedding planes or interfaces; and that a few millimeters of movement along subhorizontal discontinuities such as bedding planes, laminations are sufficient to bring these to residual condition.

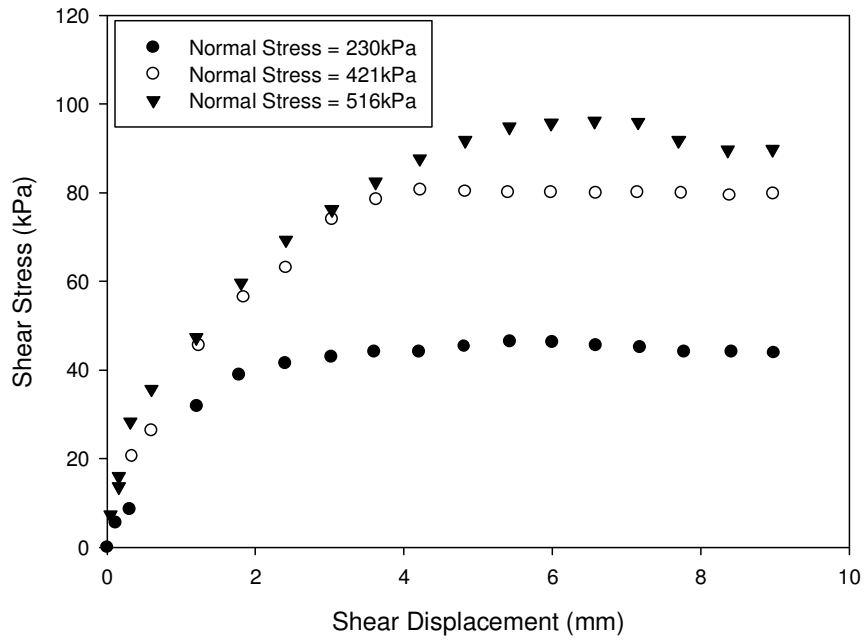


Figure 4.27 - Direct shear test results for 0.035 mm/min shearing rate (modified from Cevik, 2003)

The nonlinear envelope for $I_p=40\%$ shows most compatible curve with the laboratory measured residual values of Çevik (2003) (Figure 4.28).

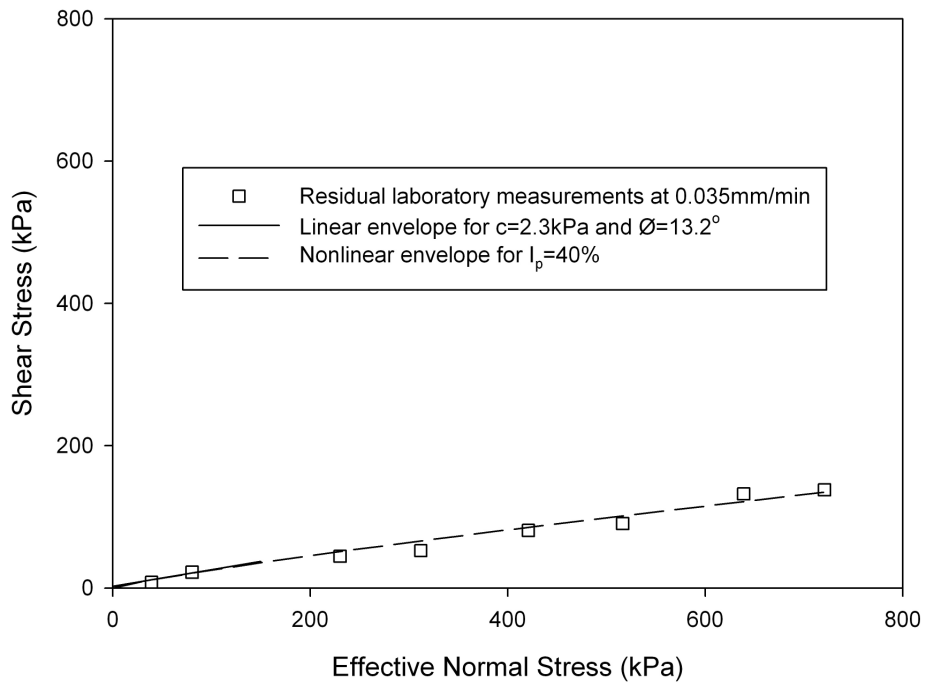


Figure 4.28 – Shear stress envelope for the Babadag landslide

Thereby the equation of the nonlinear envelope is determined as $s(r) = 0.501(\sigma')^{0.850}$. The curve is plotted for the stress range of 0 to 720 kPa considering the maximum effective normal stress extracted from the back-analysis of the slope.

In dry case with $I_p=40$ % the factor of safety is 0.698. When 10 kPa surcharge is added for certain locations of settlement in addition to same conditions, the factor of safety is found as 0.690. The effect of the surcharge is not significant but it slightly changes the level of the instability.

The back-calculated shear strength mobilized at two local, dry and shallow slope failures near Babadag landslide corresponding to $c=2.3$ kPa and $\phi=13.2^\circ$ (Çevik and Ulusay, 2005) is included in the normal stress-shear stress plot. The normal stress range in these two small slope failures is decided to be between 0 and 150 kPa by considering the maximum thickness above the sliding surface of both of the translational failures along bedding planes.

The main sliding body is theoretically divided into 3 portions (upper, middle and lower) to illustrate the displacement behavior of the landslide (Figure 4.29). At each portion a number of representative displacement measurement stations are considered in the analysis.

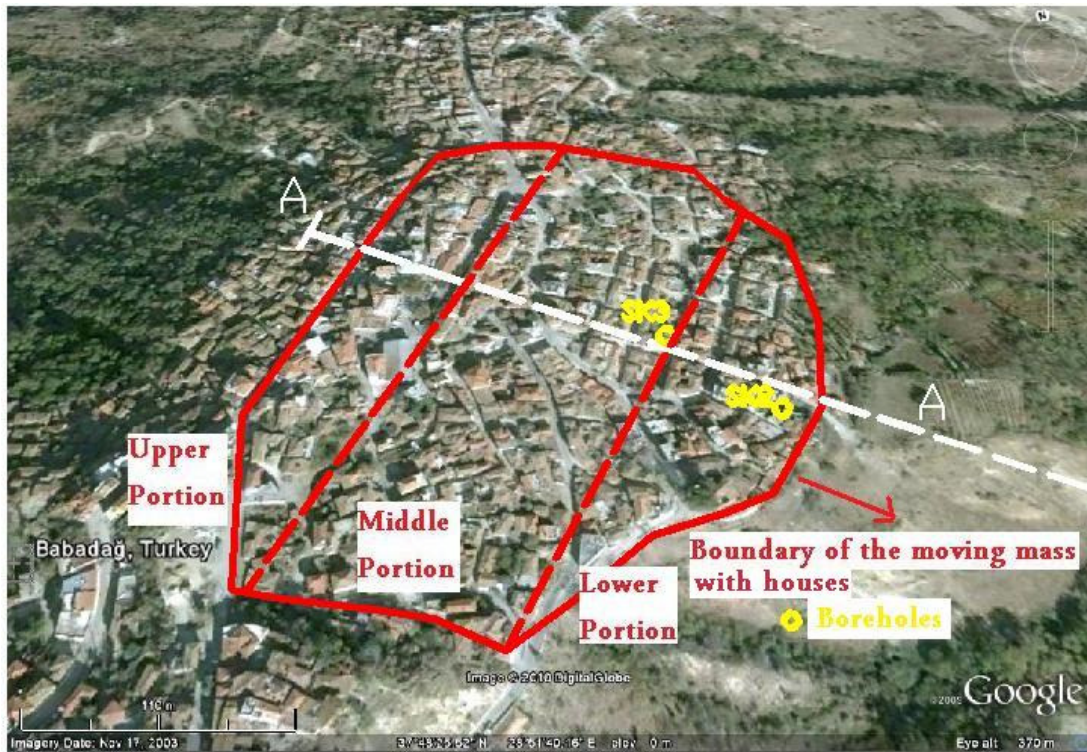


Figure 4.29 - A view from the landslide showing main sliding body and its components

The groundwater conditions due to different piezometric levels are taken into account through averaging the pore pressures under each slice resulting in respective average pore pressure coefficients (r_u) for each condition. Hence the average displacement rates are calculated and compared with the available data of Cevik (2003) between September 2002 and October 2002. Figures 4.30 and 4.31 show relationships between pore pressure coefficient with slide velocity and relative factor of safety. Pore pressure coefficients calculated at the borehole SK2 have values almost twice as values of the entire slope for the same relative factor of safety. It shows that pore pressure coefficient at an individual location may not be a representative of the pore pressure distribution for a slope. It would be wise to take into account more pore pressure measurements covering the whole slope, if possible. However, practically, for real landslides, observation of water level at one location is more applicable rather than observing at several locations and obtaining an average r_u value for the whole slope.

Drastic differences in the ranges of slide velocities between three portions of the slide can be seen from Figure 4.31. In addition, as the movement rates at middle and upper portions of the slide are almost constant, the lower portion accelerates once pore pressure coefficient reaches a value of about 0.08. Especially after the field visit carried out in February 2011, it was very clear that there was some sort of internal deformation within the sliding mass, which caused buildings to tilt and settle in various different directions, rather than a consistent deformation pattern in the direction of slope movement. Therefore the deformations may not correlate well with groundwater level fluctuations in the case of Babadag landslide. However, an attempt is carried out in this study as presented below.

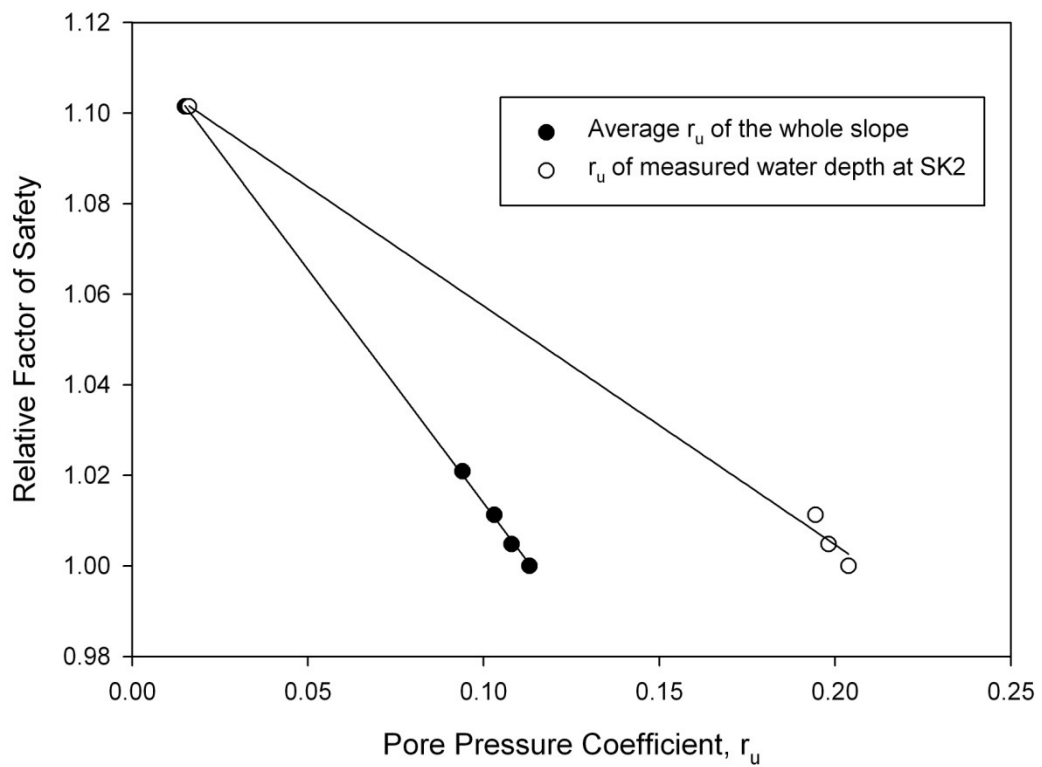


Figure 4.30 – Relation between relative factor of safety and pore pressure coefficient of Babadag landslide

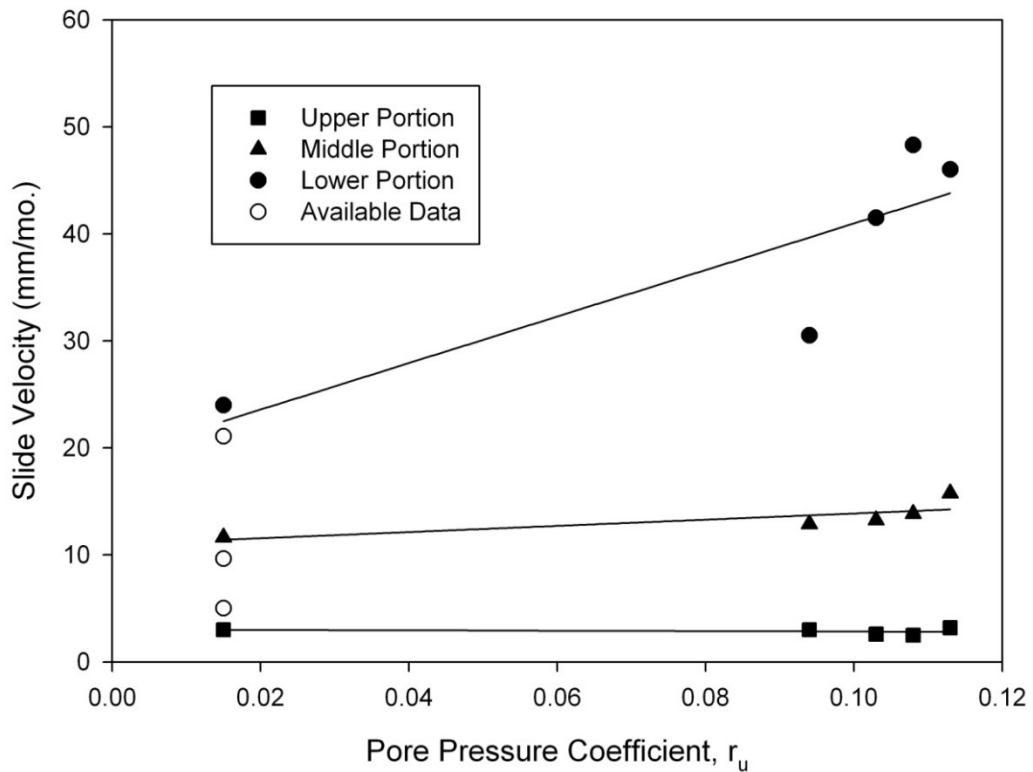


Figure 4.31 – Relation between slide velocity and pore pressure coefficient of Babadag landslide

4.6 Finite Element Analyses

As explained in the “Methodology” chapter, deformation behavior of slides are compared with the results of finite element analysis using Plaxis 2D. Since the elastic properties of slope forming materials are not known, elastic moduli of layers and the shear surface are changed for each analysis and a parametric study is executed.

As examples, total displacements of simplified San Martino landslide at water table configuration of P3 are shown as shadings and as arrows, at Figure 4.32 and Figure 4.33, respectively. The displacements shown by arrows are three times scaled. It can be seen from both figures that displacements mostly occur in the colluvial cover and in the weathered marl zone where slip surface is modeled.

Results are plotted on Figures 4.34, 4.35 and 4.36. The effect of the selected elastic moduli are shown, such that on the y-axis the ratio of elasticity modulus of layer above the shear surface to the one of the shear surface is represented where on the x-axis the average ratio of calculated velocity to measured velocity is given. The plots cover the results of 60, 98 and 99 different performed analyses with different piezometric conditions and elastic moduli, for San Martino, Steinernase and Vallcebre landslides, respectively. Drained residual shear strength parameters that are used are given in Appendix Table A.2.

The slope geometries are simplified as much as possible in order to overcome unrealistic solutions and to prevent difficulty of interpretation and to avoid creation of numerical difficulties that can mask the real solution.

As the hydraulic properties, the information on the amount of runoff and evapotranspiration of the slopes are lacking, therefore it was impossible to model time dependent groundwater flows. Instead of that, groundwater levels are modeled by separately introducing measured piezometric levels at different times. Consequently, the rate of movements are calculated by considering the time intervals during which corresponding piezometric levels stay effective.

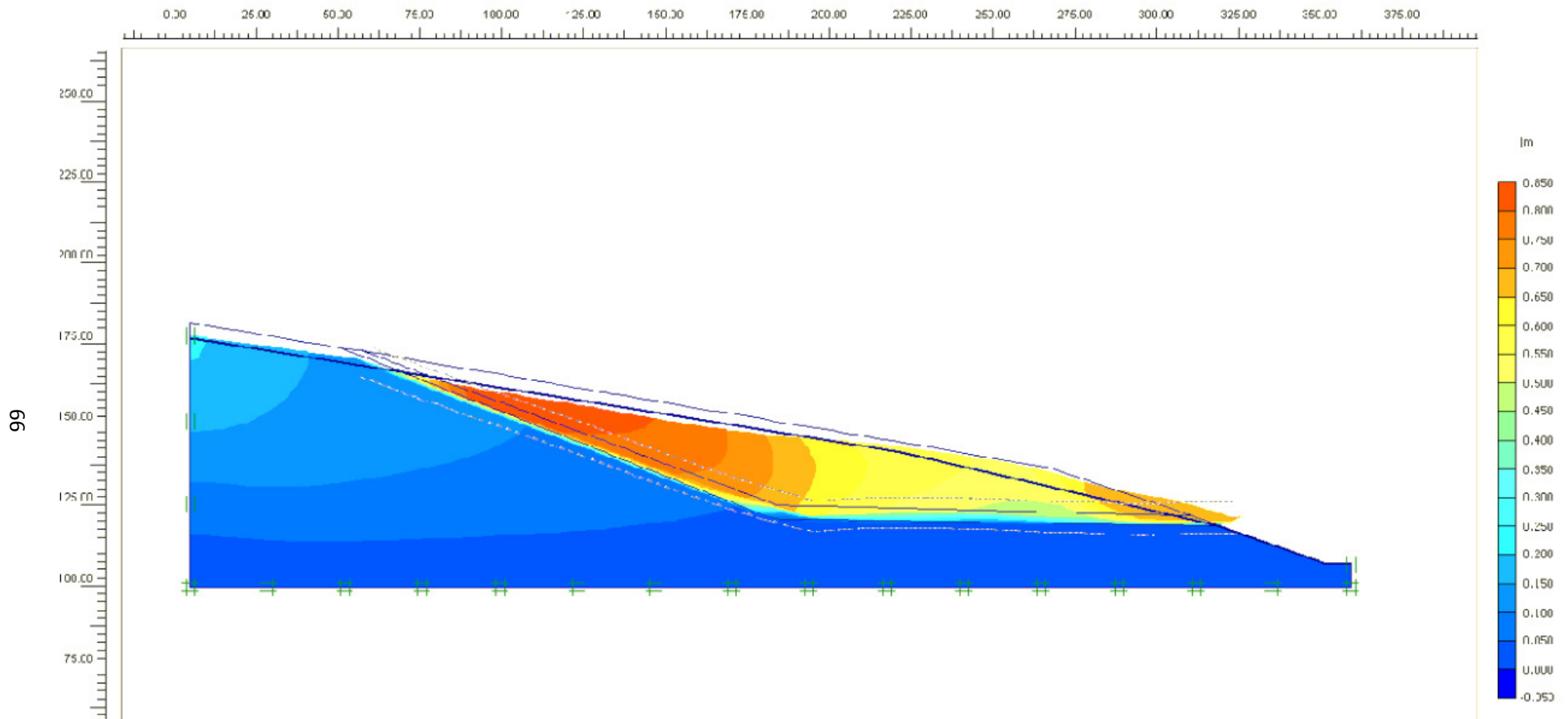


Figure 4.32 – Total displacements (as shading) of simplified San Martino landslide model at time P3

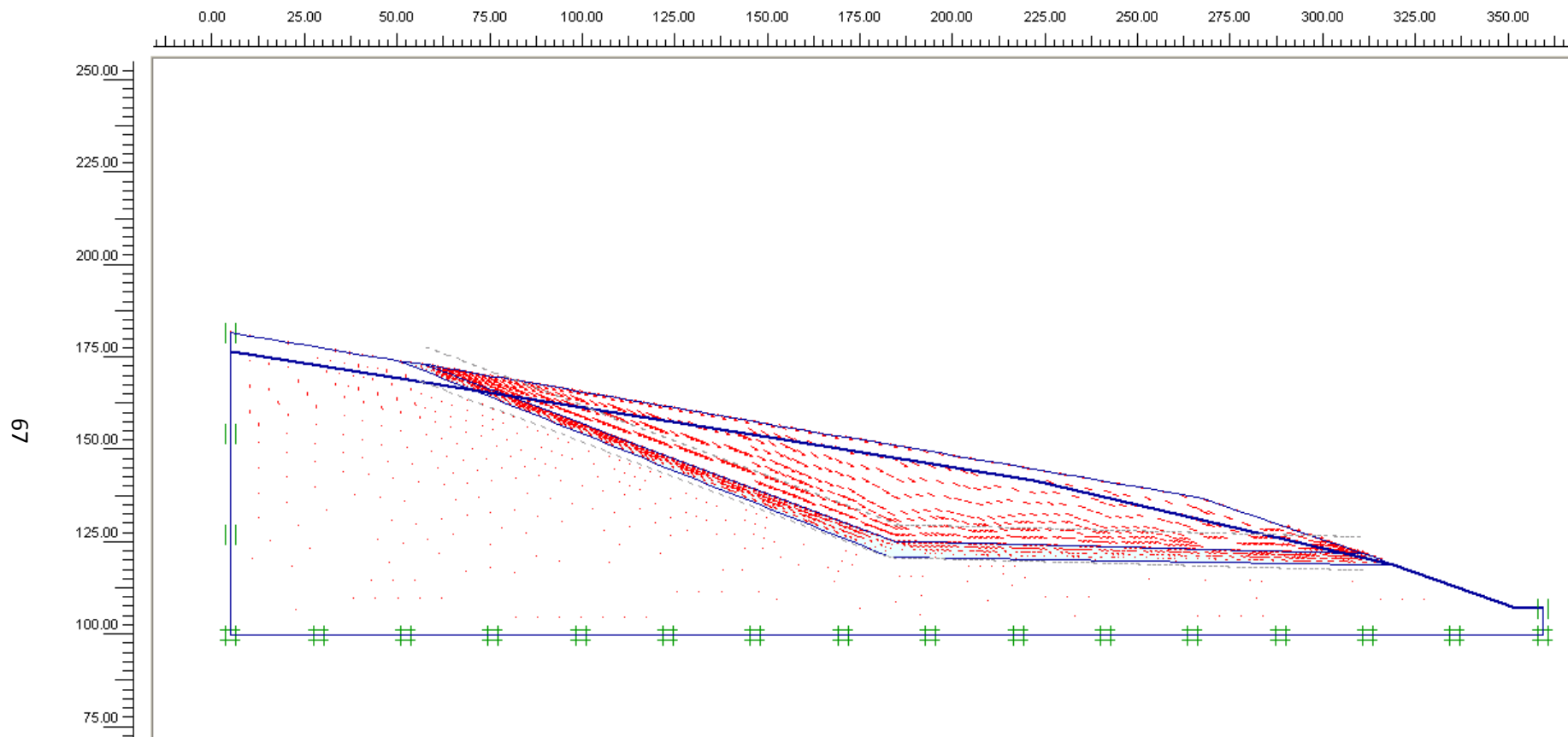


Figure 4.33 – Total displacements (as arrows) of simplified San Martino landslide model at time P3

Actual inclinometer readings give displacements perpendicular to the axis direction where the borehole axis of all selected cases are vertical. Therefore horizontal displacements are to be compared with analysis readings, so that horizontal displacements are read from outputs. The nodes of which readings are to be done are selected carefully in order to represent the location of each inclinometer.

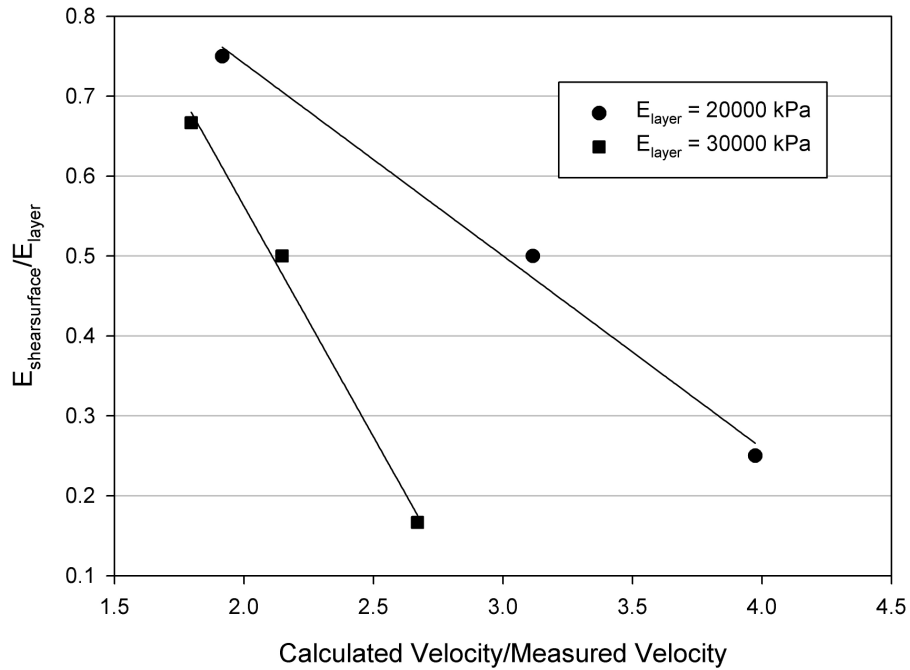


Figure 4.34 – Deformation analyses results of San Martino landslide

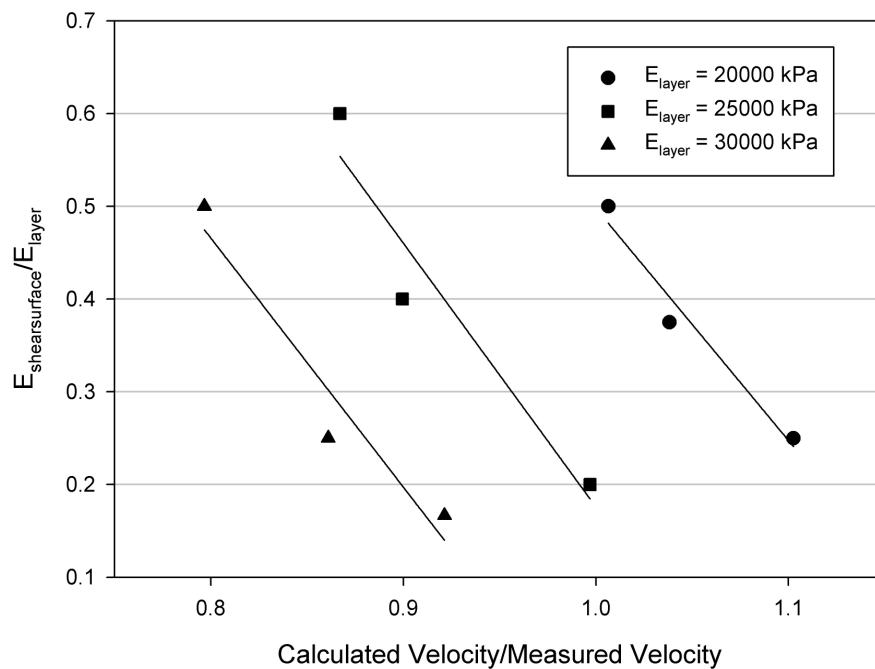


Figure 4.35 – Deformation analyses results of Vallcebre landslide

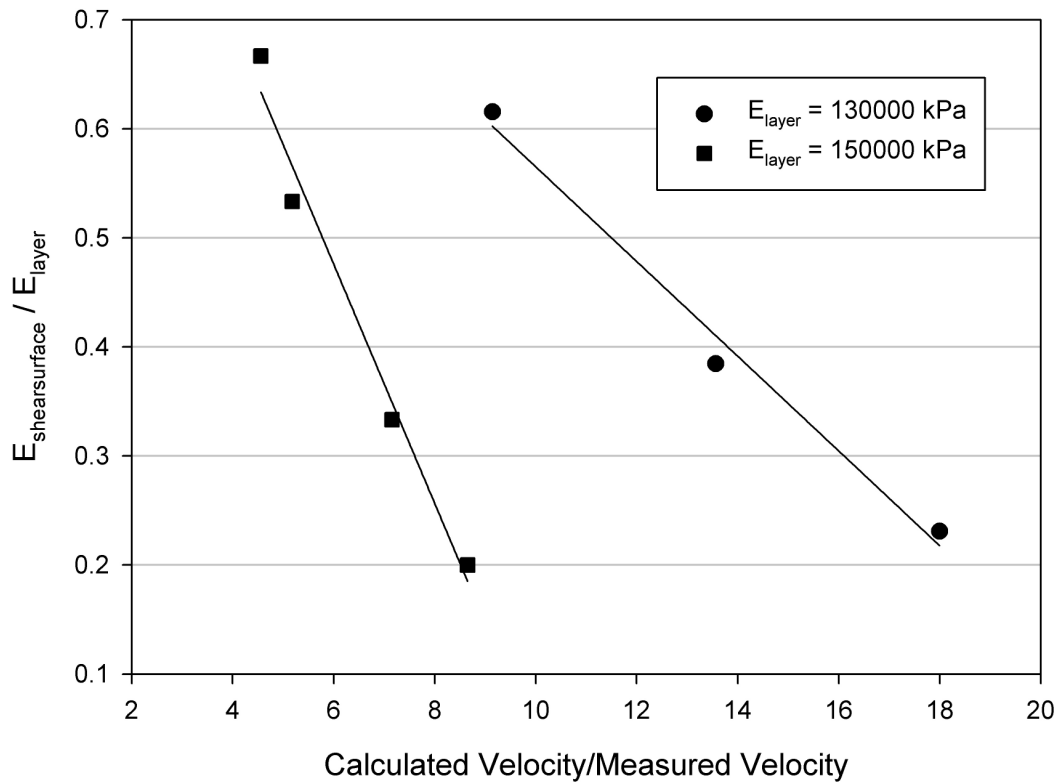


Figure 4.36 – Deformation analyses results of Steinernase landslide

It can be seen from the results of finite element deformation studies that selection of material parameters significantly affect the results obtained. The ratio of calculated velocity to the measured velocity could range from 1.0 to 15.0 for the landslide cases studied in this thesis. For Steinernase landslide, since the material is mostly sandy with about 20% fines content, a higher stiffness modulus can be used as compared to the other landslides. However, even with a very high modulus, finite element calculated velocity is still overestimating the measured velocity by about 5 to 15 times. From the results of other landslides, it can be seen that when the stiffness of the shear surface is taken to be about 0.6-0.8 times the stiffness of the overlying material, calculated velocities that are 1-2 times the measured velocities can be obtained.

If advanced constitutive models are used for the materials, especially for the material in the shear zone, we could capture the time dependent creep deformation behavior.

However, for practical purposes, it is suggested here that, parametric analyses can be conducted for each specific landslide to see range of the ratio calculated/measured velocity. Based on this information for that specific landslide, correlations can be developed for deformations that could lead to rough guidelines for early warning alarm levels. For example, if it is discovered that the calculated velocities are about 5 times the measured velocity, this factor can be taken into account in calibrating the deformations obtained from the numerical analysis. Even if no such factor is applied, forecasting larger movement rates as compared to real rates, would lead to giving unnecessary false alarms, rather than the more dangerous case of giving no-alarms. However, both of these wrong alarms could harm the trustability of an early warning system.

4.7 Kinematic Analyses

Nonlinear empirical relationships between factor of safety and rate of displacement of four of landslides are given in Figure 4.37. These relationships are formed using the values for minimum and maximum velocities, relative maximum factor of safety given in Table 4.2. The meaning of each parameter related to the Equation 3.2 is explained under “Methodology” chapter.

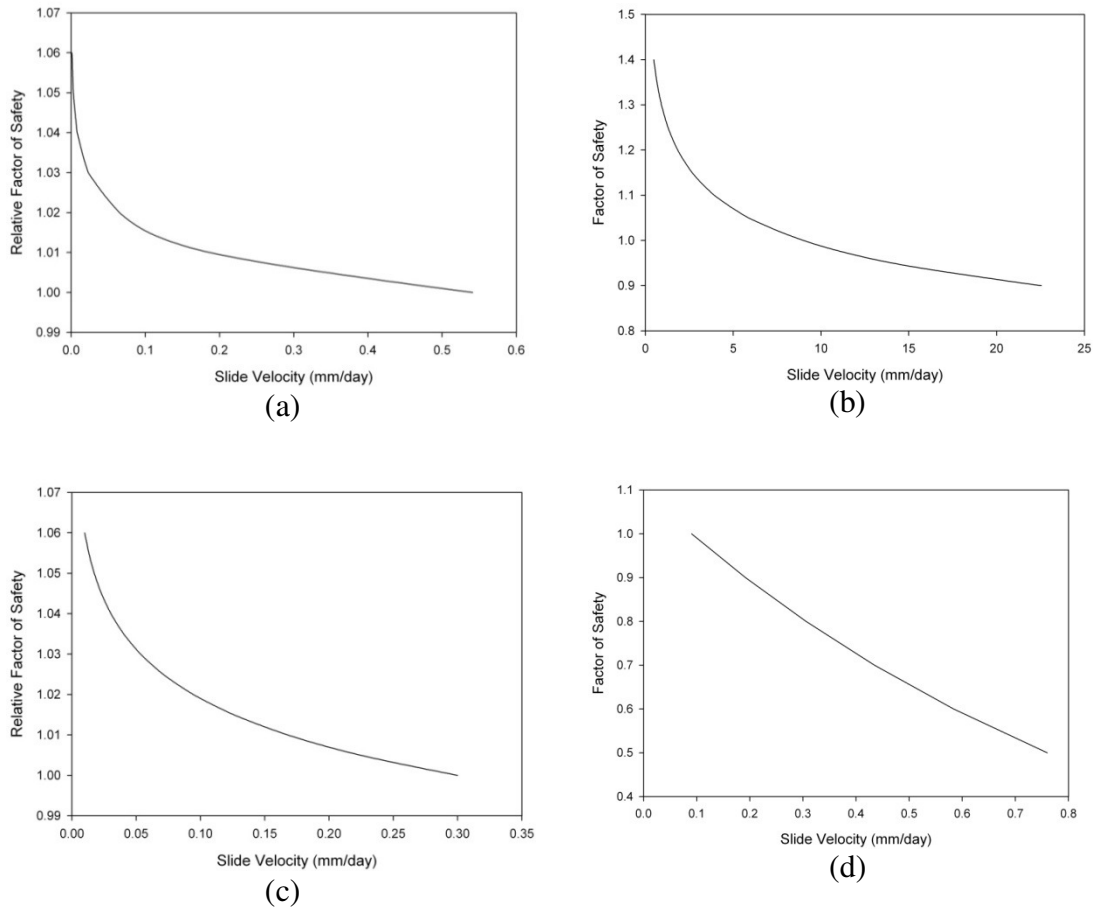


Figure 4.37 - Nonlinear empirical relationship between relative factor of safety and rate of displacement for (a) Triesenberg, (b) Vallcebre, (c) San Martino, (d) Steinernase landslides

The results of analyses are given in Figures 4.38-4.41 in comparison with measured values during the given time interval. Correlation coefficients between measured and calculated values of slide velocities are also indicated in Table 4.2.

Table 4.2 – Parameters used in kinematic analyses with correlation coefficients

	San Martino	Triesenberg	Vallcebre	Steinernase
v_{\min} (mm/day)	0.050	0.136	1.200	0.010
v_{\max} (mm/day)	4.000	0.541	9.000	0.080
Rel. F_{\max}	1.080	1.013	1.260	1.098
Corr. Coeff.	0.982	0.912	0.899	0.966

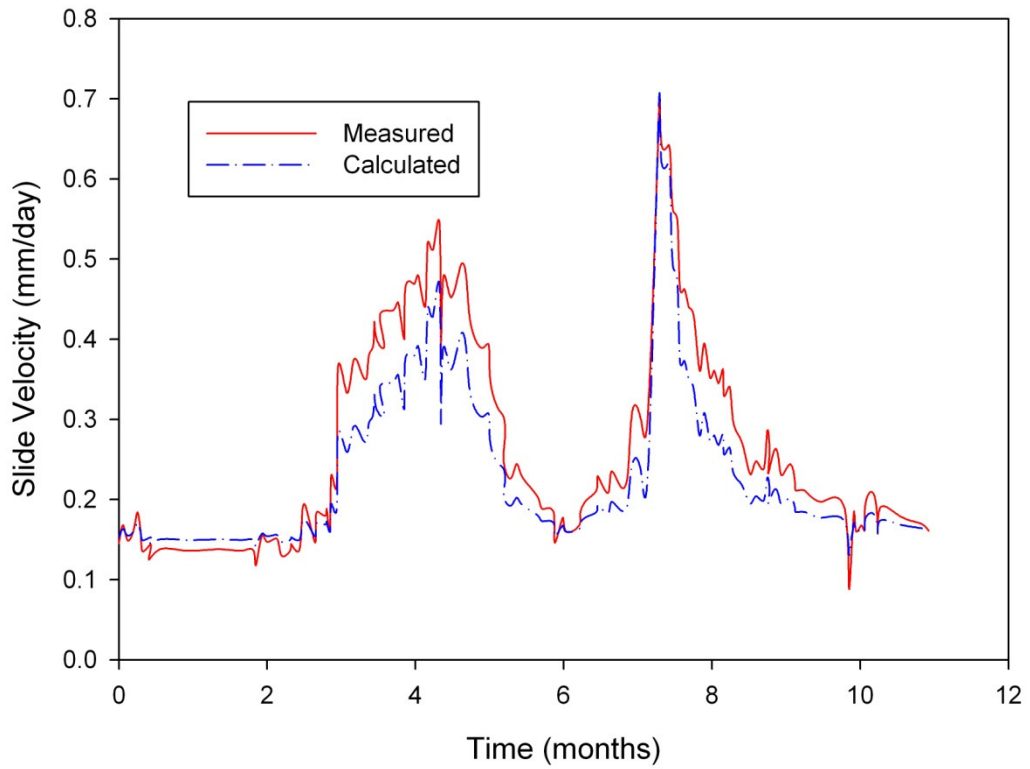


Figure 4.38 – Results of kinematic analysis for Triesenberg landslide

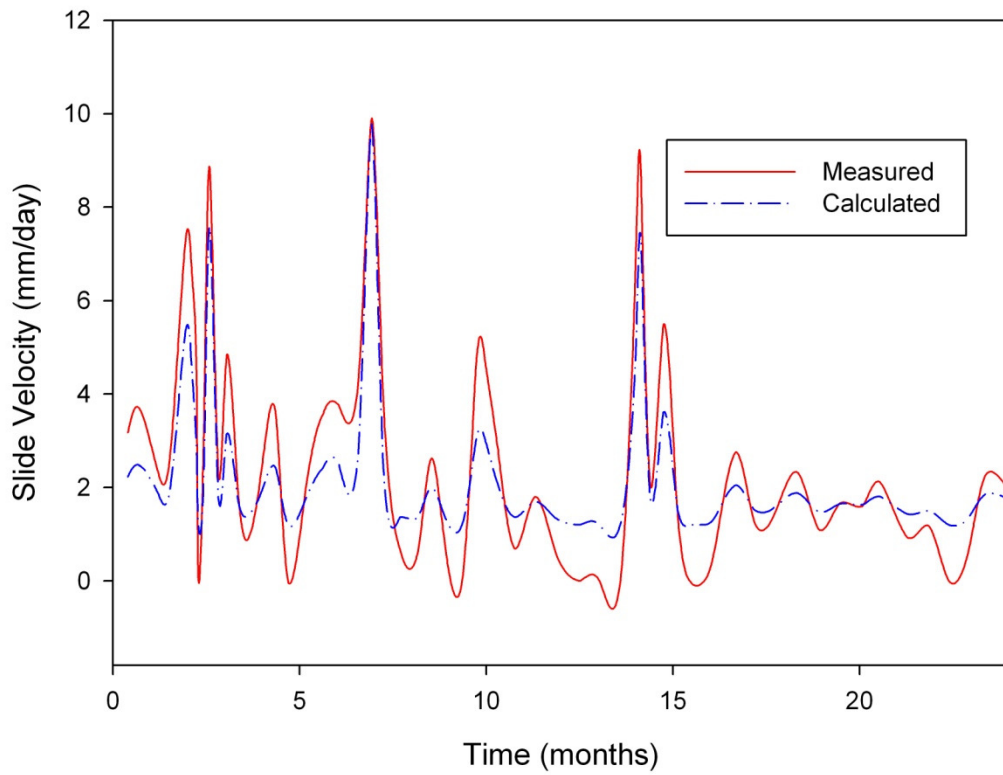


Figure 4.39 - Results of kinematic analysis for Vallcebre landslide

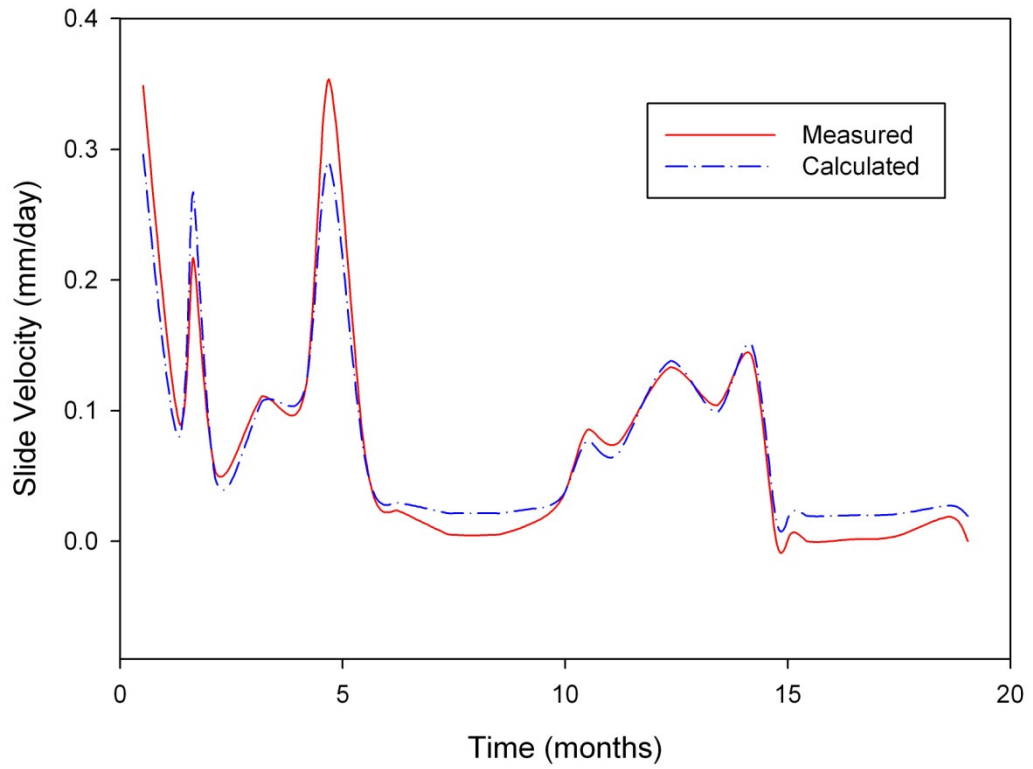


Figure 4.40 - Results of kinematic analysis for San Martino landslide

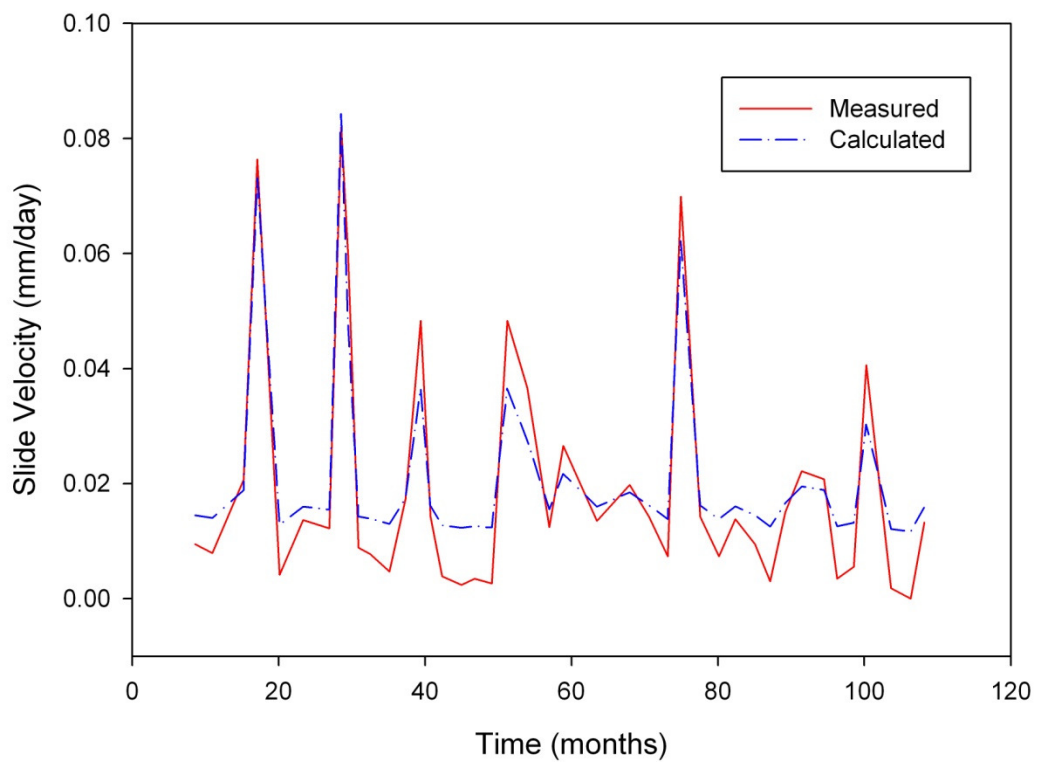


Figure 4.41 - Results of kinematic analysis for Steinernase landslide

CHAPTER 5

DISCUSSION OF RESULTS

5.1 Results of Stability Analyses

The relationships between pore water pressure, factor of safety and rate of movement in slow-moving reactivated landslides in cohesive soils are investigated through five landslide cases. In this chapter the results of analyses of each slide are gathered in order to evaluate from a more general point of view. Similar studies in the literature are also incorporated to compare the results and to possibly support conclusions. At each landslide case instant slide velocities are calculated at each measured displacement data and coupled with factor of safety values for the corresponding dates. At Figure 5.1 slide velocities are plotted against relative factor of safety for all selected cases and also for the cases reported in the literature by Bonnard and Glastonbury (2005). Thus the deformation behavior of slow landslides are demonstrated illustratively. The deformation behavior of some earthflows and debris slides were similarly analyzed by Bonnard and Glastonbury (2005).

Since the slow slides that are discussed in this thesis are reactivated/active and continuously moving, the concept of relative factor of safety can be quite acceptable. It is worth to mention that the term “continuously” here refer to the state of mobility for a given respectively long period of time not to the phenomenon of sliding without any stopping. In fact, this type of landslides becomes stable during dry seasons; i.e. the movements are intermittent. It should be noted that the calculated factor of safety values are not necessarily representative of the overall stability of the whole slide, as in the case of “F.S.>1.0 stable, F.S.<1.0 unstable” which is not very meaningful for a landslide that already has F.S. at or very close to 1.0, and already moving.

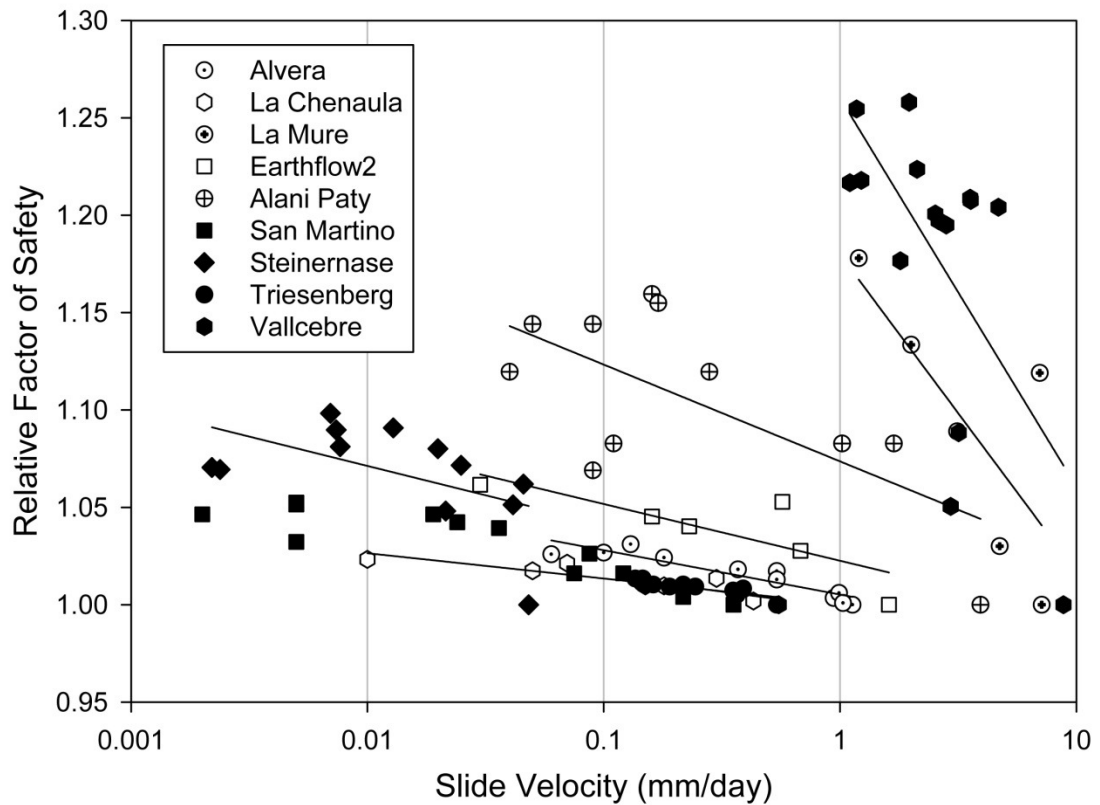


Figure 5.1 - Relative factor of safety against slide velocity of the four selected landslides in this study (shown by black symbols) in comparison with results of other slides reported by Bonnard and Glastonbury (2005)

From relative factor of safety against slide velocity plot one can derive that relative sensitivity of the slide to fluctuations of pore pressure is related to velocity of movement and relatively faster moving slides have reduced sensitivity to groundwater changes as indicated by the steep slopes of lines in Figure 5.1. For “very slow” and “extremely slow moving” landslides (velocity <4 mm/day), the slope of the lines in Figure 5.1 are less steep indicating that small increase in the F.S. can significantly decrease the slope movement rate.

Similar to Bonnard & Glastonbury (2005), relative change in factor of safety for 10-fold change in velocity is evaluated (Table 5.1). In this table the material name, angle and thickness of the moving mass and r_u -range of the slopes are given, too. The relative change in factor of safety for 10-fold change in velocity refer to the

sensitivity of the slide movements to fluctuations of groundwater tables. Small values of this parameter indicate that a slight increase in the F.S. can reduce the rate of movements drastically. For example, for Steinernase landslide in Figure 5.1 it can be calculated that 6.8% increase in F.S. can change the velocity of the sliding mass by 1 order of magnitude. Extensive database of such correlations may allow prediction of landslide movement behavior for a certain material/slope/region. This information can be useful in planning remediation works. For example, as part of a remediation study, we can decide on the range of allowable velocity for an actively moving mass, e.g. 0.1 mm/day, and we try to achieve corresponding F.S. value by trying different slope stabilization alternatives.

Table 5.1 – Percent change in factor of safety for 10-fold change in velocity

Name	Material	Average Slope Angle (deg.)	Thickness of the sliding mass (m)	r_u -range	% change in F.S. for 10-fold change in velocity
San Martino	Weathered marly clay	8-10	24	0.41 - 0.47	2.2
Steinernase	Colluvial cover	17	14	0.23 - 0.33	6.8
Triesenberg	Clayey silt matrix	24	33	0.14 - 0.54	1.6
Vallcebre	Fissured shales	10	30	0.28 - 0.44	23
Babadag	Sandstone & marl	16	30	0.01 - 0.11	--
La Mure*	Varved clay & silt	15	5	0.16 - 0.29	16.3
Alani Paty*	Basalt & tuff	12	6-10	0.21 - 0.34	5.0
Earthflow 2*	High plasticity clay shale	10.5	6	0.14 - 0.19	2.9
Alvera*	Sandstone, marl, mudstone	7.5	17	0.42 - 0.44	2.3
La Chenaula*	Argillaceous strata	11	12	0.31 - 0.40	1.3
Ragoletto**	Weathered limestone	10	30	0.05 - 0.27	25.7
Slide 114**	Schist foliation	21	27.8	0.14 - 0.20	3.4
Slide 90**	Schist foliation	31	26	0.00 - 0.21	31.9
Slide 10**	Schist foliation	21-27	16	0.09 - 0.21	56.7
Slide 7**	Quartz schist	27	93	0.00 - 0.01	0.6
Slide 15**	Quartz schist	26	47	0.07 - 0.08	4.7
Slide 113**	--	--	8	0.00 - 0.13	--
Slide 111**	Schist foliation	25	31	0.04 - 0.29	24.8
Brewery Creek**	--	--	23	0.27 - 0.28	0.4
Slide 115**	Grey mica schist	18-24	15.5	0.11 - 0.12	0.5

* Mudslides, ** Translational debris flows (Bonnard and Glastonbury, 2005)

Pore pressure parameter r_u can also be used in the correlations with rate of movement, therefore eliminating the need for the F.S. parameter. This can only be done for slopes, the stability of which are known to be governed only by the changes in pore pressures in the ground. If there are other mechanisms, e.g. toe erosion by a river, earthquake triggering etc. there would not be a clear correlation between r_u and movement rates. The correlation between pore pressure coefficient and slide velocity is plotted on Figure 5.2. Such a figure can be helpful to decide on the desired depth of groundwater to slow down the movement to acceptable rates (< 50 mm/year; shown as “typical creep rate”) in planning the level of remedial work required and in risk mitigation. The groundwater level to be considered is located at the piezometer/piezometers which is/are used to represent the whole slope. The depths of water level are to be calculated from pore pressure coefficient values at this specific piezometer. It should be reminded that correlation can be expected between r_u value and slide velocity, if the only mechanism controlling the movements is the changes in pore pressures.

The value of “allowable/tolerable movement rate” comes into play in relation to landslide stabilization works for slow moving landslides. This allowable rate is to be decided for each specific area of slope stabilization. Based on an extensive literature search on landslides, in addition to laboratory creep movement measurements, typical creep rates that is occurring in all slopes composed of clayey soils are determined to be on the order of 2-50 mm/year (Huvaj-Sarihan, 2009). If there are important structures at the toe of a slope, we may not want to allow rates of movement larger than creep rates (on the order of <50 mm/year, i.e. <0.14 mm/day). However, for a landslide in a rural area where there is only a village road passing through the slope area, we can take a higher risk and accept allowable/tolerable velocity as 10 mm/day. This decision is case specific and cannot be generalized, however creep rates can be considered as acceptable in the case of no other information. During the observed period of the Steinernase landslide the velocities fall into typical creep rates but an increase of pore pressure coefficient above 0.3 may result in crossing to the unacceptable rates of movement. San Martino landslide however passed to higher rate levels (>0.14 mm/day) on occasion. These emphasize

the importance of continuous monitoring of pore water pressure for critical extremely slow and very slow landslides.

The values of r_u that are closer to 0.5 indicate that the ground water level is close to ground surface (e.g. San Martino in Figure 5.3). Similar to San Martino landslide two other cases, Alvera and La Chenaule slides, from Bonnard and Glastonbury (2005) are closer to 0.5 with r_u -ranges between 0.40 and 0.44. It is noted that, these three slides have very small percent changes in factor of safety per 10-fold change in velocity, having ranges between 1.3 and 2.3. These similarities can be the result of similar properties of slope forming material and infill material as (i) Plasticity index = 15-30 %, (ii) Activity index (ave.) = 0.6, (iii) Residual angle of friction of slide mass = 20° , (iv) Residual angle of friction of infill material = $16-17^\circ$, and, (v) Thickness above the slip surface = 17-24 m, which affects the average effective normal stress acting on the shear surface. With development of extensive database of case histories, which have detailed material properties and monitoring information, more of such conclusions can be obtained.

From Figure 5.3, it can also be seen that slightly faster moving (but still in “slow” category) landslides, display less sensitivity to changes in r_u value, i.e. significant reduction in r_u (e.g. a decrease in ground water level) is needed to reduce movement rates to slow acceptable rates.

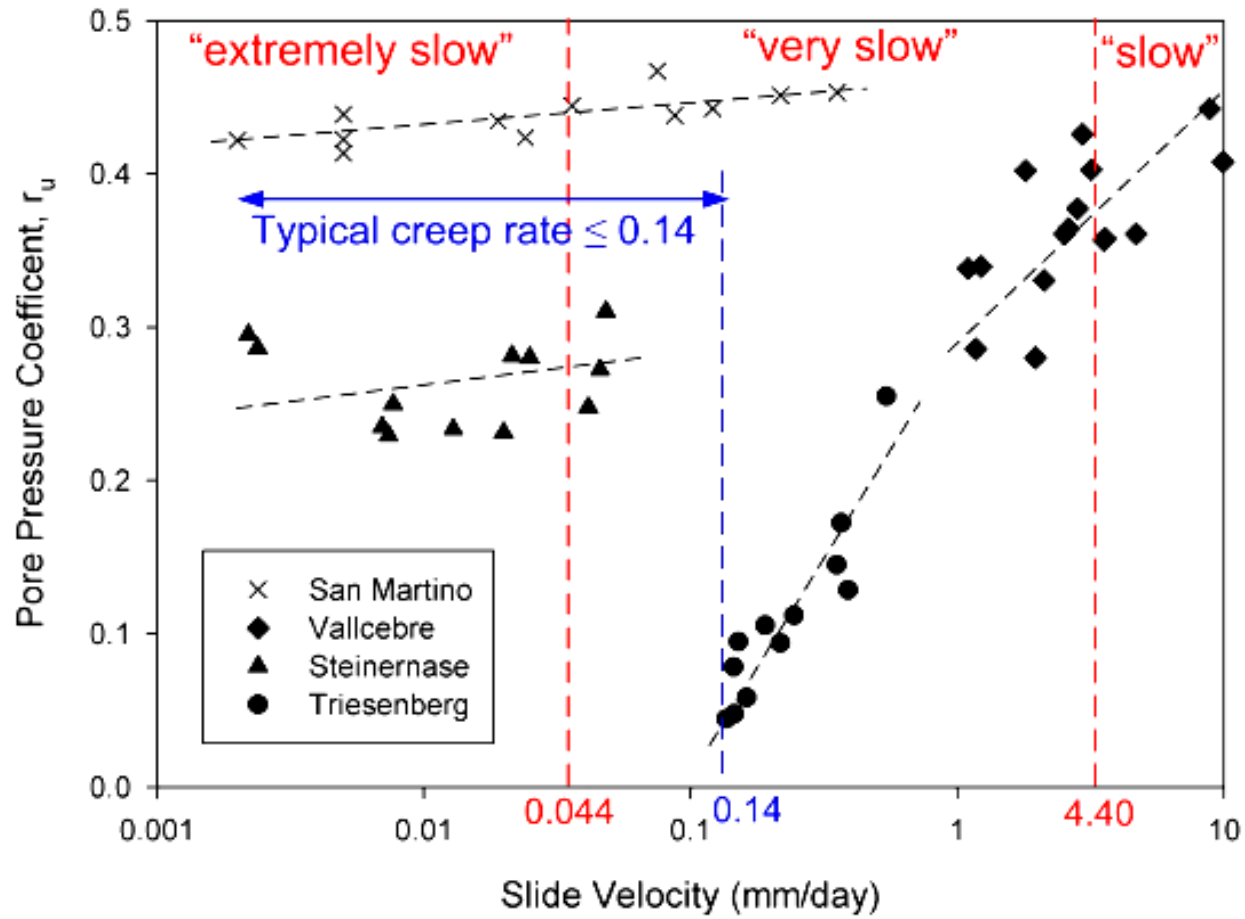


Figure 5.2 – Relation between landslide velocity and pore pressure coefficient r_u of selected cases

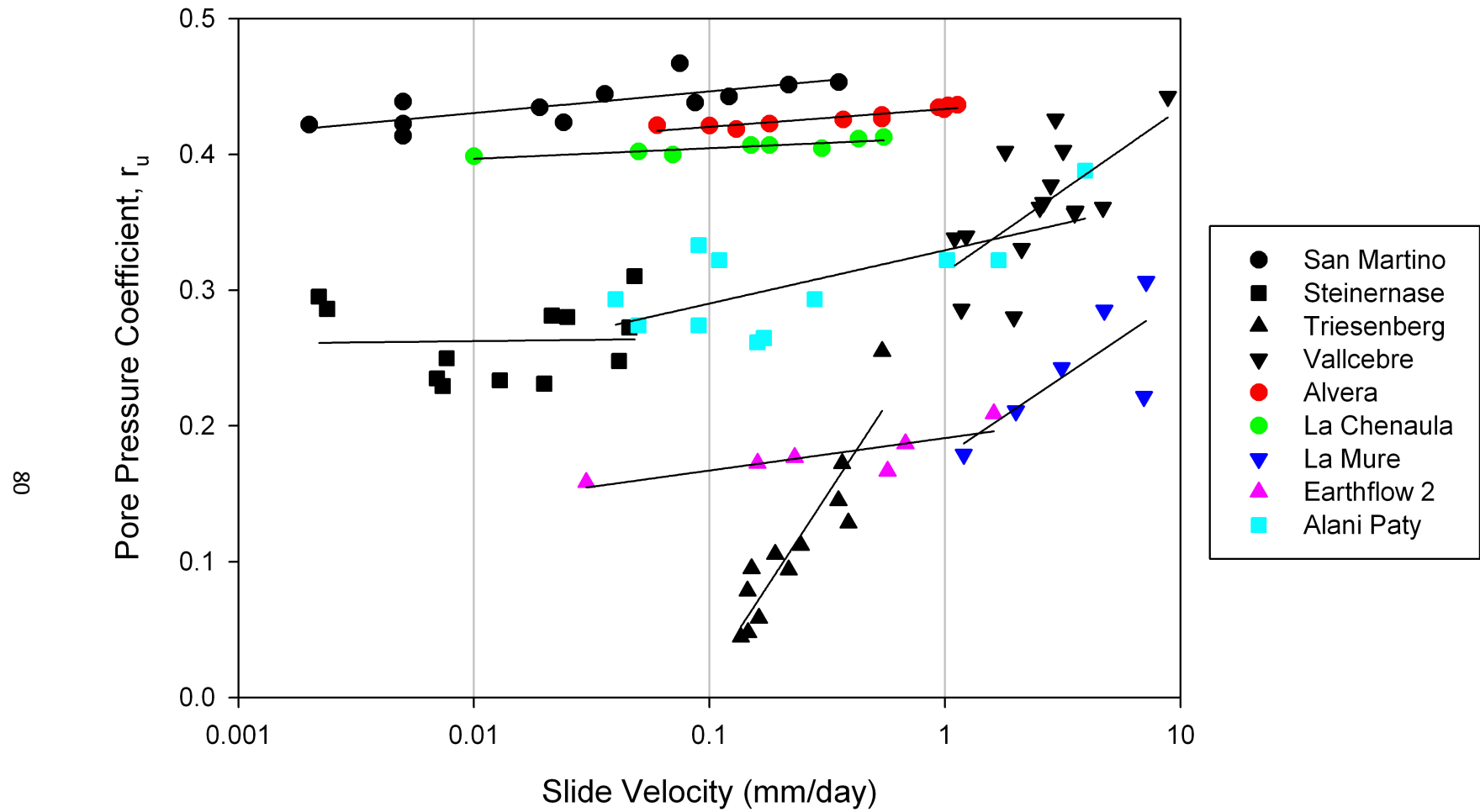


Figure 5.3 – Relation between landslide velocity and pore pressure coefficient r_u of selected cases with mudslide cases of Bonnard and Glastonbury (2005)

The change in pore pressure coefficient r_u for 10-fold change in velocity is calculated for the cases studied in this thesis (Table 5.2). Greater values of this percentage indicate greater ranges of groundwater table fluctuations. The fluctuations of groundwater may imply the amount of rainfall/meltwater and/or hydraulic characteristics of slope materials. Moreover, this information is very useful for stabilization works, as it was also the case for F.S.. With the knowledge of “change in pore pressure coefficient for 10-fold change in velocity” for a slope, we can propose to stabilize a slope by reducing r_u value, being monitored at a point along the slope, to such a value rate of movements will reduce to allowable rates.

Table 5.2 – Change in r_u for 10-fold change in velocity

Landslide Name	Change in pore pressure coefficient for 10-fold change in velocity
Vallcebre	16 %
San Martino	1 %
Steinernase	2 %
Triesenberg	39 %

Therefore, a sensitivity parameter is proposed to indicate the significance of changes in pore pressures on the factor of safety of a slope and the sensitivity of slopes to groundwater level fluctuations. This sensitivity parameter is denoted here as $\Delta\text{FS}/1\text{m}$, and it represents the decrease in F.S. for a 1-m-rise in the water level (i.e. an increase in the $r_u = u / \gamma h$ value by about 0.05 for a 10 m thick translational slide). For the four landslides in this study the sensitivity values range between 0.003 and 0.05, the latter being the more sensitive slope (Table 5.3).

Bishop (1955) noted that “It is useful from the design point of view to know the influence of possible variations in construction pore pressure on the factor of safety, and for this purpose the factor of safety may be plotted directly against average pore pressure ratio”. Understanding the sensitivity of a slope to changes in pore water pressure is also useful in order to quantify the significance of the error in the pore water pressures used in the slope stability analyses. This was pointed out by Bishop (1955), as well as by Yucemen & Tang (1975) in their study of evaluation of uncertainties in the long term stability of soil slopes.

Table 5.3 - Change of FS for 1 m rise in groundwater level

Material	Reference	Landslide Name	Calculated FS using the most likely pore water pressure at failure	Decrease in the value of F.S. for 1 m rise in groundwater level	Ratio = FS(1 m increased) / FS(most likely)	Approx. slope (ground surface) angle (degrees)	Max. soil thickness (m)	Failure type	Shear surface material properties
Boulder clay till	Bishop (1955)	---	1.38	0.10	0.93	20	16	Circular	$\gamma=22.8 \text{ kN/m}^3$, (lab direct shear $c=17 \text{ kPa}$, $\phi=37.5^\circ$)
Weathered marly clay	Bertini et al. (1984)	San Martino	1.061	0.033	0.969	8-10	24	Translational	$I_p=27\%$, $CF=25-50\%$, $\gamma=21 \text{ kN/m}^3$, CL , Particles $<0.02 \text{ mm}=76-93\%$, $c_p=15 \text{ kPa}$, $\phi_p=24 \text{ deg.}$, $c_r=0 \text{ kPa}$, $\phi_r=27 \text{ deg}$
Fissured shales	Corominas et al. (2005)	Vallcebre	1.026	0.050	0.951	10	30	Translational	$\gamma=22 \text{ kN/m}^3$, $c_p=0 \text{ kPa}$, $\phi_p=38.7 \text{ deg.}$, $c_r=0 \text{ kPa}$, $\phi_r=7.8 \text{ deg}$
Colluvial cover	Laloui et al. (2008)	Steinernase	0.984	0.024	0.976	17	14	Translational	$CF=15-28\%$, Particles $<0.02 \text{ mm}=48-65\%$, $c_p=0 \text{ kPa}$, $\phi_r=24 \text{ deg.}$
Clayey silt matrix	François et al. (2007)	Triesenberg	0.975	0.003	0.997	24	33	Translational	$I_p=11\%$, Particles $<0.02 \text{ mm}=38\%$, SC , $c_p=11 \text{ kPa}$, $\phi_p=30 \text{ deg.}$

5.2 Results of Deformation Analyses

Deformation analysis is done by utilizing a 2D plane strain finite element code. The results of analyses gave an insight of deformation behavior of slow landslide cases while the deformation properties as the elastic modulus and poisson's ratio are not known. By proportioning the calculated velocity to measured velocity for different elastic moduli of the shear surface and layers above it, the effect of elastic moduli is observed. For some cases such as the Vallcebre landslide the velocity ratio around unity is found. In this case the selected elastic moduli may represent the real condition but it should not be forgotten that the failure criteria for the shear surface is defined by Mohr-Coulomb failure criteria like all of other layers. Advanced constitutive models can be used to accurately calculate the deformation behaviour, however, they require more input parameters, which may not be available.

5.3 Results of Kinematic Analyses

Kinematic analysis is essentially useful if a groundwater analysis is conducted or groundwater levels are monitored continuously. In this study measured groundwater levels and sample displacement data are used to compute rate of displacements for a given certain time interval. If a groundwater analysis can be conducted without lacking the water retention (i.e. soil moisture characteristic) curves and permeability functions of all slope materials as well as net and gross rainfall amounts, then there will not be any need to observe groundwater levels. Instead, only rainfall data can be inputted into kinematic analysis. High correlation coefficients found between measured and calculated data imply reliable compatibility of relationships between velocity and factor of safety of limited measurement data with the data that is continuously measured. In other words, this indicates how well the sample data represents the population data. The compatibility among these is important since for some landslides continuous monitoring may be costly and/or hard or even impossible.

CHAPTER 6

CONCLUSIONS

6.1 Conclusions

In this study, relations between the pore water pressure, factor of safety and the rate of movement in reactivated slow moving landslides are investigated. These landslides are typically deep landslides (>5 m thickness) occurring in cohesive soils, especially in stiff clays and clay shales, and moving along a distinct basal shear. They display movement as a rigid body such that, the movement observed at the ground surface is not significantly different from the movement at the shear surface at depth. Their rate of movement is strongly correlated with variations in pore water pressure in the ground. Such relations could be useful in establishment of early warning systems and alarm levels. The conclusions reached at the end of this study are:

- 1) General characteristics of slow moving reactivated landslides are gathered and confirmed by four additional case histories. These characteristics were summarized in section 2.3.1.
- 2) There seems to be a nonlinear correlation between the F.S., pore water pressure represented by r_u parameter, and the landslide movement rates. These relations are developed for selected landslide cases in section 4. The relation between pore water pressure, factor of safety and movement rate of a landslide can be useful (1) to understand the significance of a possible error in the pore water pressures, on the calculated factor of safety of the slope (Bishop, 1955), (2) in classifying slow moving reactivated landslides in terms of their sensitivity, which may help in prioritization of allocation of money and resources in monitoring and early warning works for more critical slopes,

(3) in early warning systems, (4) in planning required level of remediation, for example, to decide on how many meters the ground water level should be lowered at a certain piezometric measurement location, so that the stability increases to a desired level of F.S., and movement rates are reduced to an acceptable slow rate.

- 3) Percent change in factor of safety for 10-fold change in velocity, as proposed by Bonnard and Glastonbury (2005), is used for the selected landslide cases. The values are 1.6 to 23% for the landslides cases studied. In this thesis, their approach was improved (i) by using nonlinear shear strength envelope for the material in the shear zone which is more realistic, (ii) by using limit equilibrium slope stability analysis instead of assuming infinite slope, (iii) by incorporating pore pressure coefficient r_u , in addition to “relative F.S.” in our correlations.
- 4) The change in pore pressure coefficient r_u for 10-fold change in velocity is also used in this study. The values range from 1 to 39% for the four landslides cases used in this study (Table 5.2). The values of r_u that are closer to 0.5 indicate that the ground water level is close to ground surface. For slopes with higher r_u values (e.g. San Martino in Fig. 5.2), “extremely slow” movement rates are expected and this type of landslides show more sensitivity to changes in pore pressures, indicated by a less steep slope of the relation between r_u and slide velocity in Fig.5.2. Landslides which have low r_u values (e.g. Triesenberg in Fig. 5.2) develop relatively faster rate of movements (still in the “very slow” to “slow” rates) and they are less sensitive to changes in pore water pressures as represented by a steeper slope in r_u -velocity plot. It is suspected that the slopes that are more r_u -velocity-sensitive, would occur in more plastic clays with flatter ground surface inclinations, and the second group of landslides that display less sensitivity in r_u -velocity plot would occur in less plastic materials with slightly steeper ground surface inclinations. With development of extensive database of such case histories, which have detailed material properties and monitoring information, more of such conclusions can be obtained.

- 5) This information is very useful for stabilization works. With the knowledge of “change in pore pressure coefficient for 10-fold change in velocity” for a slope, it can be proposed to stabilize a slope by reducing r_u value, being monitored at a point along the slope, to such a value that rate of movements will reduce to allowable rates. This will be also useful for determining the priority in allocating money for remediation works for the more critical/sensitive slopes in a region. Therefore, a sensitivity parameter is proposed to indicate the significance of changes in pore pressures on the factor of safety of a slope and the sensitivity of slopes to groundwater level fluctuations. This sensitivity parameter is denoted here as $\Delta FS/1m$, and it represents the decrease in F.S. for a 1-m-rise in the water level (i.e. an increase in the $r_u = u / \gamma h$ value by about 0.05 for a 10 m thick translational slide). For the four landslides in this study the sensitivity values range between 0.003 and 0.05, the latter being the more sensitive slope (Table 5.3).
- 6) Kinematic analyses proposed by Calvello et al. (2008) are also utilized in this study. The method seems to be working for the four landslide cases analyzed in this thesis.

6.2 Future Work Recommendations

Relations between changes in groundwater level, factor of safety and the rate of movement in reactivated landslides are presented for a possible use in early warning systems. For a slow moving landslide monitoring of deformation and pore water pressures can be very useful in developing these relations. Therefore, attention should be given to monitor these parameters for a long period of times, covering the area of the slide, but at least located at points where the most displacement occurs. Efficient slope deformation monitoring techniques, especially remote sensing techniques as airborne SAR and LIDAR interferometry, can be investigated.

In future it will be worth (i) to investigate more cases to see whether a trend exists in these correlations and generalization can be made for certain material/region (ii) to incorporate rainfall relation to ground water level, so that threshold rates of rainfall might be directly used in early warning.

Further studies are needed on this topic, however, such relations seem to be a promising tool to be used in local landslide forecasting, early warning and effective remediation based on drainage.

Such correlations can possibly be incorporated with rainfall and be used in predicting the slope movement behaviour in early warning systems. However it should be noted that the relationships given in this study are of landslides which have very close correlation with rainfall, i.e. the triggering mechanism is assumed to be only from rainfall and related changes in hydrologic boundary conditions. If other triggering mechanisms are also valid, they needed to be incorporated by means of more complex relations.

For finite element deformation analysis, selecting a more advanced failure criteria for the shear surface will give more reliable results. To accomplish this, necessary laboratory tests are needed to be conducted.

The incorporation of groundwater flow analysis with finite element deformation analysis will eliminate the need of individual introduction of piezometric levels at every piezometric location and remove the related interpolation/extrapolation errors.

REFERENCES

- Bertini, T., Cugusi, F., D'Elia, B., & Rossi-Doria, M. (1984). Climatic conditions and slow movements of colluvial covers in central Italy. *Proc. IV Int. Symp. on landslides, Toronto*. Toronto.
- Bishop, A. W. (1955). The use of the slip circle in the stability analysis of slopes. *Geotechnique*, 5(1), 7-17.
- Bonnard, C., & Glastonbury, J. (2005). Risk assessment for very large natural rock slopes. *Landslide Risk Management, Proc. Intl. Conf. on Landslide Risk Management*.
- Brooker, E. W. & Peck, R. B. (1993). Rational design treatment of slopes in overconsolidated clays and clay shales. *Canadian Geotechnical Journal*, Vol. 30, No. 3, pp. 526-544.
- Calvello, M., Cascini, L., & Grimaldi, G. M. (2009). Displacement scenarios of a rainfall-controlled slow moving active slide in stiff clays. *Georisk: Assessment and Management of Risk for Engineered Systems and Geohazards*, 3(3), 116-125.
- Calvello, M., Cascini, L., & Sorbino, G. (2008). A numerical procedure for predicting rainfall-induced movements of active landslides along pre-existing slip surfaces. *Int. J. Numer. Anal. Meth. Geomech.*, 32, 327-351.
- Cascini, L., Calvello, M., & Grimaldi, G. M. (2010). Groundwater modeling for the analysis of active slow-moving landslides. *Journal of Geotechnical and Geoenvironmental Engineering*, 136(9), 1220-1230.
- Cevik, S. Y. (2003). Babadağ (Denizli) ilçesindeki kütle hareketlerinin nedenleri, mekanizması ve modellenmesi üzerine bir araştırma, MSc. Thesis. *Hacettepe Üniversitesi Fen Bilimleri Enstitüsü*.

- Cevik, S. Y., & Ulusay, R. (2004). Babadağ (Denizli) ilçesini etkileyen uzun süreli kaya şevli duraysızlığının statik ve dinamik koşullar açısından araştırılması. *KAYAMEK'2004-VII. Bölgesel Kaya Mekaniği Sempozyumu*. Sivas.
- Cevik, S. Y., & Ulusay, R. (2005). Engineering geological assessments of the repeated plane shear slope instability threatening Babadag (Turkey) and its environmental impacts. *Environmental Geology*, 47, 685-701.
- Corominas, J., Moya, J., Ledesma, A., Lloret, A., & Gili, J. A. (2005). Prediction of ground displacements and velocities from groundwater level changes at the Vallcebre landslide (East-ern Pyrenees, Spain). *Landslides*, 2, 83-96.
- Corominas, J., Moya, J., Lloret, A., Gili, J. A., Angeli, M. G., Pasuto, A., et al. (2000). Measurement of landslide displacements using a wire extensometer. *Engineering Geology*, 55, 149-166.
- Corsini, A., Pasuto, A., Soldati, M., & Zannoni, A. (2005). Field monitoring of the Corvara landslide (Dolomites, Italy) and its relevance for hazard assessment. *Geomorphology*, 66, 149-165.
- Cruden, D. M., & Varnes, D. J. (1996). Landslide types and processes. In: Turner, K.A., Schuster, R.L. (Eds.), *Landslides :investigation and mitigation*, 247, 36-75.
- Dai, F. C., Lee, C. F., & Ngai, Y. Y. (2002). Landslide risk assessment and management: an overview. *Engineering Geology*(64), 65-87.
- Dixon, N., & Brook, E. (2006). Impact of predicted climate change on landslide reactivation: case study of Mam Tor, UK. *Landslides*.
- Enegren, E. G., & Imrie, A. S. (1996). Ongoing requirements for monitoring and maintaining a large remediated rockslide. *Landslides*, 1677-1682.
- Eshraghian, A. (2007). Hazard analysis of translational earth slides in the Thompson River Valley, Ashcroft, British Columbia. PhD. Thesis. *Department of Civil and Environmental Engineering, University of Alberta, Edmonton, Alta.*

- Eshraghian, A., Martin, C. D., & Morgenstern, N. R. (2008). Hazard Analysis of an active slide in the Thompson River Valley, Ashcroft, British Columbia, Canada. *Canadian Geotechnical Journal*, 45, 297-313.
- Fell, R., Hungr, O., Leroueil, S., & Riemer, W. (2000). Geotechnical engineering of the stability of natural slopes, and cuts and fills in soil. *Proc. GeoEng2000*, Melbourne, Australia.
- François, B., Tacher, L., Bonnard, C., Laloui, L., & Triguero, V. (2007). Numerical modelling of the hydrogeological and geomechanical behaviour of a large slope movement: The Triesenberg landslide (Liechtenstein). *Canadian Geotechnical Journal*, 44(7), 840-857.
- Glastonbury, J. P. (2002). The Pre- and Post-Failure Deformation Behaviour of Rock Slopes, PhD. Thesis. *The University of New South Wales*.
- Glastonbury, J., & Fell, R. (2002). *Report on the analysis of slow, very slow and extremely slow natural landslides*. The University of New South Wales, Australia, School of civil and environmental engineering. Sydney: UNICIV.
- Glastonbury, J., & Fell, R. (2008). Geotechnical characteristics of large slow, very slow and extremely slow landslides. *Can. Geotech. J.*, 984-1005.
- Gökçe, O., Özden, Ş., & Demir, A. (2008). *Türkiye'de afetlerin mekansal ve istatistiksel dağılımı afet bilgileri envanteri*. Ankara: T.C Bayındırlık ve İskan Bakanlığı Afet İşleri Genel Müdürlüğü Afet Etüt ve Hasar Tespit Daire Başkanlığı.
- Huvaj-Sarıhan, N. (2009, February). Movement of reactivated landslides, Ph.D. Thesis. *University of Illinois at Urbana-Champaign*.
- International Federation of Red Cross and Red Crescent Societies. (2009). *World Disaster Report: Focus on early warning, early action* .
- IUGS. (1995). A suggested method for describing the rate of movement of a landslides. IUGS Working Group on Landslides. *International Association of Engineering Geology, Bulletin*, 52, 75-78.

- Kayıhan, K., & Demirci, R. (2007). Babadağ ilçesi Gündoğdu Mahallesi Heyelan Afeti Uygulaması ve Yasal Süreç. *TMMOB Afet Sempozyumu*. Ankara.
- Laloui, L., Ferrari, A., & Bonnard, C. (2008). Geomechanical modeling of the Steinernase landslide (Switzerland).
- Leroueil, S. (2001). Natural slopes and cuts: movement and failure mechanism. *Geotechnique*, 51(3), 195-244.
- Leroueil, S., Locat, J., Vaunat, J., Picarelli, L., Lee, H., & Faure, R. (1996). Geotechnical characterization of slope movements. *Landslides*, 53-74.
- Lupini J.F., Skinner A.E., Vaughan P.R., 1981, The drained residual strength of cohesive soils: *Géotechnique*, v. 31, no. 2, p. 181–213
- MacFarlane, D. F., & Jenks, D. G. (1996). Stabilisation and performance of No.5 Creek slide, Clyde Power Project, New Zealand. *Proceedings of the 7th International Symposium*, 3, s. 1739-1746. Trondheim.
- Mansour, M. F. (2009). Characteristic Behaviour of Slow Moving Slides, PhD. Thesis. *University of Alberta*.
- Mansour, M. F., Morgenstern, N. R., & Martin, C. D. (2010). Expected damage from displacement of slow-moving slides. *Landslides*.
- Matsuura, S., Asano, S., & Okamoto, T. (2008). Relationship between rain and/or meltwater, pore-pressure and displacement of a reactivated landslide. *Engineering Geology*, 101, 49-59.
- Mesri, G., & Abdel-Ghaffar, M. (1993). Cohesion intercept in effective stress analysis. *J. Geotech. Eng.*, 119(8), 1229-1249.
- Mesri, G., & Shahien, M. (2003). Residual Shear Strength Mobilized in First-Time Slope. *Journal of Geotechnical and Geoenvironmental Engineering*, 129(1), 12-31.

- Mikkelsen, P. E. (1996). *Field instrumentation*. In: Turner, A.K., Schuster, R.L. (Eds.). Washington DC: Landslides Investigation and Mitigation, Transportation Research Board, Special Report 247, National Research Council.
- Montrasio, L., Valentino, R., & Losi, G. L. (2009). Rainfall-induced shallow landslides: a model for the triggering mechanism of some case studies in Northern Italy. *Landslides*, 6, 241-251.
- Ozpinar, Y., Köseoğlu, M., Cobanoğlu, İ., & Ok, R. (1999). Babadağ (Denizli) ilçe merkezi Gündoğdu heyelanı. 1. Babadağ Sempozyumu. Denizli: Pamukkale Üniversitesi.
- Picarelli, L. (2007). Considerations about the Mechanics of Slow Active Landslides in Clay. K. Sassa, H. Fukuoka, F. Wang, & G. Wang içinde, *Progress in Landslide Science* (s. 27-45). Springer.
- Picarelli, L., Urciuoli, G., & Russo, C. (2004). Effect of groundwater regime on the behaviour of clayey slopes. *Canadian Geotechnical Journal*(41), 467-484.
- Picarelli, L., Urciuoli, G., Mandolini, A., & Ramondini, M. (2006). Softening and instability of natural slopes in highly fissured plastic. *Natural Hazards and Earth System Sciences*, 529-539.
- PLAXIS b.v. (2002). *PLAXIS, Finite Element Code for Soil and Rock Analyses*. A.A. Balkema Publishers.
- Pockoski, M., & Duncan, J. (2000). *Comparison of computer programs for analysis of reinforced slopes*. Center for Geotechnical Practice and Research, Virginia Polytechnic Institute and State University, .
- Rutter, E. H., Arkwright, J. C., Holloway, R. F., & Waghorn, D. (2003). Strains and displacements in the Mam Tor landslip, Derbyshire, England. *Journal of the Geological Society, London*, 160, 735-744.

- Skempton, A. W. (1964). The long term stability of clay slopes. *Geotechnique*, 14, 77-101
- Skempton, A. W. (1985). Residual strength of clays in landslides, folded strata and the laboratory. *Geotechnique*, 35(1), 3-18.
- Skempton, A. W., Leadbeater, A. D., & Chandler, R. J. (1989). The Mam Tor landslide, North Derbyshire. *Phil. Trans. R. Soc. Lond. A*, 329, 503-547.
- Stark, T. D., & Eid, H. T. (1993). Modified Bromhead ring shear apparatus. *ASTM Geotech. J.*, 16(1), 100-107.
- Stark, T. D., & Eid, H. T. (1994). Drained residual strength of cohesive soils. *J. Geotech. Engng Div., ASCE*, 120(5), 856-871.
- Stark, T. D., Choi, H., & McCone, S. (2005, May). Drained Shear Strength Parameters for Analysis. *Journal of Geotechnical and Geoenvironmental Engineering*, 131(5), 575-588.
- Tacher, L., Bonnard, C., Laloui, L., & Parriaux, A. (2005). Modelling the behaviour of a large landslide with respect to hydrogeological and geomechanical parameter heterogeneity. *Landslides*, 2, 3-14.
- Tano, H., Aydan, Ö., Ulusay, R., & Kumsar, H. (2006). *Şev hareketleri üzerinde etkili olan jeo-çevresel faktörlerle ilgili ortak araştırma: Babadağ(Türkiye)'daki krip türü şev duyarsızlığının incelenmesi.*
- Ulusay, R., Ayadan, Ö., Tano, H., & Kumsar, H. (2006). *Babadağ Gündoğdu mah. krip türü heyelanın araştırılması ara raporu.* Ankara.
- USACE. (2003). *Slope Stability - Engineering Manual.* Washington: USACE Engineering and Design.
- Van Asch, T. J., & Buma, J. T. (1997). Modelling groundwater fluctuations and the frequency of movement of a landslide in the Terres Noires region of Barcelonnette (France). *Earth Surf. Processes Landforms*, 22, 131-141.

- Van Asch, T. W., Van Beek, L., & Bogaard, T. A. (2007). Problems in predicting the mobility of slow-moving landslides. *Engineering Geology*, 91, 46-55.
- Varnes, D. J. (1978). *Slope movement types and processes*. In: Schuster R. L. & Krizek R. J. Ed., *Landslides, analysis and control*. Transportation Research Board Sp. Rep. No. 176. Nat. Acad. of Sciences.
- Vaunat, J., Leroueil, S., & Faure, R. (1994). Slope movements: a geotechnical perspective. *Proc. 7th Cong. Int. Assoc. Engng Geol., Lisbon*, (s. 1637-1646).
- Vulliet, L., & Hutter, K. (1988). Viscous-type sliding laws for landslides. *Can. Geotech. J.*, 25(3), 467-477.
- Walstra, J., Chandler, J. H., Dixon, N., & Dijkstra, T. A. (2004). Time for change-Quantifying landslide evolution using historical aerial photographs and modern photogrammetric methods. *XXth USPRS Congress* (s. 1682-1750). Istanbul: International Society for Photogrammetry and Remote Sensing.
- Walstra, J., Dixon, N., & Chandler, J. H. (2007). Historical aerial photographs for landslide assessment: two case histories. *Quarterly Journal of Engineering Geology and Hydrogeology*, 40, 315-332.
- Waltham, A. C., & Dixon, N. (2000). Movement of the Mam Tor landslide, Derbyshire, UK. *Quarterly Journal of Engineering Geology and Hydrogeology*, 33, 105-123.
- WP6. (2008). *Slope Monitoring Methods: A State of the Art Report*. The ClimChALp partnership.
- Yucemen, M. S., & Tang, W. H. (1975). Long term stability of soil slopes: a reliability approach. In Edgar Schutze (ed.). *Proceedings of the 2nd International Conference on Applications of Statistics and Probability in Soil and Structural Engineering*, (s. 215-229).

APPENDIX A

Table A.1 - General information about landslide cases

Landslide Name:		San Martino	Vallcebre	Babadag	Steinernase	Triesenberg
Main Source:		Bertini et al. (1984)	Corominas et al. (2005)	Cevik&Ulusay (2005)	Laloui et al. (2008)	François et al.(2007)
Landslide Type:		Translational	Translational	Translational	--	Translational
Average Velocity (cm/year):		2	73 - 180	3.8 - 15	0.07 - 1.5	0 - 3
Velocity Description:		Very Slow	Slow	Very Slow	Extremely Slow	Very Slow
Bedrock:		Marly Clay	Limestone	Schist	Limestone	Schist-limestone
Geological Age:		Pliocene	U. Creta. –L. Palaeo.	Palaeocene	Quaternary	Quaternary
Maximum Soil Thickness (m):		24	30	30	14	33
Dimensions:	Length (m):	--	1200	650	230	2300
	Width (m):	--	600	430	300	1500 - 3200
	Area (km²):	--	0.8	0.3	0.07	3.1
	Volume (m³):	--	20 E+6	1.42 E+6	--	37 E+6
Average Slope Angle (°):		8 - 10	10	16	17	24
Toe:		San Martino Stream	Vallcebre Torrent Bed	Gokdere River	Rhine River	Rhine Alluvia
Shear Surface:	Type:	--	Lateral thin basal	Planar	Multi-surface	--
	Inclination (°):	8 - 10	10	14 -24	15 - 17	24
	Depth (m):	11 - 26	10 - 15	10 - 30	7.5 - 17.5	10 - 20
	Thickness (m):	4	0.3	0.3	--	1

Table A.2 - Material properties of landslide cases

Landslide Name	Materials	Unit Weight (kN/m ³)	Average Atterberg Limits			CF (%)	Fine Particles <0.02mm (%)	USCS Classification	Shear Strength Parameters			
			LL (%)	PL (%)	PI (%)				Peak		Residual	
									c (kPa)	∅ (deg.)	c (kPa)	∅ (deg.)
San Martino	Colluvium	21	42	20	22	40-50	80 - 93	CL	25	27	10	21
	Weathered Marly Clay	21	46	22	24 - 27	25-50	76 - 93	CL	15	24	0	27
	Unweathered Marly Clay	22	46	22	24	25-50	76 - 93	CL	--	--	--	--
Vallcebre	Fissured Shales	22	--	--	60	--	--	--	0	38.7	0	7.8
	Clayey Siltstone	20	55	35	20	--	--	--	0	38.7	0	14.7
	Limestone	20	--	--	--	--	--	--	--	--	--	--
Babadag	Heavily Wathered Rock	--	--	--	--	--	--	--	--	--	--	--
	Sandstone - Marl	18.5	--	--	40	--	--	--	2.9	11.2	0.6	10.8
Steinernase	Soil Cover	20	--	--	--	15 - 28	48 - 65	--	0	24	0	20
	Rhine Alluvium	20	--	--	--	--	--	--	--	--	0	27
	Bedrock	20	--	--	--	--	--	--	--	--	--	--
Triesenberg	Loose Soil	20	26	13	13	--	50	CL	0	25	0	20
	Slip Surface Material	20	22	11	11 - 20	--	38	SC	11	30	--	--
	Bedrock	20	--	--	--	--	--	SC	17	30	--	--

APPENDIX B

Table B.1 – Slope stability analyses input and results with corresponding velocities (Vallcebre)

Station		S9			S2			S5			F.S	Rel. F.S	Velocity (mm/day)
GWL No.	Date	GWL (m)	Depth (m)	ru	GWL (m)	Depth (m)	ru	GWL (m)	Depth (m)	ru			
P1	Dec-97	43.54	1.32	0.44	57.96	0.79	0.46	70.10	1.61	0.42	0.872	1.000	8.828
P2	Dec-96	43.22	1.64	0.43	57.96	0.79	0.46	--	--	--	0.911	1.045	--
P3	Nov-96	43.08	1.78	0.43	57.86	0.89	0.45	--	--	--	0.916	1.050	2.940
P4	May-97	42.59	2.27	0.41	56.57	2.18	0.40	69.55	2.16	0.39	0.920	1.055	--
P5	Initial	42.45	2.41	0.40	56.71	2.04	0.41	--	--	--	0.949	1.088	3.177
P6	Jan-98	42.43	2.43	0.40	52.93	5.82	0.26	66.06	5.65	0.24	1.026	1.177	1.801
P7	Aug-97	41.75	3.11	0.38	52.77	5.98	0.25	66.06	5.65	0.24	1.042	1.195	2.816
P8	Jun-97	41.40	3.46	0.36	52.95	5.80	0.26	66.12	5.59	0.24	1.044	1.197	2.615
P9	Jan-97	41.30	3.56	0.36	52.91	5.84	0.26	66.16	5.55	0.24	1.047	1.201	2.529
P10	Jul-97	41.30	3.56	0.36	52.77	5.98	0.25	66.10	5.61	0.24	1.050	1.204	4.680
P11	Feb-97	41.22	3.64	0.36	52.69	6.06	0.25	66.04	5.67	0.24	1.053	1.208	3.573
P12	Mar-97	41.18	3.68	0.36	52.75	6.00	0.25	65.98	5.73	0.24	1.054	1.209	3.558
P13	May-98	40.68	4.18	0.34	52.83	5.92	0.25	66.04	5.67	0.24	1.061	1.217	1.100
P14	Mar-98	40.72	4.14	0.34	52.75	6.00	0.25	66.02	5.69	0.24	1.062	1.218	1.230
P15	Jun-98	40.47	4.39	0.33	52.73	6.02	0.25	65.92	5.79	0.23	1.067	1.224	2.117
P16	Aug-98	39.24	5.62	0.29	52.51	6.24	0.24	65.89	5.82	0.23	1.094	1.255	1.175
P17	Final	39.08	5.78	0.28	52.49	6.26	0.24	65.92	5.79	0.23	1.097	1.258	1.959

Table B.2 – Slope stability analyses input and results with corresponding measured velocities (San Martino)

Station		B3			C6			F.S	Rel. F.S	Velocity (mm/day)
GWL No.	Date	GWL (m)	Depth (m)	ru	GWL (m)	Depth (m)	ru			
P1	Feb-80	154.81	0.69	0.45	143.65	0.05	0.47	0.995	1.004	0.217
P2	Apr-80	154.43	1.07	0.44	143.18	0.52	0.46	1.007	1.016	0.121
P3	May-80	154.89	0.61	0.45	142.88	0.82	0.45	0.991	1.000	0.354
P4	Jun-80	154.23	1.27	0.44	142.60	1.10	0.44	1.017	1.026	0.087
P5	Jul-80	153.60	1.90	0.42	142.13	1.57	0.44	1.033	1.042	0.024
P6	Aug-80	153.16	2.34	0.41	141.97	1.73	0.43	1.042	1.051	0.005
P7	Oct-80	154.51	0.99	0.44	142.71	0.99	0.45	1.030	1.039	0.036
P8	Dec-80	155.50	0.00	0.47	143.70	0.00	0.47	1.007	1.016	0.075
P9	Apr-81	154.26	1.24	0.44	142.46	1.24	0.44	1.023	1.032	0.005
P10	May-81	153.52	1.98	0.42	141.72	1.98	0.43	1.037	1.046	0.002
P11	Jun-81	153.55	1.95	0.42	141.75	1.95	0.43	1.043	1.052	0.005
P12	Jul-81	154.07	1.43	0.43	142.27	1.43	0.44	1.037	1.046	0.019
P13	Aug-81	153.96	1.54	0.43	142.16	1.54	0.44	1.039	1.048	0.000
P14	Sep-81	153.10	2.40	0.41	142.33	1.37	0.44	1.038	1.047	--
P15	Oct-81	152.97	2.53	0.41	142.00	1.70	0.43	1.045	1.054	--
P16	Oct-81-2	152.88	2.62	0.41	142.16	1.54	0.44	1.044	1.053	--
P17	Nov-81	152.63	2.87	0.40	142.35	1.35	0.44	1.046	1.055	--
P18	Dec-81	152.69	2.81	0.40	142.74	0.96	0.45	1.040	1.049	--

Table B.3 - Slope stability analyses input and results with corresponding measured velocities (Steinernase)

Station		B3C			B3E			F.S	Rel. F.S	Velocity (mm/day)
GWL No.	Date	GWL (m)	Depth (m)	ru	GWL (m)	Depth (m)	ru			
P1	Jan-00	321.66	7.18	0.30	326.80	13.03	0.09	1.010	1.079	
P2	Feb-00	320.97	7.87	0.28	329.45	10.39	0.17	1.003	1.072	0.025
P3	Mar-00	320.69	8.16	0.27	331.30	8.54	0.23	0.994	1.062	0.046
P4	Apr-00	319.84	9.01	0.25	330.65	9.19	0.21	1.012	1.081	0.008
P5	Jun-00	321.20	7.64	0.29	329.36	10.48	0.17	1.001	1.069	0.002
P6	Jul-00	319.28	9.56	0.23	329.30	10.54	0.17	1.028	1.098	0.007
P7	Aug-00	321.54	7.31	0.30	328.40	11.43	0.14	1.002	1.071	0.002
P8	Sep-00	319.08	9.77	0.23	330.93	8.91	0.22	1.020	1.090	0.007
P9	Jan-01	322.71	6.13	0.33	332.37	7.47	0.26	0.957	1.022	
P10	Mar-01	322.10	6.74	0.31	335.43	4.40	0.36	0.936	1.000	0.048
P11	Jun-01	319.77	9.08	0.25	333.99	5.84	0.31	0.984	1.051	0.041
P12	Sep-01	319.23	9.61	0.23	330.59	9.25	0.21	1.021	1.091	0.013
P13	Nov-01	319.14	9.70	0.23	331.88	7.96	0.25	1.011	1.080	0.020
P14	Dec-01	321.01	7.83	0.28	332.31	7.53	0.26	0.981	1.048	0.021

Table B.4 - Slope stability analyses input and results with corresponding measured velocities (Triesenberg)

Station		B4			B8			F.S	Rel. F.S	Velocity (mm/day)
GWL No.	Date	GWL (m)	Depth (m)	ru	GWL (m)	Depth (m)	ru			
P1	Jan-00	1101.64	47.90	--	909.51	7.95	0.08	0.979	1.011	0.145
P2	Feb-00	1101.34	48.21	--	908.86	8.60	0.04	0.981	1.013	0.136
P3	Mar-00	1101.80	47.74	--	909.83	7.63	0.09	0.978	1.010	0.151
P4	Apr-00	1102.32	47.22	--	911.33	6.13	0.17	0.973	1.005	0.366
P5	May-00	1105.80	43.75	--	912.92	4.54	0.25	0.968	1.000	0.541
P6	Jun-00	1102.19	47.36	--	910.48	6.98	0.13	0.976	1.008	0.389
P7	Jul-00	1101.61	47.93	--	908.92	8.54	0.05	0.981	1.013	0.146
P8	Jul-00-2	1101.83	47.71	--	909.81	7.65	0.09	0.978	1.010	0.217
P9	Sep-00	1103.39	46.16	--	910.80	6.66	0.15	0.975	1.007	0.353
P10	Oct-00	1101.56	47.99	--	910.16	7.30	0.11	0.977	1.009	0.244
P11	Nov-00	1101.86	47.69	--	909.13	8.33	0.06	0.978	1.010	0.162
P12	Nov-00-2	1101.69	47.85	--	910.04	7.42	0.11	0.977	1.009	0.190